Pricing CPPI Capital Guarantees:
A Lagrangian Framework

by

Christopher Stephen Band Morley

A thesis
presented to the University of Waterloo
in fulfilment of the
thesis requirement for the degree of
Master of Mathematics
in
Applied Mathematics

Waterloo, Ontario, Canada, 2011

Author's declaration

I hereby declare that I am the sole author of this thesis. This is a true copy of the thesis, including any required final revisions, as accepted by my examiners.

I understand that my thesis may be made electronically available to the public.

Abstract

A robust computational framework is presented for the risk-neutral valuation of capital guarantees written on discretely-reallocated portfolios following the Constant Proportion Portfolio Insurance (CPPI) strategy. Aiming to address the (arguably more realistic) cases where analytical results are unavailable, this framework accommodates risky-asset jumps, volatility surfaces, borrowing restrictions, nonuniform reallocation schedules and autonomous CPPI floor trajectories. The two-asset state space representation developed herein facilitates visualising the CPPI strategy, which in turn provides insight into grid design and interpolation. It is demonstrated that given a deterministic process for the risk-free rate, the pricing problem can be cast as solving cascading systems of 1D partial integro-differential equations (PIDEs). This formulation's stability and monotonicity are studied. In addition to making more sense financially, the limited borrowing variant of the CPPI strategy is found to be better suited than the classical (unlimited borrowing) counterpart for bounded-domain calculations. Consequently, it is demonstrated how the unlimited borrowing problem can be approximated by imposing an artificial borrowing limit. For implementation validation, analytical solutions to special cases are derived. Numerical tests are presented to demonstrate the versatility of this framework.

Acknowledgements

I am grateful to my co-supervisors, Dr. Peter Forsyth and Dr. George Labahn, for their forthright guidance in all matters conceptual, computational and editorial. I would also like to thank Dr. Yuying Li and Dr. Justin Wan for reviewing my thesis. I was fortunate to receive additional mentorship from Jen Nissen, Dr. Wing-Ki Liu and Dr. Theophanis Stratopoulos. Thanks to all of you for sharing your time and wisdom.

Helen Warren deserves special praise for her approachability and for her ability to answer all of my numerous administrative questions.

I have enjoyed many interesting and intellectually uplifting discussions with my departmental colleagues. I would like to single out my officemate Kelly: thank you for tolerating all of my eccentricities! Alex and Antonio: thank you for easing the transition from Kingston to Waterloo. Kathleen and Amenda: your departmental representation and event organisation efforts are greatly appreciated. Dhanaraja and Michael: thanks for sharing your unbounded cheerfulness with us all.

Outside of my department, I owe a great deal of thanks to my friends, near and far. Michelle, Jan and the rest of the Guelphites provided a welcome change of scenery, entertaining me with first-rate hospitality in their home city. Mike and Karen did likewise in Kingston and Toronto. Anna, Court, Randy and Vris helped expand my cultural horizons.

Over the course of my stay in Waterloo, I had the pleasure of sharing accommodations with Jason, Josh, Rahul, Hani, Michał, Linda, Kyle and Kirstin. In particular I thank them for their good humour and for involving me in their adventures, both culinary and otherwise.

Last but not least, a warm thank you to my family for their sustained encouragement and interest in my progress. I am especially indebted to my parents and I feel blessed for having had their unconditional love and support since day one.

Chris Morley

In honour of my grandparents Colleen, Elmer, Peter and Pris

Contents

List of Tables

List of Figures

List of Symbols

Latin symbols

$.^k$	Shorthand for the value of a function $(S, B, W$ or $F)$ at $\cdot(t_\mathrm{o}^k)$	7
$.^{k\pm}$	Shorthand for the value of a function $(S, B, W$ or $F)$ at $\cdot(t_\mathrm{o}^k) \pm \epsilon$	7
$\cdot_t$	Continuous-time process	53
$\mathbf{1}_A(x)$	Indicator function	51
$\mathcal{A}^k$	The image (k^{th} allocation locus) of f^k	10
$\mathcal{A}^k_{\vert}$	The vertical segment of $\mathcal{A}^k$	10
$\mathcal{A}^k_{\backslash}$	The oblique segment of $\mathcal{A}^k$	10
$\hat{\mathcal{A}}^k$	The image (k^{th} allocation locus) of $\hat{f}^k$	12
B	State variable for value of 'risk-free' component in CPPI portfolio	6
$B^\star$	Dummy state variable	—
$B^k_{\min}$	Minimum B ordinate of k^{th} grid	28
$\hat{B}^k$	Borrowing limit imposed on k^{th} grid	12
$\hat{B}$	Fixed borrowing limit	12
$\mathcal{C}(S; X, T)$	Time-0 value of a European call w. spot S, strike X and mat. T	42
$\mathscr{C}(K)$	Relates to an upper bound for $v^0_J(W_0, 0)$ (see text)	45
$\bar{C}_t$	Continuously-reallocated discounted cushion process	53
CR	Convergence ratio	61
$\frac{\mathrm{D}V}{\mathrm{D}\tau}$	Lagrangian derivative	19
$d_{u,\ell}$	A family of arguments for Φ $(u \in \{1, 2\})$	45
$\mathrm{d}q_t$	An increment in the Poisson process governing the occ. of a jump	15
$\mathrm{d}Z_t$	Wiener increment for time t	15
$\mathcal{E}(\cdot)_t$	Doléans-Dade (stochastic) exponential	53
$\mathrm{E}^{\mathbb{Q}}$	Expectation with respect to the measure $\mathbb{Q}$	16
E_ℓ	ℓ^{th} term of the series rep'n for $\mathcal{C}(m; e^{r\delta}(m-1), \delta)$ (see text)	50
F^k	Prevailing CPPI floor (reference value) at t_o^k	7
F_T	Final CPPI floor, at t=T	7
f^k	Classical CPPI jump condition at t_o^k	10
$\hat{f}^k$	Limited-borrowing CPPI jump condition at t_o^k	13
G	Shorthand for an argument of Φ	51

Latin symbols (continued)

$\bar{g}_{\ell,j}$	Probability used in FFT interpolation	38
i	Grid index (abscissa)	—
$\mathcal{J}$	Operator representing jump dynamics	18
J_t	Magnitude of a jump from S_{t^-} to $J_t S_{t^-}$ at time t	15
j	Grid index (ordinate)	—
K	Number of CPPI portfolio reallocations	7
k	Reallocation index	—
$\mathcal{L}$	Operator representing jump-free dynamics	18
$(L^{\mathrm{A}})_t$	Comp. of cont. CPPI dyn. that will not $(a.s.)$ cause a shortfall	56
$(L^{\mathrm{B}})_t$	Comp. of cont. CPPI dyn. that will $(a.s.)$ cause a shortfall	56
ℓ	Dummy index	—
$\mathbf{M_{j,k}}$	LHS matrix of the 1D PIDE's fully implicit discretisation	39
m	CPPI multiplier (leverage factor)	9
$\mathcal{N}$	Set of FFT indices	38
n	Timestep index	—
$\mathrm{P}^{\mathbb{Q}}$	Risk-neutral probability	56
$p(J)$	Probability density when J_t is lognormally distributed	16
$\mathbb{Q}$	Risk-neutral probability measure	15
r	'Risk-free' interest rate	16
RE	Relative error	62
RL	Grid refinement level	60
S	State variable for value of risky component in CPPI portfolio	6
$S^{\star}$	Dummy state variable	—
$S_{\mathcal{A}^k_{\setminus}}$	The abscissa of $\mathcal{A}^k_{\setminus}$ at $B = B^k_{\min}$	42
T	Investment horizon	7
t	Time	6
t^0_{o}	Instant of initial CPPI portfolio allocation, corresponding to $t = 0$	7
t^k_{o}	Instant of the k^{th} CPPI portfolio reallocation	7
t^{k-}_{o}	The instant before t^k_{o}	7
t^{k+}_{o}	The instant after t^k_{o}	7
t^{K+1}_{o}	Instant of CPPI portfolio liquidation, corresponding to $t = T$	7
$\bar{t}$	Dummy variable	—
$t^{\star}$	First instant when $\bar{C}_t$ goes negative	57
u	Dummy variable	—

Latin symbols (continued)

V_I	Risk-neutral expected value of a CPPI portfolio with guarantee	7
V_J	Risk-neutral expected value of a CPPI capital guarantee	23
V_L	Risk-neutral expected liability to a CPPI guarantor	7
V	Generic representation for V_I, V_J and V_L	8
v^k	Generic representation of k^{th} stage solution (with deferred interest)	19
$v^n_{i,j}$	Discretised version of v^k	38
$v^0(W_0, 0)$	The solution to V for initial wealth W_0	23
$\bar{v}^k$	v^k, as a function of X^k	30
W	Wealth	6
W_0	Initial wealth	6
$W^{k+}_{\min}$	Minimum wealth provided by k^{th} grid	28
$W^{k+}_{\max}$	Maximum wealth provided by k^{th} grid	28
X^k	CPPI analogue to strike price	29
z	Generic scale factor	—

Greek symbols

1 Introduction

1.1 Overview

Capital guarantees are structured investment products that provide (typically leveraged) exposure to upside risks, and limited exposure to downside risk, with a *portfolio insurance* feature that guarantees a minimum portfolio value at maturity [31]. Consequently, such instruments offer an investor the safety of a bond during falling markets and the earning potential of a leveraged equity portfolio during rising markets [6]. This arrangement appeals to investors with low risk tolerance, or with a bearish outlook over the term of the contract. On the other side of the deal, the counterparty acting as *guarantor* faces a liability when at the product's maturity the value of the managed portfolio falls short of the guaranteed amount. Banks issuing this product will as a result charge a premium that (ideally) fully offsets this risk. In this work we will study the pricing of these premia for the class of capital guarantees that are structured using a Constant Proportion Portfolio Insurance (CPPI) strategy.

The issuer is able to offer such a service by, at the outset of of the contract, constructing a portfolio to superreplicate the guaranteed amount at maturity. In other words, the maturity value of the portfolio—under all market movements—should be worth at least as much as the guaranteed amount. One approach is for the issuer to buy a zero-coupon bond worth the guaranteed amount at its maturity, and then invest the rest of the endowed wealth in the risky asset or a contingent claim written thereon [31]. However, such a *buy-and-hold* strategy could easily be executed by the client without professional wealth management. Moreover, this *static* strategy fails to react to changing market conditions.

A more sophisticated approach would be to use a *dynamic* allocation strategy [42], where the portfolio's composition is monitored and adjusted accordingly. Such control is beneficial because otherwise, as a portfolio's constituent assets evolve, the portfolio will deviate in trajectory from the investment goal. The CPPI strategy belongs to this class, and its optimality is examined in [29, 10, 23] and other references therein. We stress that the aforementioned strategies are predetermined and algorithmic, as opposed to those where a portfolio manager reallocates as needed, based on their own outlook and revisions thereof.

The two assets comprising a CPPI portfolio are (i) a *risky asset*, typically an equity fund or index; and (ii) a *risk-free asset*, such as a position in a sovereign zero-coupon bond. Of course, no financial asset is truly free of risk. CPPI contracts have also used funds-of-funds, credit products [37] and commodities [36] for the underlying risky asset. Different asset classes will naturally have different modelling requirements.

The CPPI strategy is attributed to Perold [41], with seminal papers by Black and Jones [7], Perold and Sharpe [42] and Black and Perold [6]. A *classical* CPPI contract specifies a constant leverage *multiplier* (also known as a *gearing factor*), and a guaranteed amount (*floor*). At each adjustment, the allocation strategy considers the difference, or *cushion*, between the portfolio's value and the discounted floor. If the cushion is positive then the risky asset exposure is set equal to the product of the cushion and the multiplier. Otherwise, the strategy is deemed to be *knocked-out* [37] (alternatively, *closed-out* [13]) and the risky asset exposure is set to zero. Leveraged upside exposure is achieved by choosing a multiplier greater than 1. A *self-financing* condition dictates that any surplus portfolio value (or debt) be invested in the risk-free asset. Consequently, CPPI strategies can dictate a short position in the risk-free asset. At expiration the investor's payoff is the larger of the guaranteed amount and the portfolio value. Conversely, the guarantor's liability is the difference between the guaranteed amount and the portfolio value, if a shortfall exists.

For a capital guarantee based on a CPPI-managed portfolio, the premium charged by the issuer at the inception of the contract should compensate for (i) the costs of managing the CPPI portfolio, and (ii) the risk assumed by its obligation to cover any shortfall. In the literature the second item is called the *CPPI gap risk*, and can be attributed to sudden, steep drops in the risky asset value occurring before the portfolio manager can rebalance the portfolio. One measure of gap risk is the present value of the claim's risk-neutral expected shortfall. This quantity represents the cost of hedging the gap risk. If a bank underestimates the magnitude of this risk (through model error) then it could end up in a position where the premium charged is insufficient to defray the knock-out liability. Such a scenario can also occur if the financial institution underprices its product in order to be competitive.

Recent works demonstrate that the gap risk is non-negligible for discontinuous risky asset time series [15] or when the CPPI portfolio is rebalanced infrequently [4]. These results show that the 'PI' in CPPI is a misnomer: in practice a CPPI strategy has a probability of failure that should not be neglected from the risk assessment, and it is the premium—rather than the CPPI strategy itself—that mitigates shortfalls. However, until lately, most articles in the CPPI literature used the same Black-Scholes-Merton assumptions prevalent when portfolio insurance was first introduced: (i) perfect liquidity, (ii) perfect unit divisibility, (iii) continuous reallocation, (iv) free transactions, (v) asset price continuity and (vi) constant market volatility. As noted in [15], such conditions also lead to the dubious result that the expected portfolio value can increase unboundedly with the leverage factor. Indeed, these classical assumptions (especially (v) and (vi)) are now regarded as overly simplistic.

Following the papers of Cont and Tankov [15] and Balder et al. [4] there has been renewed CPPI research activity. In [12] Brandl continues his work from [4], developing a discrete-reallocation model that accommodates borrowing limits, triggered reallocation, transaction costs and variable CPPI floors for the jump-free case. These extensions are achieved using Laplace transforms. Jessen [26] has developed a gap risk model that incorporates discrete reallocation, jump diffusions, transaction costs, profit lock-in and borrowing limits. Her results are obtained through Monte Carlo simulations. In [39] and [40] Paulot and Lacroze examine conditions under which CPPI-based claims can be formulated as a Markov process in one variable.

Despite these developments, the CPPI gap risk literature lags behind the products used in industry. Since 1986, practitioners and academics alike have proposed numerous variants of the classical CPPI strategy, with features such as borrowing limits, volatility caps [37], management fees, minimum exposures, early exercise, variable gearing factors, and floor ratcheting (profit lock-in) [13]. Other exotic variants are presented in [36]. Of the ones listed, only the first three can be classified as directly lowering the guarantor's gap risk. This is where we focus. The others serve to improve the investor's expected return, with the consequence of the guarantor assuming even more gap risk—and being able to charge a larger premium for this service. Our objective for this work is to develop a framework versatile enough to accommodate guarantees on a diverse range of CPPI variants.

1.2 Contributions of this thesis

The focus of this work is the development of a mathematical framework for computing the fair-market values of capital guarantees written on CPPI-style portfolios. This is useful to consumers, guarantors and regulators alike. Our treatment of CPPI gap risk is not the first, but it aims to be the most versatile. The CPPI gap risk papers described previously consider special cases under which a CPPI product can be calculated analytically or with minimal computation; in this thesis we take a contrary philosophy, proceeding with minimal assumptions about the contract or the underlying model. In summary:

- We present a general-purpose numerical framework for pricing claims on a CPPI portfolio. Our design permits
  - discrete reallocation, with apparent convergence to the continuous case,
  - nonuniform reallocation schedules,
  - underlying risky assets with finite-activity jump discontinuities,
  - any deterministic risk-free rate function,
  - any deterministic CPPI floor function (defined by either an equation or a table of values),
  - volatility surfaces, and
  - absolute limits on borrowing.
- We demonstrate that our framework is consistent with special cases from the literature.
- We design a time-varying sequence of computational grids with efficient convergence in mind. Additionally, we consider the construction of these grids for situations where a *similarity extrapolant* (in the sense of [47]) is not appropriate.
- We demonstrate that CPPI products with borrowing limits make sense both financially and computationally.

1.3 Economic relevance

CPPI-based capital guarantees have significant market presence and are of regulatory interest. Regarding the first point, we cannot quote a worldwide figure, owing to the diversity of products and the reluctance of banks to disclose their structuring strategies. Rather, we demonstrate CPPI prominence locally. In Canada, capital protected products are classified as segregated funds and market-linked instruments [34]. Segregated funds are payable upon death and are discussed elsewhere; our interest is in the latter product, where the maturity is contractually specified. Market-linked instruments are also known as market-linked guaranteed investment certificates, principal protected notes (PPNs) [34] and deposit notes on principal protected products [1]. In [24] it is estimated that of active PPNs in March 2005, 24% were written on hedge funds, and at one time this segment alone was managing \$7.7 billion in assets. By November of 2006, the entire Canadian PPN industry was controlling \$14 billion, up from \$1.9 billion in 2001 [9]. Furthermore, we have on the authority of practitioners that CPPI is a leading management strategy for Canadian [34, 9] and British [37] capital guarantees.

As to the second point, structured capital guarantee products have attracted criticism and the attention of regulators. A portfolio managed by a CPPI strategy decreases its risky-asset exposure when the underlying equity decreases in value. In the event of a significant negative market shock, such a 'buy-high, sell-low' strategy dictates selling that further lowers the price. This positive feedback behaviour can lead to a downward spiral unless checked by other market forces. Part of the blame for the 1987 stock market crisis was assigned to this same behaviour when it was exhibited by another portfolio insurance strategy; later analysis has since advocated a weaker verdict of "not proven" [32]. More recently, a 2007 report the Organisation for Economic Co-operation and Development (OECD) identified the gap risk of CPPI and related structured products as a "potential stability issue" and "a major area of policy interest" [8]. The Bank of England elaborates, recognizing that CPPI-backed guarantees have several consequential, interconnected drawbacks that can affect financial stability in a manner contrary to the product's advertised objective [37]. This same authority did not find the positive feedback effect of CPPI strategies to be gravely detrimental during market upheaval in 2007; however, it was noted that this may have masked price signals. Other reported concerns are (i) calibration error, (ii) issuers experiencing higher-than-expected volatility and therefore incurring more gap risk, and (iii) the scarcity of hedging instruments leading to deliberately imperfect hedges. These issues deserve attention, and while our design cannot address all of them, it can aid the sensitivity analyses of exotic CPPI claims.

1.4 Outline

The remainder of this thesis is organised as follows. In Chapter 2 we lay a mathematical framework for describing this problem, and then recast the problem in a form that is easier to solve. This leads into Chapter 3, where we discretise the problem so that it may be solved on a computational grid. Here we also study our numerical approach's convergence properties. In Chapter 4 we derive analytical results for a few special cases of this problem. In Chapter 5 we present our numerical results and validate them against the results obtained in the previous chapter. This is followed by concluding remarks and suggestions for future work in Chapter 6.

2 CPPI with jumps and discrete reallocation

A capital guarantee can be viewed as a contingent claim; our ultimate objective is to price contingent claims written on a discretely-reallocated CPPI portfolio. In this chapter we introduce a state space framework for describing CPPI portfolios and their discrete-time reallocation dynamics. From this, we model the payoffs and inter-rebalancing dynamics of a CPPI claim. The resulting system is transformed into a system of one-dimensional partial integro-differential equations (PIDEs) which in between reallocations can be solved in parallel.

2.1 Preliminaries

Before we mathematically model the discrete-time CPPI strategy (Section 2.2) and characterise the CPPI capital guarantee (Section 2.3), let us first introduce some notation.

2.1.1 Notation

Modelling a discrete-time version of the CPPI strategy described in Section 1.1 requires notation for the observation times, guaranteed amount and the CPPI portfolio's composition. Our approach differs from that of Balder, Brandl and Mahayni [4]: we track the values of the CPPI portfolio's constituent assets rather than the units held of each.

Recall that at time $t = 0$ an *investor* endows their *portfolio manager* with *initial wealth* $W_0 > 0$. This capital is immediately invested to create a two-asset portfolio consisting of

1. a risky, liquid stock or index fund worth $S(t)$ at time t, and
2. a risk-free, fixed-income asset worth $B(t)$ at time t.

Models for these assets' dynamics will be introduced in Section 2.4. It follows that at any time t the portfolio has a value $W(t) \equiv S(t) + B(t)$.

To represent the contractually predetermined *observation times* we partition the investment horizon $[0,T]$. Denote this partition by $\left\{t_{\mathrm{o}}^{k}\right\}_{k=0}^{K+1}$, such that

$$t_{\mathrm{o}}^{0} \equiv 0 < t_{\mathrm{o}}^{1} < t_{\mathrm{o}}^{2} < \ldots < t_{\mathrm{o}}^{K-1} < t_{\mathrm{o}}^{K} < t_{\mathrm{o}}^{K+1} \equiv T.$$

By this notation, the CPPI strategy is initially applied at the *allocation event* t_{o}^{0} and reinforced at each of K *reallocation events*. Finally, at the *payoff event* t_{o}^{K+1} the portfolio is liquidated and the proceeds are paid to the investor. The observation times need not be uniformly spaced.

We introduce the function $F(t)$ to represent the value of the *CPPI floor* at time t. This allows us to study cases where this reference value behaves independently of the risk-free asset. The values of the CPPI floor at each observation time are defined contractually; $F_T \equiv F(T)$ represents the guaranteed amount of the CPPI claim at maturity.

For convenience, we employ the following notation:

- $S^{k^-} \equiv S(t_{\mathrm{o}}^{k} - \epsilon)$ to represent the risky asset exposure at the instant before reallocation;
- $S^{k} \equiv S(t_{\mathrm{o}}^{k})$ to represent the risky asset exposure at the instant of (re)allocation;
- $S^{k^+} \equiv S(t_{\mathrm{o}}^{k} + \epsilon)$ to represent the risky asset exposure at the instant after (re)allocation.

The same conventions apply to t_{o}^{k}, B, W and F. However, $F^{k^-} = F^{k} = F^{k^+}$ since F is contractually defined and is not affected by reallocation.

2.1.2 State space

In this work we use the ordered pair (S,B) to represent the composition (or *state*) of the CPPI portfolio at any given time. Since the strategies we will consider prohibit short stock positions but do allow borrowing money, our *state space* is situated within

$$\Omega \equiv \Big\{(S,B) \in \mathbb{R}_{\geq 0} \times \mathbb{R}\Big\}.$$

Our objective can now be stated as determining the $t=0$ value for the functions $V_I(S,B,t)$ and $V_L(S,B,t)$, respectively representing the risk-neutral value of a CPPI claim to an investor and the risk-neutral liability of this claim to the guarantor. Apart from the payoffs introduced in Section 2.3 and the boundary conditions of Section 3.2, these claims behave identically, and thus in the following sections we will often treat them collectively as V. Later in this chapter we will show a parity relationship between these two functions, so that it is only necessary to compute one of them.

Remark 2.1.1. Our choice of state variables is natural and intuitive for describing this problem, but there are other, less apparent alternatives that simplify computation. Indeed, in Section 2.5 we will apply a state space transformation for this very reason.

In some special cases it is possible to use a scalar state variable; other authors track the cushion process $(S(t) + B(t) - F(t))$ and the discounted cushion process [15]. The tradeoff is that it is no longer straightforward to impose important position-dependent features such as borrowing restrictions and local volatilities. ■

2.2 Discrete-time reallocation strategies

We complete our discrete-time CPPI model by describing how portfolio compositions are altered at each reallocation. In the literature equations of this type are called *jump conditions*. It is these dynamics that characterise the CPPI strategy. In addition to the classical CPPI, we will also develop jump conditions for a variant with borrowing restrictions. The following introductory observations are common to both flavours of CPPI claim.

When executing a discrete-time CPPI strategy, the observation instants $\left\{t_{\mathrm{o}}^{k}\right\}_{k=0}^{K}$ are met in ascending order, and the asset allocation at each t_{o}^{k+} is a result of the state at t_{o}^{k-}. However, using a dynamic programming approach to price a CPPI-backed capital guarantee, we solve the problem backwards in time from T, and thus these observation events are met in descending order. Therefore the values of the pricing function V at t_{o}^{k-} depend on the information at t_{o}^{k+}.

The discrete-time strategy, as we model it, prescribes what amount of the total wealth should be invested in each of the assets. In practice, these proportions would be converted into the number of units to be held for each asset. These values are calculated using the spot prices at t_{o}^{k}, and then held constant until t_{o}^{k+1}. In contrast, the portfolio value will fluctuate over this interval, and it is this that necessitates reapplication of the control strategy. It is assumed permissible to hold each asset in any quantity, including fractional units.

The self-financing condition, along with the assumptions that rebalancing is achievable (i) instantaneously without affecting the market price, and (ii) without transaction costs, implies that wealth is conserved at each allocation adjustment. We express this symbolically as

$$W^{k^-} = W^k = W^{k^+}, \tag{2.2.1}$$

or alternatively as

$$B^{k^-} + S^{k^-} = B^{k^+} + S^{k^+}. \tag{2.2.2}$$

Moreover, the value of a claim written on a wealth-preserving instrument should also remain unchanged across rebalancing instants. We therefore have the general jump condition

$$V(S^{k^-}, B^{k^-}, t_{\mathrm{o}}^{k^-}) = V(S^{k^+}, B^{k^+}, t_{\mathrm{o}}^{k^+}).$$

CPPI strategies prescribe a portfolio reallocation to the state (S^{k^+}, B^{k^+}) based on the old state (S^{k^-}, B^{k^-}), for each reallocation instant t_{o}^k. A significant consequence of this is that only the information on the *(re)allocation locus* $\left\{(S^{k^+}, B^{k^+})\right\}$ is propagated backwards in time at t_{o}^k—all other information is discarded. This does not mean that we can ignore all other states in Ω, since the inter-observation dynamics will still require this information (as will be seen in Section 2.5). However, in solving the system at $t_{\mathrm{o}}^{k^+}$, we want our calculations to achieve the highest accuracy on the k^{th} allocation locus, and this requires knowing the shapes of the loci in this family. The next section explains and examines S^{k^+} and B^{k^+} for the classical CPPI claim. The section after that will repeat the analysis for a CPPI variant where borrowing is restricted.

2.2.1 Classical discrete-time CPPI jump conditions

Recall from Section 1.1 that the new risky-asset exposure S^{k^+} depends on the state of the *cushion*—the surplus portfolio wealth $W^k = S^{k^-} + B^{k^-}$ with reference to the prevailing CPPI floor value, F^k. So, formally stated, the cushion value used to make the reallocation decision at time $t_{\mathrm{o}}^{k^+}$ is the quantity $(W^k - F^k)$. Based on this, a portfolio following the classical CPPI strategy falls in one of two classes.

In the *positive-cushion* case, S^{k^+} is set proportional to the cushion by a leverage factor $m > 1$. Since the strategy is intended to be self-financing, excess wealth (or debt) is allocated to B^{k^+}. This yields

$$\begin{cases} S^{k^+} = m(W^k - F^k) \\ B^{k^+} = W^k - S^{k^+} \end{cases} .$$

This strategy will typically result in a position in S that is larger than the current portfolio value, thus necessitating a negative position in B. This represents borrowing.

If, on the other hand, the cushion is negative then all wealth is invested in B. In this case, the prescribed reallocation is given by

$$\begin{cases} S^{k^+} = 0 \\ B^{k^+} = W^k \end{cases} .$$

Combining these cases results in the following sequence of mappings, at (re)allocation instants t_o^0 through t_o^K, and for all states (S, B) in Ω, setting $W^0 = W_0$:

$$\begin{cases} V(S^{k^-}, B^{k^-}, t_\text{o}^{k^-}) & = V(S^{k^+}, B^{k^+}, t_\text{o}^{k^+}) \\ W^k & = S^{k^-} + B^{k^-} \\ S^{k^+} & = m \cdot \max\left\{W^k - F^k, 0\right\} \\ B^{k^+} & = W^k - S^{k^+} \end{cases} . \tag{2.2.3}$$

As a consequence of (2.2.3), at any reallocation instant t_o^k, all discrete-time CPPI portfolios with the same wealth W^k will be rebalanced to the same CPPI-prescribed portfolio, also worth W^k. A case-wise manipulation of (2.2.3), substituting (2.2.1) and (2.2.2), yields the following characterisation of the jump condition mappings' images:

$$\begin{aligned} \mathcal{A}^k &\equiv \mathcal{A}_|^k \cup \mathcal{A}_\backslash^k, \qquad (2.2.4) \\ \text{where } \mathcal{A}_|^k &\equiv \left\{ \left(S^{k^+}, B^{k^+}\right) \,\middle|\, S^{k^+} = 0,\ B^{k^+} < F^k \right\} \\ \text{and } \mathcal{A}_\backslash^k &\equiv \left\{ \left(S^{k^+}, B^{k^+}\right) \,\middle|\, S^{k^+} > 0,\ B^{k^+} = F^k - \tfrac{m-1}{m} S^{k^+} \right\}. \end{aligned}$$

We will call (2.2.3) the k^{th} *classical reallocation mapping*, denoted by $f^k : \Omega \to \mathcal{A}^k$.

A representative example of the locus $\mathcal{A}^k$ is illustrated in Figure 2.1. The vertical segment $\mathcal{A}_|^k$ corresponds to the negative-cushion states, and the oblique segment $\mathcal{A}_\backslash^k$ corresponds to positive-cushion states following the normal CPPI allocation strategy. The arrows illustrate

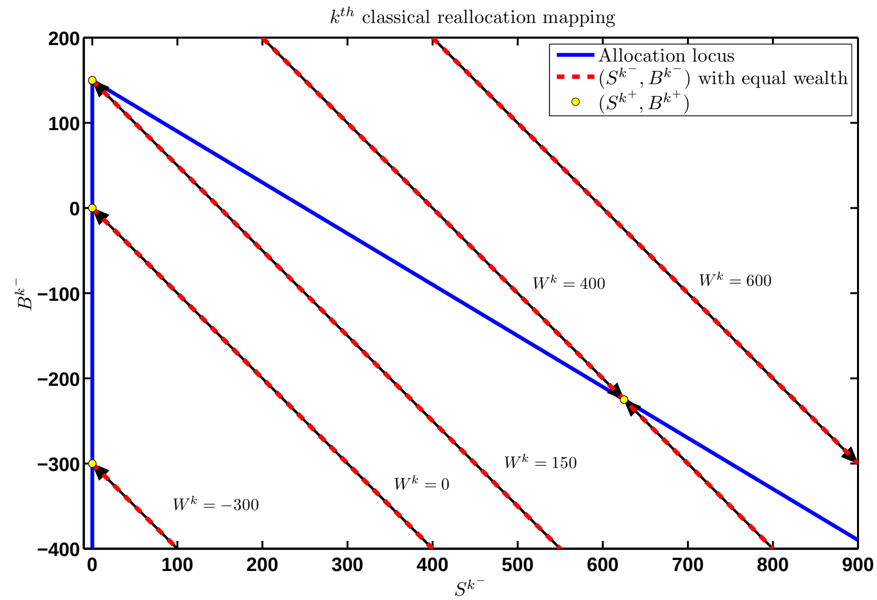

Figure 2.1: Image of a typical classical reallocation mapping, for $F^k = 150$ and $m = 2.5$. Portfolios with $W = 600$ reallocate to $(1125, -525)$ which is not shown.

that portfolios of the same wealth are reallocated identically. Portfolios (S^{k^-}, B^{k^-}) with wealth greater than F^k and below the oblique segment are rebalanced so that a smaller proportion of the wealth is allocated to the risky asset. Conversely, portfolios situated above the oblique segment are rebalanced to take on increased risk. A property of this strategy is that short stock positions are not prescribed. Furthermore, risk-free positions worth more than the prevailing CPPI floor value are not attainable at the instant of rebalancing, although they may later exceed the CPPI floor through appreciation.

Further examination of Figure 2.1 reveals that any portfolio (S^{k^-}, B^{k^-}) with wealth greater than 510 will reallocate to a portfolio outside the bounds of this plot[1]. As will be seen in Section 3.5, a qualification of our numerical algorithm (stemming from our model in Section 2.4.4) is that solving for a portfolio on $\mathcal{A}^k$ requires information from the region above $\mathcal{A}^k$. Hence, iteratively applying these forward mappings causes our analytical domain of dependence to grow unboundedly. One workaround is presented in Section 3.3.2, involving a special-case relation between portfolio values. Another option is to impose an

[1]More precisely, f^k is an *expansive mapping* (in an L^2 sense) when restricted to the region above $\mathcal{A}^k$. This can be verified using Figure 2.1 and geometric arguments.

artificial *borrowing limit* (i.e. a lower bound) on the amount that can be borrowed.

2.2.2 Limited-borrowing discrete-time CPPI jump conditions

For this variant on the classical CPPI strategy the contract is modified so that there is a lower bound $\hat{B}^k$ on the CPPI-prescribed risk-free position B^{k^+}. If $\hat{B}^k$ does not vary with k, then the borrowing limit is *fixed*. Otherwise, the borrowing limit is *variable*. As a special case of the latter, the borrowing limit is *floating* if $F^k - \hat{B}^k$ does not vary with k. Note that $\hat{B}^k$ only makes financial sense if it is less than F^k. A negative value of $\hat{B}^k$ corresponds to a borrowing limit.

There are two reasons why this modification is an improvement over the classical CPPI contract. Firstly, limiting leverage has value from regulatory and risk management standpoints. For example, laws exist that prohibit capital guarantees written on a mutual fund from exceeding 100% equity exposure [36]. This corresponds to a fixed borrowing limit of $\hat{B} = 0$. Secondly, while this mapping still has subdomains in which it is expansive, we are now able to design our grid to offset this effect. We will return to this point in the next chapter.

The result of imposing this restriction on (2.2.3) is the following sequence of mappings, at (re)allocation instants t_o^0 through t_o^K, and for all states (S, B) in Ω, setting $W^0 = W_0$:

$$\begin{cases} V(S^{k^-}, B^{k^-}, t_o^{k^-}) & = V(S^{k^+}, B^{k^+}, t_o^{k^+}) \\ W^k & = S^{k^-} + B^{k^-} \\ B^{k^+} & = \max\left\{W^k - m \cdot \max\left\{W^k - F^k, 0\right\}, \hat{B}^k\right\} \\ S^{k^+} & = W^k - B^{k^+} \end{cases} . \tag{2.2.5}$$

The image of of this mapping is shown in Figure 2.2 and is described by the k^{th} *limited-borrowing allocation locus*,

$$\begin{aligned} \hat{\mathcal{A}}^k \equiv \quad & \left\{\left(S^{k^+}, B^{k^+}\right) \middle| \, S^{k^+} = 0,\ B^{k^+} \in [\hat{B}^k, F^k]\right\} \\ & \bigcup \left\{\left(S^{k^+}, B^{k^+}\right) \middle| \, S^{k^+} \in [0, \varsigma^k],\ B^{k^+} = F^k - \tfrac{m-1}{m} S^{k^+}\right\} \\ & \bigcup \left\{\left(S^{k^+}, B^{k^+}\right) \middle| \, S^{k^+} > \varsigma^k,\ B^{k^+} = \hat{B}^k\right\}, \end{aligned} \tag{2.2.6}$$

where

$$\varsigma^k \equiv \tfrac{m}{m-1}\left(F^k - \hat{B}^k\right)$$

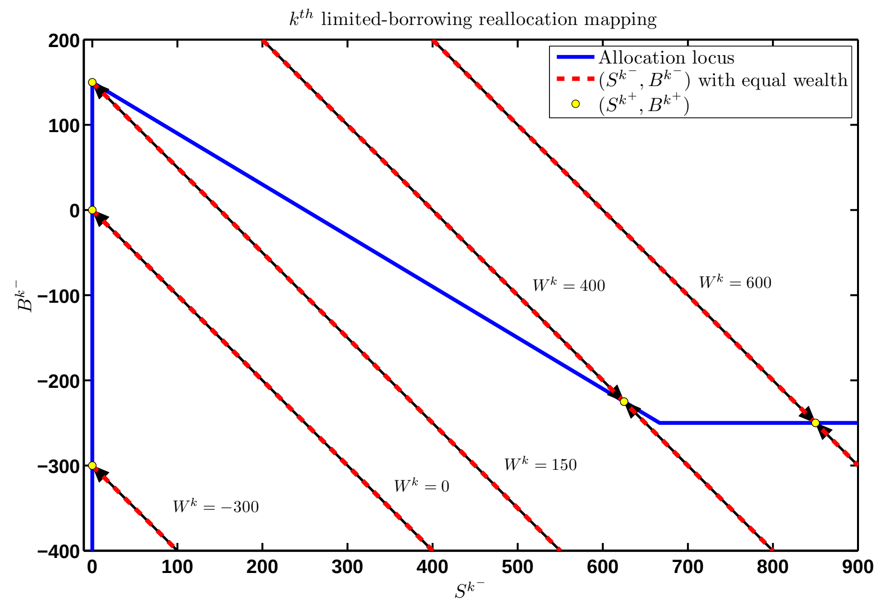

Figure 2.2: Image of a typical limited-borrowing reallocation mapping, for $F^k = 150$, $\hat{B}^k = -250$ and $m = 2.5$.

is the risky-asset exposure at which the limited-borrowing strategy deviates from the classical strategy. We will call this mapping the k^{th}*limited-borrowing reallocation mapping* $\hat{f}^k : \Omega \to \hat{\mathcal{A}}^k$.

2.3 Payoffs

Having modelled the discrete-time CPPI strategy, we are now able to characterise a CPPI-based capital guarantee.

An investor holding a CPPI claim is guaranteed at least F_T at time T, so their payoff is

$$\begin{aligned} V_I(S, B, T) &= \max\{S + B, F_T\} \\ &= \max\{S - (F_T - B), 0\} + F_T. \end{aligned} \tag{2.3.1}$$

Likewise, an institution issuing a CPPI claim has a liability of

$$\begin{aligned} V_L(S,B,T) &= -\max\{F_T - S - B, 0\} && (2.3.2)\\ &= -\max\{(F_T - B) - S, 0\}. && (2.3.3) \end{aligned}$$

Offering the insured aspect of a capital guarantee (i.e. an instrument with payoff (2.3.2)) is equivalent to having a short position in a European put option written on the CPPI portfolio with strike price F_T. Cont and Tankov [15] call (2.3.3) a *CPPI-embedded option* and, like Cipollini [13], explore the hedging relationship between this and a sequence of forward vanilla puts.

In our implementation, we exploit the fact that for each fixed value of B (a row of the state space Ω), Equation (2.3.3) is the payoff of a vanilla European put with strike $F_T - B$. Correspondingly, (2.3.1) is that of a European call with the same strike, along with a zero-coupon bond with maturity F_T.

We conclude with a result that shows the problem need only be solved for one of the payoffs.

Proposition 2.3.1 (CPPI parity result)**.** *A relationship akin to put-call parity exists for* V_I *and* V_L*:*

$$V_I(S,B,t) + V_L(S,B,t) = S(t) + B(t), \tag{2.3.4}$$

and most importantly,

$$V_I(S,B,0) + V_L(S,B,0) = S(0) + B(0) = W_0. \tag{2.3.5}$$

Proof. We start with the observation (using (2.3.1) and (2.3.3)) that

$$V_I(S,B,T) + V_L(S,B,T) = S(T) + B(T).$$

Intuitively, this is justified by noting that any investor who holds a capital guarantee on a CPPI product and has issued an identical guarantee on the same product is left with an unprotected CPPI-managed portfolio. At maturity this unprotected portfolio is worth the sum of its components, so the risk-neutral expected value of this portfolio at time t_{o}^{K+} is simply the sum of the time–t_{o}^{K+} values of its components. Under the risk-neutral measure, both components of the CPPI portfolio are martingales, hence

$$V_I(S,B,t_{\text{o}}^{K+}) + V_L(S,B,t_{\text{o}}^{K+}) = S(t_{\text{o}}^{K+}) + B(t_{\text{o}}^{K+}).$$

Moreover, since the CPPI jump conditions (Section 2.2) are wealth-preserving,

$$V_I(S, B, t_o^{K-}) + V_L(S, B, t_o^{K-}) = S(t_o^{K-}) + B(t_o^{K-}). \tag{2.3.6}$$

The final result is obtained by repeatedly applying this reasoning, descending in k. ■

2.4 Dynamics between observations

Until now our approach has been independent of the underlying asset dynamics. However, we cannot proceed further without committing to models for the two portfolio assets and the CPPI floor value's trajectory. From these we model the dynamics of the CPPI claim between observations.

2.4.1 Risky asset dynamics

We model the risky asset process (under the risk-neutral measure $\mathbb{Q}$) as a geometric Brownian motion with finite-intensity jumps [35]

$$\frac{\mathrm{d}S_t}{S_{t^-}} = (r_t - \lambda\kappa)\,\mathrm{d}t + \sigma(S_t^-, t)\,\mathrm{d}Z_t + (J_t - 1)\,\mathrm{d}q_t, \tag{2.4.1}$$

where

S_{t^-}	is the previous state,
r_t	is the 'risk-free' interest rate
λ	is the jump frequency,
κ	is $\mathrm{E}^{\mathbb{Q}}\{J_t - 1\}$,
σ	is the local volatility,
J_t	belongs to a sequence of independent and identically distributed (*iid*) random variables representing jump intensity,
$\mathrm{d}Z_t$	is a Wiener process increment, and
$\mathrm{d}q_t$	is a Poisson process increment with jump probability λ.

For simplicity we exclude dividends in our model and we follow the common assumption that J_t and dq_t are independent. Additionally, λ and J_t are both modelled as time-homogeneous: λ is constant and J_t is stationary.

Since we are using the risk-neutral measure, λ and J_t (and therefore $\mathrm{d}q_t$ and κ) are market-calibrated quantities. More precisely, λ and the parameters characterising J_t's distribution must all be fitted to prevailing market data. The $\lambda\kappa$ term compensates the processes' drift rate for jumps, so that the risk-neutral expectation for $\frac{\mathrm{d}S_t}{S_t}$ grows at the risk-free rate:

$$\begin{aligned}\mathrm{E}^{\mathbb{Q}}\left\{\frac{\mathrm{d}S_t}{S_{t^-}}\right\} &= \left(\mathrm{E}^{\mathbb{Q}}\left\{r_t\right\} - \lambda\kappa\right)\mathrm{d}t + \mathrm{E}^{\mathbb{Q}}\left\{J_t - 1\right\}\mathrm{E}^{\mathbb{Q}}\left\{\mathrm{d}q\right\} \\ &= \left(\mathrm{E}^{\mathbb{Q}}\left\{r_t\right\} - \lambda\kappa\right)\mathrm{d}t + \kappa\lambda\,\mathrm{d}t \\ &= \mathrm{E}^{\mathbb{Q}}\left\{r_t\right\}\,\mathrm{d}t.\end{aligned}$$

If $\lambda = 0$ then the jump component vanishes and we have a regular geometric Brownian motion. Typically J is assumed to be lognormally-distributed [35, 3], with density

$$p(J) = \frac{\exp\left(-\frac{(\ln(J)-\mu)^2}{2\gamma^2}\right)}{\sqrt{2\pi}\gamma J}, \tag{2.4.2}$$

so that $\ln J$ is normally-distributed with mean μ and variance γ^2. In this situation we have $\kappa = e^{\mu+\frac{1}{2}\gamma^2} - 1$. Calibration details are given in [3]. A popular alternative is the double-exponential density proposed by Kou [30]. Indeed, our framework is general enough to accommodate any choice of density function.

More generally, jump diffusions are modelled as Lévy processes, which are studied in a CPPI context in [15] but will not be addressed here. We also exclude stochastic volatility from our model because this would add another dimension to our state space and make our framework too computationally taxing for practical use. Instead, our framework accommodates volatility surfaces, as was done in [47].

2.4.2 Risk-free asset dynamics

The interest rate governing the process B_t will in practice behave stochastically. However, for the same dimensionality reasons as above, we restrict our risk-free interest rate model to a deterministic function, $r(t)$. The risk-free asset therefore follows

$$\frac{\mathrm{d}B_t}{B_{t^-}} = r(t)\,\mathrm{d}t, \tag{2.4.3}$$

which has the unique solution

$$B(t) = B(\bar{t}) \cdot \exp\left(\int_{\bar{t}}^{t} r(u)\,\mathrm{d}u\right)$$

for some fixed reference time $\bar{t}$. For convenience we define

$$\rho_k^{k+1} \equiv \exp\left(\int_{t_\mathrm{o}^k}^{t_\mathrm{o}^{k+1}} r(u)\,\mathrm{d}u\right) \tag{2.4.4}$$

to represent the appreciation of the risk-free asset between reallocation events.

2.4.3 CPPI floor dynamics

The flexibility of this framework allows us to use any deterministic function $F(t)$ to describe the CPPI floor dynamics. Furthermore, F need only be defined for each observation instant t_o^k, thus allowing the function to be defined tabularly. Financially, it makes the most sense for F to be monotonically increasing in t_o^k. Another constraint is that $F(T) = F_T$. For our analysis we will assume this function is of the form

$$F(t) = F_T \cdot \exp\left(-\int_{t}^{T} \varrho(u)\,\mathrm{d}u\right),$$

where $\varrho(t)$ is any positive-valued function (typically chosen to be constant). When $\varrho \neq r$, the CPPI floor value is said to be *autonomous* or independent of the risk-free rate.

Remark 2.4.1 (Effect of independent floors on the CPPI strategy)**.** When $\varrho(t) \geq r(t)$ for all t, a portfolio experiencing a shortfall at time t_o^k can be considered *knocked-out* since there is never any possibility—under either the classical or limited-borrowing CPPI strategies—of the portfolio reverting to a positive-cushion state over the interval $(t_\mathrm{o}^k, T]$.

However, we are careful to distinguish between a portfolio being negative-cushion and knocked-out; under our formulation it *is* possible for a negative-cushion portfolio to eventually re-achieve positive-cushion status, such as when $\varrho(t) < r(t)$ for all t (a capital guarantee with this feature has more downside than an investment in a risk-free bond). Our CPPI jump conditions should therefore be considered *nonabsorbing*. The conversion to the absorbing case is straightforward. ■

2.4.4 CPPI claim dynamics

Applying Itō's lemma and a hedging argument for systematic jump risk [21] yields the following partial integro-differential equation (PIDE):

$$\begin{aligned}\frac{\partial V}{\partial t} &= -\left(\mathcal{L}+\mathcal{J}\right)V - r(t)B\frac{\partial V}{\partial B}, \\ \text{where } \mathcal{L}V &\equiv \frac{1}{2}\sigma(S,t)^2 S^2\frac{\partial^2 V}{\partial S^2} + \big(r(t)-\lambda\kappa\big)S\frac{\partial V}{\partial S} - \big(r(t)+\lambda\big)V, \\ \text{and } \mathcal{J}V &\equiv \lambda\int_0^\infty V(JS,B,t)p(J)\,\mathrm{d}J \\ \text{for } t &\in \bigcup_{k=0}^{K}\left(t_{\mathrm{o}}^{k}, t_{\mathrm{o}}^{(k+1)}\right).\end{aligned} \tag{2.4.5}$$

This formulation may therefore be viewed as a sequence of cascading 2D PIDEs. Connecting these PIDE stages are jump conditions (Section 2.2), applied at each t_{o}^{k}. A payoff (Section 2.3) is applied as a *terminal condition* at t_{o}^{K+1}. We will refer to the interval $\left(t_{\mathrm{o}}^{k}, t_{\mathrm{o}}^{(k+1)}\right)$ as the k^{th} *stage* of the inter-observation dynamics.

2.5 Deferred-interest state space transformation

Linear PIDEs such as Equation (2.4.5) are challenging to solve numerically in one spatial dimension—let alone two—because of the nonlocal nature of the integral term. A survey of techniques for solving 1D PIDEs arising in finance is provided in Chapter 12 of [14].

As noted in Section 2.2, at t_{o}^{k+} we are chiefly concerned with solving (2.4.5) along $\mathcal{A}^k$ (or in the limited-borrowing case, $\hat{\mathcal{A}}^k$), for each k. Moreover, each of these loci is comprised of a low number of line segments or rays. Our problem would therefore simplify conveniently if we had a transformation that could reduce (2.4.5) to a finite system of 1D PIDEs, with one equation for each piece of the allocation locus. However, such a transformation comes at the expense of generality. For example, a new coordinate system with origin at $(S,B)=(0,F^k)$, aligned with the two pieces of the classical allocation locus will fail to simplify (2.4.5) if F does not evolve at the risk-free rate.

The best we can do (while still retaining a degree of generality) is to reformulate the PIDE in Equation (2.4.5) as a system of infinitely many 1D PIDEs embedded in a 2D state space. Our approach is inspired by the usefulness of semi-Lagrangian discretisations in pricing Asian options [38, 17]. This technique originates in the meteorological literature and was developed to counteract numerical problems arising from overlapping reference frame trajectories (see Sections 14.3 and 14.12 of [11]). However, as will be seen, the deterministic B dynamics are simple enough that discretisation is not necessary in order to rewrite (2.4.5) in a more convenient form. Instead, we will transform the system, and then later discretise each 1D PIDE individually. The following should therefore be thought of as a fully Lagrangian state space transformation, rather than as a discretisation. The transformation does not depend on our choice of jump conditions.

In order to reduce the number of spatial dimensions in (2.4.5), we use the Lagrangian derivative. Unlike the partial derivative $\frac{\partial V}{\partial t}$, which measures the rate of change of a quantity at a stationary observation point (a Eulerian frame of reference), the Lagrangian derivative $\frac{\mathrm{D}V}{\mathrm{D}t}$ is a total derivative describing a rate of change observed with a moving reference frame.

For clarity we introduce and prove our result here, and show the details of its application in the next section. Henceforth, the notation v^k will represent the reformulation of V over $\left(t_{\mathrm{o}}^{k^-}, t_{\mathrm{o}}^{(k+1)^-}\right)$.

Proposition 2.5.1 (Lagrangian reformulation)**.** *These two formulations are equivalent:*

- *the CPPI claim dynamics of Section 2.4.4 (a sequence of 2D PIDEs), with the jump conditions of Section 2.2;*
- *the following interest-deferred dynamics (a sequence of B-parameterised 1D PIDE systems) with the system for each stage k (corresponding to $\left(t_{\mathrm{o}}^{k^+}, t_{\mathrm{o}}^{(k+1)^-}\right)$) defined by*

$$\frac{\partial v^k(S,\tau;B)}{\partial \tau} = (\mathcal{L}_k + \mathcal{J}_k)v^k(S,\tau;B), \tag{2.5.1}$$

$$\begin{aligned} \textit{where } \mathcal{L}_k v^k &\equiv \frac{1}{2}\left[\sigma(S, t_{\mathrm{o}}^{k+1}-\tau)\right]^2 S^2 \frac{\partial^2 v^k}{\partial S^2} + \big(r(t_{\mathrm{o}}^{k+1}-\tau) - \lambda\kappa\big) S \frac{\partial v^k}{\partial S} \\ &\qquad - \big(r(t_{\mathrm{o}}^{k+1}-\tau) + \lambda\big) v^k, \\ \textit{and } \mathcal{J}_k v^k &\equiv \lambda \int_0^\infty v^k(JS,\tau;B)p(J)\,\mathrm{d}J \\ \textit{for } \tau &\in \left(0, t_{\mathrm{o}}^{k+1} - t_{\mathrm{o}}^{k}\right), \end{aligned} \tag{2.5.2}$$

and with the jump conditions of Section 2.2 modified so that

$$W^k \equiv S^{k^-} + \rho_{k-1}^k B^{k^-}.$$

Consequently, solving on Ω requires solving a family of one-dimensional PIDEs parameterised by B.

In the literature it is customary to use τ to represent the *backwards time*, or time until maturity (at T). Our usage differs; we instead use τ to represent the time until the next t_o^k.

Financially, Equation (2.5.2) can be interpreted as deferring the payment of interest accrued by the risk-free asset over $\left(t_\mathrm{o}^k, t_\mathrm{o}^{k+1}\right)$ until the end of this interval, at the last instant before the rebalancing decision is made.

Proof of Proposition 2.5.1. The following applies to the k^{th} stage of Equation (2.4.5), for t in $\left(t_\mathrm{o}^{k^+}, t_\mathrm{o}^{(k+1)^-}\right)$. We address the PIDE and jump conditions separately.

Part I: PIDE transformation

Without loss of generality, consider the trajectory $\phi(t) = (\phi_1(t), \phi_2(t))$ with the departure point

$$\phi(t_\mathrm{o}^{k^+}) = (S^\star, B^\star).$$

Along this trajectory, the Lagrangian derivative for $V(S, B, t)$ is

$$\frac{\mathrm{D}V}{\mathrm{D}t} = V_t + V_S \frac{\mathrm{d}\phi_1}{\mathrm{d}t} + V_B \frac{\mathrm{d}\phi_2}{\mathrm{d}t}. \tag{2.5.3}$$

Combining (2.4.5) with (2.5.3) and choosing $\phi(t)$ to satisfy

$$\frac{\mathrm{d}\phi}{\mathrm{d}t} = (0, r(t)B), \tag{2.5.4}$$

the PIDE of interest becomes

$$\frac{\mathrm{D}V}{\mathrm{D}t} = -(\mathcal{L} + \mathcal{J})V. \tag{2.5.5}$$

Equation (2.5.4) has the unique solution

$$\phi(t) = \left(S^\star, \exp\left(\int_{t_\mathrm{o}^{k^+}}^t r(u)\, du\right) B^\star\right). \tag{2.5.6}$$

This development shows that the B dynamics can be entirely removed from our PIDE. However, the variable B cannot be discarded from our state space: B still arises in the jump conditions, so we need to retain it as a parameter in order to distinguish between Lagrangian trajectories.

Applying the transformation $\tau \equiv t_{\text{o}}^{(k+1)^-} - t$ to Equation (2.5.5) yields Equation (2.5.1).

Part II: Interest-deferred jump conditions

By construction we have, for all times t in $\left(t_{\text{o}}^k, t_{\text{o}}^{k+1}\right)$,

$$v^k\left(S, t_{\text{o}}^{(k+1)^-} - t; B\right) = V\left(S, \exp\left(\int_{t_{\text{o}}^{k^+}}^{t} r(u)\, du\right) B, t\right).$$

This holds since both sides of this equation are equivalent representations for the value of a portfolio with composition $\left(S, \exp\left(\int_{t_{\text{o}}^{k^+}}^{t} r(u)\, du\right) B\right)$ at time t. In particular, we have

$$v^k(S, 0; B) = V(S, \rho_k^{k+1} B, t_{\text{o}}^{(k+1)^-}) \tag{2.5.7}$$

and

$$v^k(S, t_{\text{o}}^{(k+1)^-} - t_{\text{o}}^{k^+}; B) = V(S, B, t_{\text{o}}^{k^+}) \tag{2.5.8}$$

at the endpoints of the k^{th} stage. Equations (2.5.7) and (2.5.8) tell us that in order to solve for $V(S^\star, B^\star, t_{\text{o}}^{k^+})$, we should solve the related 1D PIDE (2.5.1) for $v^k(S^\star, t_{\text{o}}^{(k+1)^-} - t_{\text{o}}^{k^+}; B^\star)$, with initial conditions for the $B = B^\star$ horizontal strip given by $v^k(S, 0; B^\star) = V(S, \rho_k^{k+1} B^\star, t_{\text{o}}^{(k+1)^-})$. Since the ρ_k^{k+1} factor is common to each strip, it can instead be incorporated into the jump conditions, replacing B^{k^-} with $\rho_{k-1}^{k} B^{k^-}$ in the calculation of W^k. ■

Remark 2.5.2. In Part I of the preceding proof we assigned reference frames to each point in Ω at $t_{\text{o}}^{k^+}$, and then moved each reference frame—from its individual starting point—exponentially in the B direction at the prevailing risk-free rate. The trajectory of each reference frame depended on the initial B ordinate and was independent of S. We therefore chose to group portfolios by their initial B ordinate. Financially, this amounts to identifying each portfolio at time $t \in (t_{\mathrm{o}}^{k}, t_{\mathrm{o}}^{k+1})$ by its risky position at t and its risk-free position at $t_{\mathrm{o}}^{k^+}$. We could just as well have chosen the opposite convention, since by the exponential nature of (2.5.6) there is a bijective relationship between trajectories' states at $t_{\mathrm{o}}^{(k+1)^-}$ and $t_{\mathrm{o}}^{k^+}$. ■

This Lagrangian reformulation has transformed the problem from a PIDE in two spatial dimensions to a system of PIDEs in one spatial dimension. Information is only passed between the PIDEs at the reallocation instants. The system is therefore decoupled and each element can be solved using a one-dimensional PIDE solver. For our implementation we adapt the framework described in [22].

2.6 Framework summary

We conclude this chapter with a dynamic programming algorithm for solving this problem with systems of 1D PIDEs:

1. Initialisation.
   (a) For each row (parameterised by B), compute $v^K(S,0;B)$ using the payoff
   $$v_I^K(S,0;B) \equiv \max\left\{S - (F_T - \rho_K^{K+1} B), 0\right\} + F_T \;, \tag{2.6.1}$$
   to value the claim from the investor's perspective, or
   $$v_L^K(S,0;B) \equiv -\max\left\{(F_T - \rho_K^{K+1} B) - S, 0\right\} \tag{2.6.2}$$
   from the guarantor's perspective;
   (b) Set $k = K$.
2. Iteration.
   (a) (*Working backwards from $t_{\mathrm{o}}^{(k+1)^-}$ to $t_{\mathrm{o}}^{k^+}$*) For each row (parameterised by B), determine $v^k(S, t_{\mathrm{o}}^{(k+1)^-} - t_{\mathrm{o}}^{k^+}; B)$ by solving
   $$(v^k)_\tau = (\mathcal{L}_k + \mathcal{J}_k)\, v^k \tag{2.6.3}$$
   backwards in time from $t_{\mathrm{o}}^{(k+1)^-}$ to $T - t_{\mathrm{o}}^{k^+}$, using the values computed for $v^k(S,0;B)$ as the initial condition;

(b) (*Working backwards from $t_o^{k^+}$ to $t_o^{k^-}$*) For each row (parameterised by B), determine $v^{(k-1)}(S, 0; B)$ by applying the jump conditions

$$\begin{cases} v^{(k-1)}(S^{k^-}, 0; B^{k^-}) & = v^k(S^{k^+}, t_o^{(k+1)^-} - t_o^{k^+}; B^{k^+}) \\ W^k & = S^{k^-} + \rho_{k-1}^k B^{k^-} \\ S^{k^+} & = m \cdot \max\left\{W^k - F^k, 0\right\} \\ B^{k^+} & = W^k - S^{k^+} \end{cases} \tag{2.6.4}$$

for the classical CPPI case, or

$$\begin{cases} v^{(k-1)}(S^{k^-}, 0; B^{k^-}) & = v^k(S^{k^+}, t_o^{(k+1)^-} - t_o^{k^+}; B^{k^+}) \\ W^k & = S^{k^-} + \rho_{k-1}^k B^{k^-} \\ B^{k^+} & = \max\left\{W^k - m \cdot \max\{W^k - F^k, 0\}, \hat{B}^k\right\} \\ S^{k^+} & = W^k - B^{k^+} \end{cases} \tag{2.6.5}$$

for the limited-borrowing CPPI case;

3. Repeat step 2 for each stage k, descending from (K–1) to 0 inclusive, where $W^0 \equiv W_0$.

4. Report the solution $v^0(W_0, t = 0) \equiv v^0(S^0, t_o^{1^-} - t_o^{0^+}; B^0)$, where $S^0 + B^0 = W_0$.

So, solving such a system with K rebalancing events requires K+1 stages and K+1 grids. Note that the expression for W^0 does not involve a discount factor (since no interest has accrued yet), but all subsequent wealth calculations do.

Remark 2.6.1. Depending on the PIDE solver, it may be more suitable to calculate v_I using the related payoff

$$v_J^K(S, 0; B) \equiv \max\left\{S - (F_T - \rho_K^{K+1} B), 0\right\} = v_I^K(S, 0; B) - F_T \tag{2.6.6}$$

in the above algorithm. The desired final result is recovered by linearity:

$$v_I^0(W_0, t = 0) = v_J^0(W_0, t = 0) + \rho_{K+1}^0 F_T. \tag{2.6.7}$$

This is the approach that we take when generating our results in Chapter 5.

The corresponding parity result is

$$v_L^0(W_0, t = 0) = W_0 - \rho_{K+1}^0 F_T - v_J^0(W_0, t = 0). \tag{2.6.8}$$

In the special case where $\varrho = r$, the sum of $v_L^0(W_0, t = 0)$ and $v_J^0(W_0, t = 0)$ is the CPPI cushion. ∎

3 Discretisation and convergence properties

Having formulated the CPPI pricing problem, we turn our attention towards solving it computationally. A computational approach offers the greatest versatility but cannot be directly applied to the continuous-domain formulation summarised in Section 2.6; the problem must first be discretised. This involves

- selecting a bounded, finite computational domain for our calculations (Section 3.1),
- imposing boundary conditions for situations when the inter-observation numerical scheme (Section 3.2) and the reallocation jump conditions (Section 3.3) require information outside of the computational domain,
- choosing an interpolation scheme for when the reallocation jump conditions require data in between grid points (Section 3.4), and
- choosing a numerical scheme to approximate the inter-observation dynamics (Section 3.5).

In addition, we examine the stability (Section 3.6.1) and monotonicity (Section 3.6.2) of our chosen discretisation. These two properties are imperative for any numerical implementation and are intermediate steps towards proving that the discretisation converges to the continuous-domain formulation's financially relevant solution.

3.1 Computational domain

Analytically, this problem has an infinite domain of dependence because of the integral term in Equation (2.6.3) and the expansive nature of the reallocation mappings. For computational purposes it is necessary to localise the problem to a bounded, finite computational domain. As will be seen, some bounds arise naturally and others must be artificially imposed.

We propose a computational domain that is a sequence of $K + 1$ structured grids in (S, B) space. The k^{th} *grid* applies to the k^{th} stage of the PIDE solve (Section 2.6) and exists for the time interval $(t_{\text{o}}^{k^+}, t_{\text{o}}^{(k+1)^-})$. The k-varying aspect of these grids is a departure from the fixed grids used in related studies (such as [48, 17, 47, 5]). It arises because the CPPI floor value F^k changes at each reallocation.

Only the information on the k^{th} allocation locus (either $\mathcal{A}^k$ or $\hat{\mathcal{A}}^k$, which both reside on the k^{th} grid at time $t_{\text{o}}^{k^+}$) is used to populate the terminal (time $t_{\text{o}}^{k^-}$) data of the $(k-1)^{\text{th}}$ grid. For this reason, the grids are constructed with the following pertinent properties:

- each grid's nodes are arranged in rows (indexed by the B ordinate);
- grid k has a maximum B ordinate of F^k (consistent with the highest B ordinate of the k^{th} allocation locus);
- for the limited-borrowing CPPI case, grid k's minimum B ordinate is the prevailing borrowing limit $\hat{B}^k$;
- for the classical CPPI case, grid k's minimum B ordinate is artificially-imposed and nonpositive;
- each row has
  - its leftmost node coincident with the vertical component of the k^{th} reallocation locus (at $S = 0$), as well as
  - a node coincident with the oblique segment of the k^{th} allocation locus;
- on the topmost row (where $B = F^k$) the two aforementioned nodes are coincident;
- each other row's remaining S abscissæ (including each row's artificially-imposed rightmost node) are scaled about the oblique segment of the k^{th} allocation locus.

The remaining details of our grid design are relegated to Appendix B.

These properties result in grids with convex hulls that resemble right trapezoids. The resemblance is not perfect because a lower bound is imposed on the row scaling factor to avoid complications as $B^k \to F^k$. See Section B.2 for additional information.

Figure 3.1 depicts a representative computational domain (albeit with exaggerated proportions and a simplified shape). Boundary conditions for the labelled segments will be addressed in the following two sections.

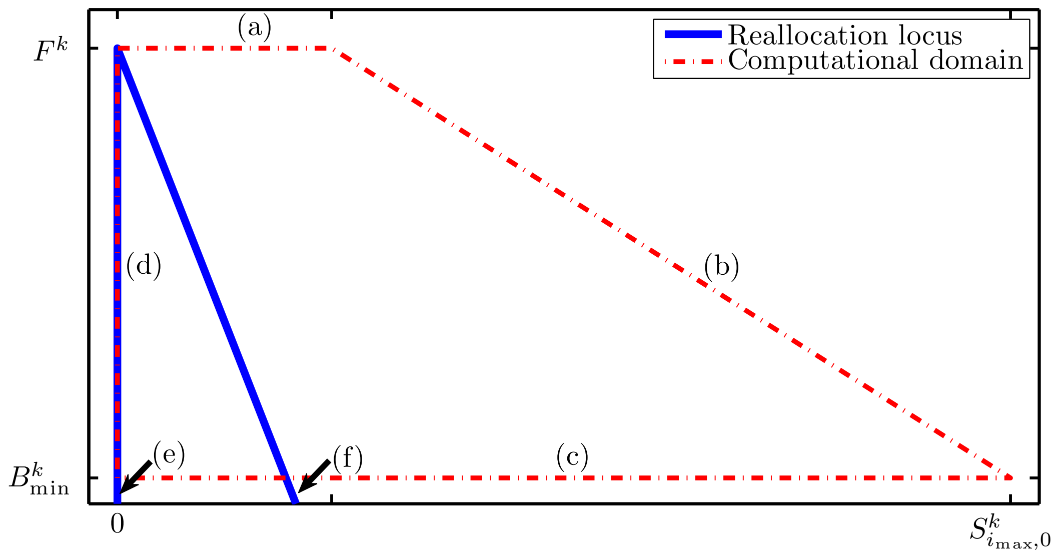

Figure 3.1: A representative computational domain, with superimposed classical reallocation locus and labelled boundaries. Boundaries (a) through (d) apply to the inter-observation dynamics. Boundary (e) applies to both the classical and limited-borrowing jump conditions. Boundary (f) only applies to the classical jump condition.

3.2 Boundary conditions between observations

Under the Lagrangian reformulation of Section 2.5, information flow only has a nonzero B component at each t^k_{o}. Consequently, between reallocations we only need to consider boundary conditions in the S direction: for the *near-field* ($S = 0$) and *far-field* ($S \to \infty$) behaviour of our 1D PIDEs. These correspond, respectively, to segments (d) and (b) of Figure 3.1; no boundary conditions are required on segments (a) and (c). Note that for both boundaries the same results would have been achieved if λ were zero; at both boundaries our PIDEs behave like classical Black-Scholes PDEs.

3.2.1 Near-field boundary between observations

When restricted to $S = 0$ our system of 1D PIDEs (2.6.3) simplifies to a family (indexed in B) of ordinary differential equations,

$$(v^k)_\tau = -rv^k, \tag{3.2.1}$$

which obey the relation

$$v^k(0, \tau = t_o^{(k+1)^-} - t_o^{k^+}; B) = \rho_{k+1}^k v^k(0, \tau = 0; B). \tag{3.2.2}$$

3.2.2 Far-field boundary between observations

Unfortunately, option pricing theory does not furnish us with a natural choice of far-field boundary condition. Instead, as is done throughout the literature, we must impose conditions that make numerical sense but financially cannot be rigorously justified. The numerical aspects of domain truncation and choice of artificial boundary conditions are examined in [28, 45].

In practice we assume $(v^k)_{SS} = 0$ for large S. Then we can write

$$v^k(S, \tau; B) = Sv_1^k(\tau; B) + v_2^k(\tau; B) \tag{3.2.3}$$

and the PIDE (2.6.3) (when S is large) collapses to

$$(v^k)_\tau = -rv_2^k = rS(v^k)_S - rv^k.$$

However, theoretical results are more readily obtainable if we additionally assume the far-field Dirichlet condition

$$\lim_{S\to\infty} V_L(S, \tau; B) = 0 \quad \text{or} \quad \lim_{S\to\infty} V_I(S, \tau; B) = S. \tag{3.2.4}$$

Numerical tests for vanilla and exotic American options [19] show that if the domain is sufficiently large in S then there is negligible difference in the results obtained with and without Equation (3.2.4).

3.3 Boundary conditions at observations

Only one grid is active at each stage of the PIDE solve. At each t_o^k the (old) k^{th} grid is used to populate its successor, the (new) $(k-1)^{\text{th}}$ grid. More precisely, each new grid's terminal values are calculated from the data on the old stage's allocation locus. The shape of the allocation locus will depend on whether the classical (2.6.4) or the limited-borrowing (2.6.5) CPPI jump condition is applied, but in either case the information on the k^{th} allocation locus is a function of $W^k = S^{k^-} + \rho^k_{k-1} B^{k^-}$.

In a computational setting the grid population operation is restricted by domain truncation. Suppose, based on the chosen grid parameters, that grid k (more precisely, grid k's convex hull) intersects with the k^{th} allocation locus in the wealth range $[W^{k+}_{\text{min}}, W^{k+}_{\text{max}}]$. Situations will arise where the lookup value W^k is outside of this interval: it was noted in the previous chapter that our jump conditions (as originally stated in Section 2.2) were expansive in regions above the allocation loci. Our interest-deferred transformation (Section 2.6) actually extends this effect to the regions below the allocation loci. However, we can offset all expansive effects by imposing boundary conditions: a *large shortfall boundary condition* for reallocation wealth $W^k < W^{k+}_{\text{min}}$, and a *large cushion boundary condition* for $W^k > W^{k+}_{\text{max}}$.

Our approach for the large shortfall boundary condition is common to both CPPI flavours and is described in the next subsection. Following that we describe a similarity extrapolant for the classical product as for $W^k > W^{k+}_{\text{max}}$. These boundary conditions respectively apply to segments (e) and (f) of Figure 3.1. For the limited-borrowing product it is possible to avoid needing a large cushion boundary condition: under mild but technical conditions on the grids' bounds, we can design a sequence of grids tailored to the *fixed-borrowing-limit* strategy. More precisely, the sequence corresponding to each grid's maximum represented wealth is bounded. The details are relegated to Section B.3 of the Appendix. We do this in order to avoid introducing extraneous notation to the main body of this text. We will not attempt to generalise this result to the variable borrowing limit case.

3.3.1 Large shortfall boundary condition

For $W^k < W^{k+}_{\text{min}}$, recursively applying the appropriate jump condition ((2.6.4) or (2.6.5)) will eventually allow the required off-grid portfolio to be expressed in terms of discounted, on-grid information from a previous stage. Consider B^k_{min}, the smallest ordinate of the k^{th} grid. It follows that $W^{k+}_{\text{min}} = B^k_{\text{min}}$. Choosing each B^k_{min} sufficiently low (so that all off-grid portfolios with a shortfall at t^k_{o} retain their shortfall status for the remaining reallocation instants t^{k+1}_{o} through t^K_{o}) allows a special case where off-grid data can be computed directly from the payoff $v^K(S, \tau = 0; B)$. The following result permits this for all sequences of CPPI floor values.

Lemma 3.3.1. *If $B^k_{\min} < 0$ for all k, then, for all $W^k < W^{k+}_{\min} = B^k_{\min}$,*

$$v^k(S = 0, \tau = t_o^{k+1} - t_o^k; B = W^k) = \rho^k_{K+1} v^K(S = 0, \tau = 0; B = \rho_k^{K+1} W^k). \quad (3.3.1)$$

Specifically,

$$\begin{aligned} & v_I^k(S = 0, \tau = t_o^{k+1} - t_o^k; B = W^k) = \rho^k_{K+1} F_T, \\ & v_J^k(S = 0, \tau = t_o^{k+1} - t_o^k; B = W^k) = 0, \\ \textit{and} \quad & v_L^k(S = 0, \tau = t_o^{k+1} - t_o^k; B = W^k) = \rho^k_{K+1}(F_T - \rho_k^{K+1} W^k) = \rho^K_{K+1} F_T - W^k. \end{aligned}$$

Proof. The valuation is the expected discounted payoff. The discounted payoff is certain for states that are guaranteed to incur a shortfall at time T. ∎

3.3.2 Large cushion boundary condition (classical CPPI case)

Definition 3.3.2 (Homogeneity of a function)**.** A function $f(x)$ is ℓ^{th}-degree homogeneous when $f(zx) = z^\ell f(x)$ for all x and nonzero z.

In [47] a *similarity extrapolant* workaround is proposed: for valuing cliquet options, off-grid information can be expressed in terms of on-grid information, by employing a homogeneity property of the solution and making the assumption that far-field local volatility is constant. Unfortunately, this approach is not directly applicable to our problem because here our valuations—unlike the cliquet valuations—are not homogeneous of degree zero. This is verified by an inspection of the payoff functions. For example:

$$\max\{F - z\rho_K^{K+1} B - zS, 0\} \neq \max\{F - \rho_K^{K+1} B - S, 0\}.$$

However—under narrow conditions—an exact first degree homogeneity relation is attainable, which when applied at a reallocation instant can serve as a similarity extrapolant. Rather than arising in terms of B, homogeneity arises in terms of an auxiliary state variable defined as

$$X^k \equiv F^{k+1} - \rho_k^{k+1} B^{k^+} = F^{k+1} - \rho_k^{k+1} B^{(k+1)^-}. \quad (3.3.2)$$

Like B under the Lagrangian reformulation, X^k is fixed over the interval $(t_o^{k^+}, t_o^{(k+1)^-})$. The dual definition of X^k therefore arises from the fact that, by construction, B^{k^+} is equal to

$B^{(k+1)^-}$. Since payoffs can now be expressed in terms of the difference $(S - X)$, X^k should be viewed as the CPPI analogue to a European option strike price, with the distinction that X^k can take negative values when $r > \varrho$ for a sufficiently large part of the interval $(t_o^{k+}, t_o^{(k+1)^-})$.

We start with a homogeneity result between portfolios at the same instant τ.

Proposition 3.3.3 (Homogeneity)**.** *Recall the interest-deferred payoffs for v_L and v_J defined in Equations* (2.6.2) *and* (2.6.6)*. If*

(H1) *the risk-free rate r and the volatility σ are piecewise constant over each interval $\left(t_o^{k+}, t_o^{(k+1)^-}\right)$,*

(H2) *the contract specifies classical CPPI reallocation (Section 2.2.1), and*

(H3) *the CPPI floor value F appreciates at the risk-free rate,*

then v_L is first-degree homogeneous in (S, X). Stated in terms of the usual interest-deferred (S, B) state space, we have

$$v_L^k\Big(zS, \tau; B = \rho_{k+1}^k \left(F^{k+1} - zX\right)\Big) = zv_L^k\Big(S, \tau; B = \rho_{k+1}^k \left(F^{k+1} - X\right)\Big) \tag{3.3.3}$$

for all positive z, S and X. The same can be said for v_J and $(v_J + v_L)$.

Proof. In the following we will work with v_L. The same reasoning holds for v_J and $(v_J + v_L)$. Although X may in general take negative values, Hypothesis (3.3.3.H3) guarantees that in this case X will be nonnegative.

Adopting the notation

$$\bar{v}^k(S, \tau; X^k) \equiv v_L^k\Big(S, \tau; B = \rho_{k+1}^k \left(F^{k+1} - X^k\right)\Big), \tag{3.3.4}$$

then Equation (3.3.3) is equivalent to

$$\bar{v}^k(zS, \tau; zX^k) = z\bar{v}^k(S, \tau; X^k), \tag{3.3.5}$$

which is the definition of first-degree homogeneity in (S, X^k).

It is now straightforward to verify that the payoff $v_L^K(S, \tau = 0; B)$ (defined in Equation (2.6.2)) is first-degree homogeneous in (S, X), so that the hypotheses of Corollary 15.1

in [27] are satisfied. From this we can conclude that v_L^K is first-degree homogeneous (in mutually nonzero coordinates (S, X), but *not* (S, B)) under *log-type* models (such as (2.4.1) under (3.3.3.H1)) for the entire K^{th} stage.

In order for this result to extend to the other K stages, the jump condition must produce first-degree homogeneous terminal data at each $t_{\text{o}}^{k^-}$. More precisely, for $k = 0, \ldots, K$, we must show

$$\bar{v}^k(zS, \tau = 0; zX^k) = z\bar{v}^k(S, \tau = 0; X^k) \tag{3.3.6}$$

for all nonzero z, S and X.

Consider the interest-deferred version of the k^{th} classical reallocation mapping f^k, stated in Equation (2.6.4). Substituting $\rho_{k-1}^k B^{k^-} = F^k - X^{k-1}$, this can be expressed as

$$f^k : \begin{bmatrix} S^{k^-} \\ B^{k^-} \end{bmatrix} \mapsto \begin{bmatrix} S^{k^+} \\ B^{k^+} \end{bmatrix} = \begin{bmatrix} m \cdot \max\left\{S^{k^-} - X^{k-1}, 0\right\} \\ S^{k^-} + F^k - X^{k-1} - m \cdot \max\left\{S^{k^-} - X^{k-1}, 0\right\} \end{bmatrix},$$

or equivalently as

$$f_X^k : \begin{bmatrix} S^{k^-} \\ X^{k-1} \end{bmatrix} \mapsto \begin{bmatrix} S^{k^+} \\ X^k \end{bmatrix} = \begin{bmatrix} m \cdot \max\left\{S^{k^-} - X^{k-1}, 0\right\} \\ F^{k+1} - \rho_k^{k+1}\left(S^{k^-} + F^k - X^{k-1} - m \cdot \max\left\{S^{k^-} - X^{k-1}, 0\right\}\right) \end{bmatrix}.$$

Only under (3.3.3.H3) do the CPPI floor terms vanish, so that

$$f_X^k\left(\begin{bmatrix} zS^{k^-} \\ zX^k \end{bmatrix}\right) = z f_X^k\left(\begin{bmatrix} S^{k^-} \\ X^k \end{bmatrix}\right), \tag{3.3.7}$$

and thus

$$\begin{aligned} \bar{v}^{(k-1)}(zS^{k^-}, zX^{k-1}, 0) &\overset{(\text{A})}{=} \bar{v}^k\Big(f_X^k(zS^{k^-}, zX^{k-1}), t_{\text{o}}^{k+1} - t_{\text{o}}^k\Big) \\ &\overset{(\text{B})}{=} \bar{v}^k\Big(z f_X^k(S^{k^-}, X^{k-1}), t_{\text{o}}^{k+1} - t_{\text{o}}^k\Big) \\ &\overset{(\text{C})}{=} z\bar{v}^k\Big(f_X^k(S^{k^-}, X^{k-1}), t_{\text{o}}^{k+1} - t_{\text{o}}^k\Big) \\ &\overset{(\text{D})}{=} z\bar{v}^{(k-1)}(S^{k^-}, X^{k-1}, 0). \end{aligned} \tag{3.3.8}$$

Here we have mildly abused our notation for $\bar{v}^k$; understand that

$$\bar{v}^k\left(f_X^k(S^{k^-}, X^{k-1}), \tau\right) \equiv \bar{v}^k\left(S^{k^+}, \tau; X^k\right).$$

Equalities A and D result from the conservation of wealth across reallocations. Equality B results from Equation (3.3.7) and C is a consequence of homogeneity at $t_{\mathrm{o}}^{k^+}$.

This confirms Equation (3.3.6), as desired. Equation (3.3.3) then follows from (3.3.4) and induction descending in k. ■

Next we extend this result across reallocation instants and remark on the stability of this approach.

Corollary 3.3.4 (Classical similarity extrapolant). *Adopt the same hypotheses as Proposition 3.3.3: assume that*

(H1) *the risk-free rate r and the volatility σ are piecewise constant over each interval $\left(t_{\mathrm{o}}^{k^+}, t_{\mathrm{o}}^{(k+1)^-}\right)$,*

(H2) *the contract specifies classical CPPI reallocation (Section 2.2.1), and*

(H3) *the CPPI floor value F appreciates at the risk-free rate (i.e $\varrho = r$).*

Then the $(k-1)^{\mathrm{th}}$ stage terminal data for all positive-cushion (portfolio wealth exceeding the prevailing CPPI floor) states (S_1, B_1) on grid $(k-1)$ can be expressed in terms of any single point (S_2, B_2) on $\mathcal{A}_\backslash^k$ from grid k:

$$v^{(k-1)}(S_1, 0; B_1)\Big|_{S_1+\rho_{k-1}^k B_1 - F^k > 0} = \frac{m(S_1 + \rho_{k-1}^k B_1 - F^k)}{S_2} v^k(S_2, t_{\mathrm{o}}^{k+1} - t_{\mathrm{o}}^k; B_2). \qquad (3.3.9)$$

Likewise,

$$v^0(W_0, t=0)\Big|_{W_0 > F^0} = \frac{m(W_0 - F^0)}{S_2} v^0(S_2, t_{\mathrm{o}}^1 - t_{\mathrm{o}}^0; B_2). \qquad (3.3.10)$$

We use this result to determine the time-t_{o}^k value for a portfolio (prescribed by the k^{th} classical reallocation mapping) that has wealth above $W_{\max}^{k^+}$. This valuation is related to that of another portfolio with coordinates (S_2, B_2). The solid locus in Figure 3.2 illustrates the set of related portfolios; computationally we require that $B_2 \in [B^k_{\min}, F^k)$. In this situation—when $\varrho = r$—the locus of related portfolios is coincident with $\mathcal{A}^k_\backslash$.

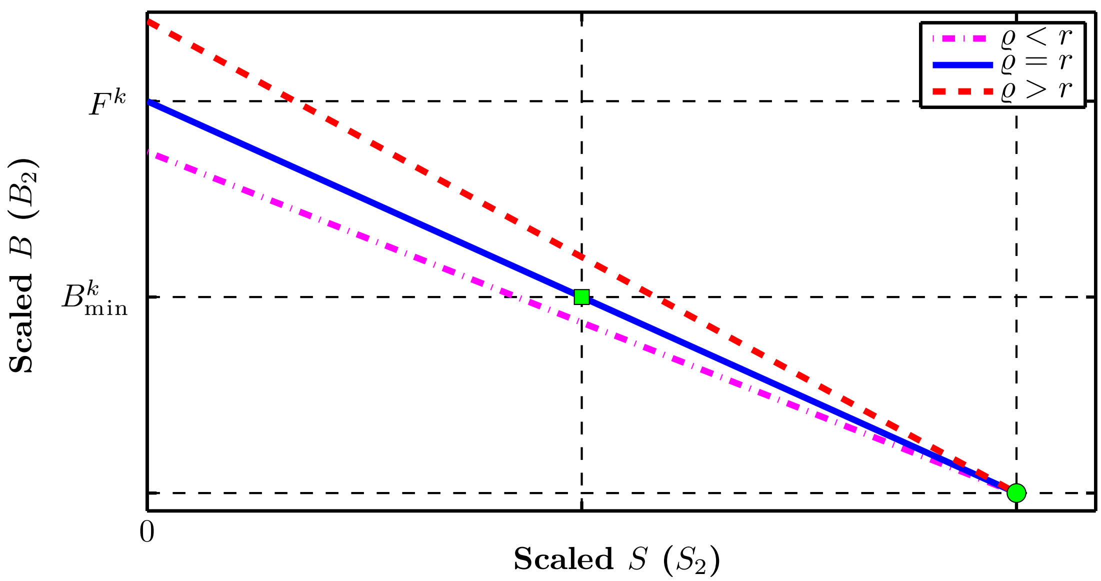

Figure 3.2: The similarity extrapolant expresses the value for an off-grid portfolio (represented by the circular marker) in terms of the value for a related on-grid portfolio. In our implementation we use the related portfolio with ordinate $B^k_{\min}$. When $\varrho = r$ this corresponds to the square marker. For comparison, loci for autonomous CPPI floor situations are also depicted; they are described by Equation (3.3.11).

Proof of Corollary 3.3.4. At t^k_o the positive-cushion portfolio (S_1, B_1) on grid $(k-1)$ maps to an equal-valued portfolio (on $\mathcal{A}^k_\backslash$) that has the risky asset position $m(S_1 + \rho^k_{k-1} B_1 - F^k)$. By the previous homogeneity result, this new portfolio can be valued in terms another portfolio (S_2, B_2) using $z = \frac{m(S_1+\rho^k_{k-1}B_1-F^k)}{S_2}$. By (3.3.4.H3) (which permits Equality B of Equation (3.3.8)), (S_2, B_2) is also on $\mathcal{A}^k_\backslash$.

Equation (3.3.10) applies to the initial allocation, where $m(W_0 - F^0)$ from the endowment W_0 (which must exceed the initial CPPI floor F^0) is invested in the risky asset at the outset of the contract. ∎

Remark 3.3.5 (Stability)**.** The factor $\frac{m(S_1+\rho^k_{k-1}B_1-F^k)}{S_2}$ in (3.3.9) is larger than unity whenever the similarity extrapolant is used as a large cushion boundary condition. From the perspective of stability this may appear problematic, but it will be shown in Proposition 3.6.4 that the factor relevant to stability is actually the value of a specific European call option divided by S_2. This quantity approaches unity as $K \to \infty$. ■

For completeness we examine how the similarity extrapolant approach can be used to approximate more exotic scenarios.

Corollary 3.3.6 (Applicability of Equation (3.3.9))**.** *Assume*

*(**i**) the risk-free rate r and the volatility σ are piecewise constant over each interval $\left(t_{\mathrm{o}}^{k+}, t_{\mathrm{o}}^{(k+1)^-}\right)$, and*

*(**ii**) the contract specifies classical CPPI reallocation (Section 2.2.1).*

Then the similarity extrapolant (Equation (3.3.9)) is exact when $\rho_{k+1}^{k} F^{k+1} = F^{k}$. Moreover,

*(**i**) when $\rho_{k+1}^{k} F^{k+1} < F^{k}$, Equation (3.3.9) overvalues v_J and undervalues v_L; and*

*(**ii**) when $\rho_{k+1}^{k} F^{k+1} > F^{k}$, Equation (3.3.9) undervalues v_J and overvalues v_L.*

These relations can also be concluded for other log-type models such as those with stochastic volatility.

Proof. Exactness when $\rho_{k+1}^{k} F^{k+1} = F^{k}$ was shown in Corollary 3.3.4.

Analogous to Equation (3.3.9), we have the more general relation

$$v^{(k-1)}(S_1, 0; B_1)\Big|_{S_1+\rho_{k-1}^{k}B_1-F^k>0} = \frac{m(S_1+\rho_{k-1}^{k}B_1-F^k)}{S_2} v^{k}(S_2, t_{\mathrm{o}}^{k+1}-t_{\mathrm{o}}^{k}; B_2), \qquad (3.3.11)$$

$$\text{where } B_2 = \rho_{k+1}^{k}F^{k+1} - S_2\left(\frac{m-1}{m} + \frac{\rho_{k+1}^{k}F^{k+1}-F^k}{m(S_1+\rho_{k-1}^{k}B_1-F^k)}\right).$$

This formula allows us to express an off-grid node in terms on an on-grid node with coordinates (S_2, B_2). It is exact as long as the inter-reallocation dynamics are first-degree homogeneous—even when the CPPI floor rate is not the same as the risk-free rate.

Note that the ordinate B_2 is linear in S_2. Furthermore, the line described by varying S_2 (i) intersects with $\mathcal{A}^k$ at $S_2 = m(S_1+\rho_{k-1}^{k}B_1-F^k)$ (corresponding to no scaling), and (ii) has a B-intercept at $B = \rho_{k+1}^{k}F^{k+1}$. This is depicted in Figure 3.2.

Since the purpose of the similarity extrapolant is to express any off-grid node (with abscissa $m(S_1 + \rho^k_{k-1}B_1 - F^k)$) in terms of an on-grid node (with abscissa S_2), we are interested in S_2 in the interval $[0, m(S_1 + \rho^k_{k-1}B_1 - F^k)]$. Over this range, the locus of (S_2, B_2) portfolios described by Equation (3.3.11) is above the allocation locus $\mathcal{A}^k$ when $\rho^k_{k+1}F^{k+1} > F^k$ and below when $\rho^k_{k+1}F^{k+1} < F^k$. As was noted earlier, when $\rho^k_{k+1}F^{k+1} = F^k$, the locus described by (S_2, B_2) is coincident with $\mathcal{A}^k_{\setminus}$. Recall from Equation (3.3.2) that lower values of B correspond to larger values of X, which in turn is analogous to the strike price of a European call. The function v_J (with a call-style payoff) is decreasing in X. Likewise, v_L is increasing in X.

Other log-type models are admissible because they too are first-degree homogeneous in the spot and strike prices [27]. ■

Remark 3.3.7 (Generalising the similarity extrapolant stability result)**.** The amount by which independent-floor variants are misvalued by the similarity extrapolant is an issue for future study. Equation (3.3.11) is a starting point for work in this direction. Note that as $K \to \infty$, Equation (3.3.11) becomes Equation (3.3.9) because the quantity $t^{k+1}_{\mathrm{o}} - t^k_{\mathrm{o}}$ implicitly decreases as K increases and $\lim_{K\to\infty}(F^{k+1} - \rho^{k+1}_k F^k) = 0$. We conclude that the similarity extrapolant is exact as $K \to \infty$, regardless of the CPPI floor dynamics (as long as the sequence $\{F^k\}^{K+1}_{k=0}$ is sampled from a continuous function). This leads us to suspect that the similarity extrapolant (in conjunction with homogeneous inter-reallocation dynamics) should have the same stability result for all continuous CPPI floor functions $F(t)$. In other words, it is likely that the stability result that will be presented for the similarity extrapolant (Proposition 3.6.4) can be generalized to cases where $\varrho \neq r$.

The applicability of the similarity extrapolant to the class of problems with nonhomogeneous models (such as those with S-dependent local volatilities) is unclear and also warrants further investigation. We conjecture that stability can also be extended to situations where the payoff is homogeneous but the inter-observation dynamics incorporate a nonhomogeneous model for the risky asset. It will be shown in Section 3.6.1 that stability relies on whether the time-τ computed value an option converges to the payoff as $\tau \to 0$. This property is expected of homogeneous and nonhomogeneous models alike. ■

Remark 3.3.8 (Other functions are not homogeneous)**.** The functions v_I and $(v_I + v_L)$ do not have homogeneous payoffs, so these functions are also not first-degree homogeneous for times before maturity. It is for this reason that we calculate v_J instead of v_I in Chapter 5. The function v_I can be recovered with Equation (2.6.7). ■

Remark 3.3.9 (Unlimited-borrowing case, large cushion boundary condition)**.** Recall that the smallest B ordinate on the k^{th} computational grid is $B^k_{\min}$. Our implementation uses the similarity extrapolant (Equation (3.3.9)), with $(S_2, B_2) = \left(\frac{m}{m-1}(F^k - B^k_{\min}), B^k_{\min}\right)$. The expression for S_2 follows from the definition of $\mathcal{A}^k_{\setminus}$ in Equation (2.2.4). ■

In the case of constant financial coefficients and lognormal jumps, there is an analytical solution for each row of the K^{th} stage of (2.6.3) [35]. Combining this fact with the results of this section allows us to price a class of classical CPPI problems analytically. This in turn can be used to help validate our computational results, which apply to a much broader class of problems. This idea will be developed in Chapter 4 and applied in Chapter 5.

Corollary 3.3.4 fails for limited-borrowing reallocation schemes because Equation (3.3.7) does not hold for points where the borrowing limit is in effect—where $B = \hat{B}^{k+1}$. We remind the reader that our limited-borrowing reallocation scheme does not require such a boundary condition when we design our grid according to Proposition B.1. However, a similarity relation does exist in special cases for the triplet $(S, X, \hat{B})$:

Proposition 3.3.10 (Limited-borrowing CPPI similarity extrapolant)**.** *If*

(H1) *the risk-free rate r and the volatility σ are piecewise constant over each interval $\left(t_{\text{o}}^{k^+}, t_{\text{o}}^{(k+1)^-}\right)$,*

(H2) *the contract specifies limited-borrowing CPPI reallocation (Section 2.2.2), and*

(H3) *the CPPI floor value F appreciates at the risk-free rate*

then

$$v^k\Big(zS, \tau; B = \rho^k_{k+1}\left(F^{k+1} - zX\right), \hat{B} = \rho^k_{k+1}\left(F^{k+1} - zX\right)\Big) \tag{3.3.12}$$

$$= zv^k\Big(\ S, \tau; B = \rho^k_{k+1}\left(F^{k+1} - \ X\right), \hat{B} = \rho^k_{k+1}\left(F^{k+1} - \ X\right)\Big), \tag{3.3.13}$$

and likewise for v_J and $(v_J + v_L)$.

Proof. This follows the proof of Proposition 3.3.3. The limited-borrowing and classical cases have the same payoffs, so the last stage of the PIDE solve is homogeneous. It is straightforward to verify that, analogously to Equation (3.3.7),

$$\hat{f}^k_X\left(\begin{bmatrix} zS^{k^-} \\ zX^k \end{bmatrix}; \hat{B} = \rho^k_{k+1}\left(F^{k+1} - zX\right)\right) = z\hat{f}^k_X\left(\begin{bmatrix} S^{k^-} \\ X^k \end{bmatrix}; \hat{B}^k = \rho^k_{k+1}\left(F^{k+1} - X\right)\right)$$

. ■

3.4 Interpolation

Recall that the k^{th} jump condition acts on the k^{th} (either classical or limited-borrowing) reallocation locus and is indexed by $W^k = S^{k^-} + \rho_{k-1}^k B^{k^-}$. Computationally, this function's domain is limited to the grid k allocation wealth range $[W_{\min}^{k^+}, W_{\max}^{k^+}]$. In the previous section boundary conditions were introduced for situations where W^k was outside this range. Now we address the situation where W^k is within this range.

The discrete nature of the grids necessitates interpolation. Recall that each grid is, by design, aligned with the appropriate allocation locus. This enables *wealth-indexed interpolation* in a single variable W^k (much like the *diagonal interpolation* scheme described in [47, 5]), instead of the more general two-dimensional interpolation in (S, B).

In our implementation we have considered four types of interpolation, each acting on a stencil of nodes that are coincident with the allocation locus:

- linear interpolation;
- standard quadratic Lagrange interpolation;
- limited quadratic interpolation, adapted from [48];
- piecewise quadratic Lagrange interpolation, with standard quadratic Lagrange interpolation on each of three intervals (corresponding to the three segments of Figure 2.2).

The latter scheme prevents interpolation across these segments' intersections, where v is generally nonsmooth.

3.5 PIDE discretisation

We use a simple extension of the numerical scheme developed in [18] for a one-dimensional jump diffusion, which in turn extends the positive coefficient discretisation method proposed in [43]. For each fixed B, stage k of our interest-deferred, inter-observation dynamics (2.6.3) discretises to

$$\begin{aligned} & v_{i,j}^{n+1}\left[1 + \left(\alpha_{i,j} + \beta_{i,j} + r + \lambda\right)\Delta\tau\right] - \Delta\tau\alpha_{i,j}v_{i-1,j}^{n+1} - \Delta\tau\beta_{i,j}v_{i+1,j}^{n+1} \\ = \quad & v_{i,j}^{n} + \left(1-\theta_J\right)\Delta\tau\lambda\sum_{\ell\in\mathcal{N}}\chi\left(v_j^{n+1}, i, \ell\right)\bar{g}_{\ell,j}\Delta x + \theta_J\Delta\tau\lambda\sum_{\ell\in\mathcal{N}}\chi\left(v_j^{n}, i, \ell\right)\bar{g}_{\ell,j}\Delta x \end{aligned} \tag{3.5.1}$$

for timesteps $n \geq 0$ and gridpoints $\left\{(S^k_{i,j}, B^k_j) \,\middle|\, 0 \leq i < i_{\max}, 0 \leq j \leq j_{\max}\right\}$, where

$v^n_{i,j}$	denotes the grid value $v^k(S^k_{i,j}, \tau^n; B^k_j)$,
τ^0	corresponds for the k^{th} stage to $t_{\text{o}}^{(k+1)-}$,
$\alpha_{i,j}$ and $\beta_{i,j}$	are non-negative finite difference coefficients defined in Appendix A,
$\Delta\tau$	is the timestep $\tau^{n+1} - \tau^n$,
$\mathcal{N}$	denotes the set of FFT indices $[-\frac{N}{2}+1, \frac{N}{2}] \cap \mathbb{Z}$ [18],
$\chi\left(v^n_j, i, \ell\right)$	is an interpolation operator that is linear and acts on the row $\left\{v^n_{i,j}\right\}_{i=0}^{i_{\max}}$,
$\bar{g}_{\ell,j}$	is related to $f(J)$ (see [18] for details),
Δx	is the grid spacing of the FFT grid, and
θ_J	determines whether the jump term is handled explicitly ($\theta_J = 1$), implicitly ($\theta_J = 0$), or using Crank-Nicolson timestepping ($\theta_J = \frac{1}{2}$).

Most of these objects vary with the PIDE stage, but for simplicity we omit the index k from the notation (i.e. $\alpha_{i,j}$ should be interpreted as $\alpha^k_{i,j}$).

Our implementation's handling of the boundary conditions is discussed in [22]. Recall that with the assumptions of Section 3.2, our PIDEs collapse to Black-Scholes PDEs at the near- and far-field boundaries. For theoretical purposes we follow (3.2.4) and additionally assume a far-field Dirichlet boundary condition:

$$v^{n+1}_{i_{\max},j} = v^n_{i_{\max},j} = \begin{cases} S^k_{i_{\max},j}, & \text{when the payoff is } V_J, \\ 0, & \text{when the payoff is } V_L. \end{cases}$$

The upcoming stability results rely upon two important properties from [18]:

- $\bar{g}_{i,j}$ is non-negative for all indices;
- $\sum_{\ell\in\mathcal{N}} \bar{g}_{\ell,j}\Delta x \leq 1$, for each row.

These properties are consequences of $\bar{g}$ approximating a probability mass function.

3.6 Convergence

Assuming that our problem formulation satisfies a strong comparison result, then a unique viscosity solution exists [5]. This is the financially-relevant solution to our problem [20].

In order to prove our numerical scheme converges to the viscosity solution it is sufficient to demonstrate stability, monotonicity and consistency; for the sake of robustness our implementation should (in theory) obey these three criteria even as K tends to infinity. We shall examine the first two requirements.

3.6.1 Stability

In the following we address the stability of the fully implicit PIDE discretisation (Equation (3.5.1) with $\theta_J = 0$).

Notation

Let v_j^n be a vector representing the data on the j^{th} row of grid k at timestep n. The corresponding update equation for the fully implicit PIDE discretisation scheme (Equation (3.5.1) with $\theta_J = 0$ and boundary conditions (3.2.1), (3.2.3) and (3.2.4)) is

$$\mathbf{M_{j,k}} v_j^{n+1} = v_j^n, \tag{3.6.1}$$

with each $\mathbf{M_{j,k}}$ defined such that

$$[\mathbf{M_{j,k}} v^{n+1}]_i = \begin{cases} (1 + r\Delta\tau) v_{i,j}^{n+1}, & i = 0 \\ \left[1 + (\alpha_{i,j} + \beta_{i,j} + r + \lambda)\,\Delta\tau\right] v_{i,j}^{n+1} - \Delta\tau\alpha_{i,j} v_{i-1,j}^{n+1} & \\ \quad -\Delta\tau\beta_{i,j} v_{i+1,j}^{n+1} - \Delta\tau\lambda \sum_{\ell\in\mathcal{N}} \chi\left(v_j^{n+1}, i, \ell\right) \bar{g}_{\ell,j}\Delta x\ , & 1 \le i \le i_{\max} \\ v_{i,j}^{n+1}, & i = i_{\max} \end{cases}$$

and with $i_{\max}$ corresponding to the the rightmost node of row j.

PIDE stability

We begin with a general result for the stability of the one dimensional PIDE in between reallocations. This result mostly follows [18], although it is not explicitly stated there.

Proposition 3.6.1 (ℓ^∞ stability)**.** *The fully implicit PIDE discretisation scheme described by Equation* (3.6.1) *is ℓ^∞-stable for all bounded initial conditions. Moreover, local and time-independent bounds exist: if, for functions $H_{j,k}^+$ and $H_{j,k}^-$,*

$$H_{j,k}^-(S_{i,j}^k, B_j^k) \le \left[v_j^0\right]_i \le H_{j,k}^+(S_{i,j}^k, B_j^k) \text{ for all } i$$
$$\text{then } H_{j,k}^-(S_{i,j}^k, B_j^k) \le \left[v_j^n\right]_i \le H_{j,k}^+(S_{i,j}^k, B_j^k) \text{ for all } i \text{ and all } n.$$

Proof. The term $\chi\left(v_j^{n+1}, i, \ell\right)$, as defined in [18], is an interpolation between two other interpolated values. By this and the properties of Section 3.5, $\sum_{\ell \in \mathcal{N}} \chi\left(v_j^{n+1}, i, \ell\right) \bar{g}_{\ell,j} \Delta x$ multiplied by $-\Delta\tau\lambda$ contributes a term bounded by $[-\Delta\tau\lambda, 0]$ to each element of $\mathbf{M_{j,k}}$ (except for those on the top and bottom rows). Additionally, the row sums of these contributions are each exactly $-\Delta\tau\lambda$.

Recalling the positive coefficient discretisation presented in Appendix A, it follows that for all i,

- $[\mathbf{M_{j,k}}]_{i,i} > 0$,
- $[\mathbf{M_{j,k}}]_{i,\ell} \leq 0$, for all $\ell \neq i$ and
- $[\mathbf{M_{j,k}}]_{i,i} \geq -\sum_{\ell \neq i} [\mathbf{M_{j,k}}]_{i,\ell}$ (with strict equality for the top and bottom rows).

Therefore, every entry of the inverse matrix $\mathbf{M_{j,k}}^{-1}$ is positive, since $\mathbf{M_{j,k}}$ satisfies the properties of an M-matrix [21].

Let u_j^n be a vector, such that $[u_j^n]_i$ is solely a function of the corresponding grid coordinates S_i and B_j. Consequently, if every entry of the vector $(u_j^0 - v_j^0)$ is nonpositive (respectively, nonnegative) then the same can be said for $(u_j^{n+1} - v_j^{n+1}) = \left(\mathbf{M_{j,k}}^{-1}\right)^{n+1} (u_j^0 - v_j^0)$. This proves that there exist local bounds for each gridpoint, independent of n. ■

Corollary 3.6.2 (Bounds for discrete approximations of v_J and v_L)**.** *Assume $F^k \geq \rho_{k-1}^k B_j$. If $v_{i,j}^0 = \max\{S_i + \rho_{k-1}^k B_j - F^k, 0\}$ (corresponding to a payoff for v_J) then $0 \leq v_{i,j}^n \leq S_i$ for all n. Likewise, if $v_{i,j}^0 = \max\{F^k - S_i - \rho_{k-1}^k B_j, 0\}$ (corresponding to a payoff for v_L) then $0 \leq v_{i,j}^n \leq F^k - \rho_{k-1}^k B_j$ for all n.*

Limited-borrowing case

With the preceding results, stability is now easily extended to limited-borrowing CPPI products. The following result shows that ℓ^∞ stability is achievable for the fixed-borrowing-limit case when the computational grids are attentively designed.

Proposition 3.6.3 (Stability for the fixed-borrowing-limit CPPI problem)**.** *If*

- *$\hat{B} \leq 0$,*
- *the sequence $\{F^k\}$ samples a nondecreasing function, and*

- *the computational domain is a sequence of grids (such as the one developed in Appendix B) constructed so that the following quantities are sufficiently large:*
  - $F^0 - \hat{B}$;
  - *each* $S^k_{i_{\max}-1,j}$;
  - *each* $S^k_{i_{\max},j}$,

then the numerical scheme incorporating

- *the fully implicit PIDE discretisation (Equation* (3.6.1)*),*
- *the large shortfall boundary condition of Section 3.3.1,*
- *linear or limited higher-order interpolation (Section 3.4), and*
- *the interest-deferred, fixed-borrowing-limit CPPI jump condition (Equation* (2.6.5) *with constant* $\hat{B}^k$*)*

is ℓ^∞*-stable for all* K*.*

The above conditions on the computational domain are mild but technical; see Appendix B for the details.

Proof of Proposition 3.6.3. After Corollary 3.6.2, it remains to prove that boundedness at each $t_o^{k^+}$ implies boundedness at the corresponding $t_o^{k^-}$. We proceed by induction, descending in k.

Base case: ($k = K + 1$**)** This step is trivial, because here the terminal value of v is defined by a payoff function. For example, in the case of v_L the magnitude of our gridpoints' values is bounded between 0 and $F_T + \max_j\{S^K_{i_{\max},j}\} + \rho_K^{K+1} B^K_{j_{\max}}$.

Induction step: ($0 < k < K + 1$**)** Recall that the k^{th} limited-borrowing jump condition is handled in one of two ways, depending on the lookup value W^k. A large-cushion boundary condition is not required because we have assumed the hypotheses of Proposition B.1, thus guaranteeing that $W^k \le W^{k^+}_{\max}$ for all k.

We must resort to using Lemma 3.3.1 when the lookup value W^k is below the range of available data points supplied by the k^{th} grid. The lookup value W^k is calculated from the coordinates of the $(k-1)^{\text{th}}$ grid and is therefore bounded. For v_I, Lemma 3.3.1 produces values at t_{o}^{k-} bounded by $\left[\rho_{K+1}^{0} F_T, F_T\right]$. For v_J, all results are identically zero. For v_L, the results for a given W^k are within the interval $\left[\rho_{K+1}^{0} F_T - W^k, F_T - W^k\right]$.

Wealth-indexed interpolation (Section 3.4) is used when $W^k \geq W_{\min}^{k+}$. For linear interpolation, the interpolated value lies in between the two bounded neighbouring values and is therefore also bounded. The same can be said for higher-order variants (such as the limited quadratic interpolation scheme adopted from [48]) where boundedness by neighbouring lookup values is explicitly enforced.

We conclude that the induction step is ℓ^∞-stable. ∎

Classical case with similarity extrapolant

Proving our discretisation's stability for the similarity extrapolant case (using Equation (3.3.9)) would be straightforward if we could show that $v_L^K\left(S_2, T - t_{\text{o}}^K; B_2\right) \leq \frac{S_2}{m}$, but with Corollary 3.6.2 we can only achieve the weaker upper bound of S_2. We therefore cannot use the reasoning of Proposition 3.6.3.

Our numerical results (in particular, those to be presented in Section 5.3) suggest that the implementation using Equation (3.6.1) and the similarity extrapolant is indeed convergent under conditions where the similarity extrapolant is exact. From this we conjecture that our numerical scheme for the classical CPPI product is ℓ^∞-stable. This may seem counterintuitive; earlier it was noted in Remark 3.3.5 that the similarity extrapolant multiplier is larger than unity.

To examine this discrepancy we derive an analytical solution for the classical CPPI problem. It will be shown that when the similarity extrapolant is exact, we can express the analytical CPPI valuation as a product of $K+1$ vanilla option values. We can then prove stability for this analytical special case by showing that the value of each vanilla option approaches $\frac{S_2}{m}$ as $K \to \infty$. This analytical work is later revisited in Chapter 4, towards the development of a tractable analytical solution.

Let $S_{\mathcal{A}_{\setminus}^k} \equiv \frac{m}{m-1}(F^k - B_{\min}^k)$, denoting the abscissa of $\mathcal{A}_{\setminus}^k$ at $B = B_{\min}^k$. Let $\mathcal{C}(S; X, T)$ represent the time-0 value of a European call option with spot S, strike X and maturity T. For notational convenience, model-specific arguments (such as r, σ and λ) are omitted.

The following analysis is simpler if we work with v_J. An analogous result for v_L can be obtained: instead of $(K+1)$ call values, it involves the product of K call values and one put value.

Proposition 3.6.4 (Analytical solution of the classical CPPI problem when the similarity extrapolant is exact)**.** *If*

- $B^k_{\min} \le 0$ *for all* k,
- *the risk-free rate* r *and the volatility* σ *are piecewise constant over each interval* $\left(t_{\mathrm{o}}^{k^+}, t_{\mathrm{o}}^{(k+1)^-}\right)$,
- *the contract specifies classical CPPI reallocation (Section 2.2.1), and*
- *the CPPI floor value* F *appreciates at the risk-free rate,*

then, using the large shortfall boundary condition (Lemma 3.3.1) and the classical similarity extrapolant (Corollary 3.3.4), the time-0 risk-neutral value of a CPPI claim with payoff v_J *and initial wealth* W_0 *can be expressed using the product of* $K+1$ *call option values:*

$$v_J(W_0, 0) = \max\left\{W_0 - F^0, 0\right\} \prod_{k=0}^{K} \left[\frac{m}{S_{\mathcal{A}^k_\setminus}} \mathcal{C}\left(S_{\mathcal{A}^k_\setminus}; F^{k+1} - \rho_k^{k+1} B^k_{\min}, t_{\mathrm{o}}^{k+1} - t_{\mathrm{o}}^k\right)\right]. \quad (3.6.2)$$

Proof. The hypotheses of Corollary 3.3.4 are assumed, and therefore a stage's positive-cushion terminal data can be expressed in terms of a single node from the previous grid. In the case of v_J at time t^{K^-}, the result is

$$\begin{aligned} & v_J^{(K-1)}\left(S^{K^-}, 0; B^{K^-}\right)\Big|_{S^{K^-} + \rho^K_{K-1} B^{K^-} - F^K > 0} \\ = \quad & \frac{m(S^{K^-} + \rho^K_{K-1} B^{K^-} - F^K)}{S_{\mathcal{A}^K_\setminus}} v_J^K(S_{\mathcal{A}^K_\setminus}, t_{\mathrm{o}}^{K+1} - t_{\mathrm{o}}^K; B^K_{\min}). \end{aligned} \quad (3.6.3)$$

On the other hand, with the large shortfall boundary condition (Lemma 3.3.1) we have

$$v_J^{(K-1)}\left(S^{K^-}, 0; B^{K^-}\right)\Big|_{S^{K^-} + \rho^K_{K-1} B^{K^-} - F^K \le 0} = 0, \quad (3.6.4)$$

recalling that all negative-cushion portfolios are terminally knocked-out when F evolves at or above the risk-free rate. Combining these two results yields

$$\begin{aligned} v_J^{(K-1)}\left(S^{K^-},0;B^{K^-}\right) &= \frac{m\cdot\max\left\{S^{K^-}+\rho_{K-1}^{K}B^{K^-}-F^K,0\right\}}{S_{\mathcal{A}_\setminus^K}}v_J^K\left(S_{\mathcal{A}_\setminus^K},t_{\mathrm{o}}^{K+1}-t_{\mathrm{o}}^K;B_{\min}^K\right) \\ &= \frac{m\cdot\max\left\{S^{K^-}+\rho_{K-1}^{K}B^{K^-}-F^K,0\right\}}{S_{\mathcal{A}_\setminus^K}}\mathcal{C}\left(S_{\mathcal{A}_\setminus^K};F^{K+1}-\rho_K^{K+1}B_{\min}^K,t_{\mathrm{o}}^{K+1}-t_{\mathrm{o}}^K\right). \end{aligned} \tag{3.6.5}$$

The second equality results directly from the definition of the function $\mathcal{C}$; the terminal value associated with $v_J^K\left(S_{\mathcal{A}_\setminus^K},t_{\mathrm{o}}^{K+1}-t_{\mathrm{o}}^K;B_{\min}^K\right)$ is $\max\left\{S_{\mathcal{A}_\setminus^K}-\left(F^{K+1}-\rho_K^{K+1}B_{\min}^K\right),0\right\}$ which can be thought of as a call payoff. Furthermore, there are no reallocations over the interval $(t_{\mathrm{o}}^K,t_{\mathrm{o}}^{K+1}]$, so $v_J^K\left(S_{\mathcal{A}_\setminus^K},t_{\mathrm{o}}^{K+1}-t_{\mathrm{o}}^K;B_{\min}^K\right)$ is the time-0 value of a call with spot $S_{\mathcal{A}_\setminus^K}$, strike $F^{K+1}-\rho_K^{K+1}B_{\min}^K$ and maturity $t_{\mathrm{o}}^{K+1}-t_{\mathrm{o}}^K$.

The only difference between Equation (3.6.5) (at time t_{o}^K) and the original payoff

$$\max\left\{S^{(K+1)^-}+\rho_K^{K+1}B^{(K+1)^-}-F^{K+1},0\right\}$$

(at time $t_{\mathrm{o}}^{K+1}=T$) is the decremented reallocation index (from $K+1$ to K) and a scaling by the factor

$$\frac{m}{S_{\mathcal{A}_\setminus^K}}\mathcal{C}\left(S_{\mathcal{A}_\setminus^K};F^{K+1}-\rho_K^{K+1}B_{\min}^K,t_{\mathrm{o}}^{K+1}-t_{\mathrm{o}}^K\right)$$

which is independent of both S^{K^-} and B^{K^-}. This allows us to exploit linearity and repeat the above reasoning to determine $v_J^{(K-2)}\left(S^{(K-1)^-},0;B^{(K-1)^-}\right)$, which is simply the expression for $v_J^{(K-1)}\left(S^{K^-},0;B^{K^-}\right)$ scaled by the factor

$$\frac{m}{S_{\mathcal{A}_\setminus^{K-1}}}\mathcal{C}\left(S_{\mathcal{A}_\setminus^{K-1}};F^K-\rho_{K-1}^KB_{\min}^{K-1},t_{\mathrm{o}}^K-t_{\mathrm{o}}^{K-1}\right).$$

Descending further in k introduces an additional factor at each iteration. We ultimately obtain Equation (3.6.2), recalling that $W_0=S^0+B^0$. ∎

From this result it follows that when the similarity extrapolant is exact, the analytical result for the classical case with K reallocations is bounded by

$$0 \leq v_J^0(W_0, 0) \leq \max\left\{W_0 - F^0, 0\right\}\left(\mathscr{C}(K)\right)^{\lfloor K\rfloor+1}\mathscr{C}^\dagger(K), \tag{3.6.6}$$

$$\text{where } \mathscr{C}(K) \equiv \max_{0\leq k\leq\lfloor K\rfloor}\left\{\frac{m}{S_{\mathcal{A}_\setminus^k}}\mathcal{C}\left(S_{\mathcal{A}_\setminus^k}; F^{k+1} - \rho_k^{k+1}B_{\min}^k, t_\mathrm{o}^{k+1} - t_\mathrm{o}^k\right)\right\},$$

$$S_{\mathcal{A}_\setminus^k} = \frac{m}{m-1}(F^k - B_{\min}^k), \text{ as before,}$$

and $\mathscr{C}^\dagger(K)$ is a factor that only arises when K takes a noninteger value.

Here $\lfloor\cdot\rfloor$ represents the floor function—this function determines the largest previous integer, and is not to be confused with the CPPI floor, F. We have carefully defined the upper bound in Equation (3.6.6), in a manner that facilitates studying its limit as $K \to \infty$ (calculating this requires treating K as a continuous variable). The function $\mathscr{C}^\dagger(K)$ relates to the remaining, shortened time interval that arises when the interval $[0, T]$ is partitioned into a noninteger number of equal subintervals. This function therefore varies with $\lfloor K\rfloor - K$ and is unity-valued when K is a nonnegative integer. The graph of this function looks like a sawtooth function with decaying amplitude; it is a piecewise function in K that is increasing over each subinterval, bounded below by one and bounded above by $\mathscr{C}(K)$.

Proving stability when the similarity extrapolant is exact therefore reduces to proving that $\lim_{K\to\infty}\left[\mathscr{C}(K)\right]^{K+1}$ is finite. By Corollary 3.6.2 we have $\mathscr{C}(K) \leq m$. As noted earlier, this bound is unfortunately not tight enough, because $m > 1$. We instead use the following result.

Lemma 3.6.5. *If $y(K)$ is a differentiable function with $\lim_{K\to\infty} y(K) = 1$ then*

$$\lim_{K\to\infty}\left(y(K)\right)^{K+1} = \exp\left(\lim_{K\to\infty} -(K+1)^2\frac{\partial y(K)}{\partial K}\right).$$

Proof. This is a consequence of l'Hôpital's rule and the limit definition of e^x. See Proposition 1.3.5 of [4] for details. ∎

It is straightforward to verify that $\mathscr{C}(K) \to 1$ as $K \to \infty$. As K increases, the duration between reallocations decreases, and all of the functions $\mathcal{C}$ considered in Equation (3.6.6) approach the payoff function. Hence

$$\lim_{K\to\infty}\mathscr{C}(K) = \lim_{K\to\infty}\left(m\cdot\max_{0\leq k\leq\lfloor K\rfloor}\frac{S_{\mathcal{A}_\setminus^k} + \rho_k^{k+1}\left(F^k - \frac{m-1}{m}S_{\mathcal{A}_\setminus^k}\right) - F^{k+1}}{S_{\mathcal{A}_\setminus^k}}\right).$$

The CPPI floor terms vanish from this equation when the limit is taken. This is a consequence of the assumption about F in Proposition 3.6.4. Each candidate of the optimisation therefore reduces to the same value, $1/m$, as $K \to \infty$. From this we reach the desired conclusion.

We additionally require finiteness for $\lim_{K\to\infty} -(K+1)^2 \frac{\partial \mathscr{C}(K)}{\partial K}$, but we cannot generally presume that $\frac{\partial \mathscr{C}(K)}{\partial K}$ is $\mathrm{O}\left(1/(K+1)^2\right)$—or that this derivative exists at all. This is because the largest-valued stage (corresponding to the optimal value of k) may vary with K, leading to a piecewise definition for $\mathscr{C}(K)$. Such an issue is avoided when the financial parameters are equal over each stage and the reallocation schedule is uniform. Calculations confirming this are presented in Section 4.1.2.

This analytical stability finding is encouraging. However, further study is required in order to apply this reasoning to the numerical result; it is not straightforward to extend Proposition 3.6.4 to account for truncation errors.

3.6.2 Monotonicity

Unconditional monotonicity of the fully-implicit scheme between observations follows from Lemma 3.1 of [19]. It remains to show monotonicity at the reallocation instants, and this is straightforward. In the case of wealth-indexed linear interpolation, the relevant difference is

$$\begin{aligned} &\left[v_{i,j}^{n+1} - (v_1+\epsilon_1)\,q - (v_2+\epsilon_2)\,(1-q)\right] - \left[v_{i,j}^{n+1} - v_1 q - v_2(1-q)\right] \\ =& -\left(\epsilon_1 q + \epsilon_2(1-q)\right) \\ \leq&\ 0, \end{aligned}$$

for any non-negative perturbations ϵ_1 and ϵ_2. Here v_1 and v_2 represent the two lookup table values and $0 \leq q \leq 1$ and $(1-q)$ are their respective weights. Similar calculations apply to the similarity extrapolant (using Equation (3.3.9)) and the near-field boundary (using Equation (3.2.2))—all of the coefficients in these two equations are positive. In general, higher-order interpolation schemes do not guarantee positive coefficients and therefore do not preserve monotonicity.

3.7 Summary

In this chapter we developed numerical schemes for solving the classical and limited-borrowing CPPI problem. As an assessment of robustness we sought to verify whether these schemes would theoretically converge even as $K \to \infty$. Assuming a strong comparison result holds, stability, monotonicity and consistency are sufficient to prove convergence to the viscosity solution. In demonstrating that a scheme satisfies the first two of these properties, the reallocation instants and the intervals between reallocations can be addressed separately.

For the fixed-borrowing-limit case we have proven that the jump condition (2.6.5) can be implemented in a way that preserves ℓ^∞ stability (independent of the timestep and grid refinement level) and monotonicity. These conditions are met at the reallocation instants, even as $K \to \infty$. Therefore the limited-borrowing case will be robustly stable and monotone if the discretisation of the inter-reallocation dynamics also has these properties (as our scheme does with fully-implicit timestepping and linear interpolation).

Our results are in contrast weaker for the similarity extrapolant workaround to the classical case. The monotonicity of the jump condition (2.6.4) is again unconditional (for linear interpolation), but it remains to be determined whether the similarity extrapolant approach is numerically stable. Our analytical result developed herein is encouraging; we find that stability can be achieved when truncation and roundoff errors are not present in the calculation. This, along with our numerical results, leads us to conjecture the similarity extrapolant approach is indeed stable. If this is true, then we additionally conjecture that the stability result can be generalised to accommodate classes of problems with autonomous CPPI floors and volatilities that vary with the underlying risky asset.

We recommend that computational implementations primarily use the limited-borrowing approach. In addition to making more financial sense than the classical (unlimited-borrowing) case, it is just as straightforward to implement and has fewer unresolved theoretical matters. In Section 5.6 we will investigate the suitability of limited-borrowing approach as an approximation for the classical case.

4 Analytical special cases

In this chapter we derive analytical results for the classical CPPI pricing problem. The formulæ we develop here are only suitable for pricing a special class of CPPI-backed guarantees: those with unlimited borrowing, under a model where (i) the risk-free asset and the CPPI floor both evolve at the same constant rate, and (ii) the volatility is constant. Nevertheless, these formulæ are useful for validating some of our numerical results.

4.1 Discrete case

4.1.1 Formulation

The analytical solutions of Balder, Brandl and Mahayni for a CPPI claim under discrete rebalancing [4] can be extended beyond the Black-Scholes case. Here we present an analogous result for when the risky asset evolves according to the jump diffusion described by Equation (2.4.1). It is easier to solve for v_L by indirect means, by first pricing v_J and then applying the parity relationship given by Equation (2.6.8).

Recall from Proposition 3.6.4 that the time-zero risk-neutral value of a classical CPPI claim with payoff v_J and initial wealth W_0 can be expressed using the product of $K+1$ call option values:

$$v_J(W_0, 0) = \max\left\{W_0 - F^0, 0\right\} \prod_{k=0}^{K} \left[\frac{m}{S_{\mathcal{A}^k_\setminus}} \mathcal{C}\left(S_{\mathcal{A}^k_\setminus}; F^{k+1} - \rho_k^{k+1} B^k_{\min}, t_{\mathrm{o}}^{k+1} - t_{\mathrm{o}}^k \right) \right].$$

This holds when (i) $\varrho(t) = r(t)$, (ii) r and σ are piecewise constant, and (iii) $B^k_{\min}$ is always nonpositive. As before, $S_{\mathcal{A}^k_\setminus} = \frac{m}{m-1}(F^k - B^k_{\min})$ and $\mathcal{C}(S; X, T)$ represents the time-0 price of a European call option with spot S, strike price X and maturity T. For notational convenience, model-specific arguments are omitted.

In an analytical context the choice of $B^k_{\min}$ is arbitrary because there is no domain truncation. So the above is more conveniently expressed (using homogeneity) as

$$\begin{aligned} v_J(W_0, 0) &= \max\left\{W_0 - F^0, 0\right\} \prod_{k=0}^{K} \left[\mathcal{C}\left(m; \frac{m}{S_{\mathcal{A}^k_\setminus}}\left(F^{k+1} - \rho_k^{k+1} B^k_{\min}\right), t_{\mathrm{o}}^{k+1} - t_{\mathrm{o}}^k\right)\right] \\ &= \max\left\{W_0 - F^0, 0\right\} \prod_{k=0}^{K} \left[\mathcal{C}\left(m; \rho_k^{k+1}(m-1), t_{\mathrm{o}}^{k+1} - t_{\mathrm{o}}^k\right)\right]. \end{aligned}$$

The strike price simplification results from the definition of $S_{\mathcal{A}^k_\setminus}$ and the assumption that the CPPI floor evolves at the risk-free rate.

While this result is linear (for wealth $W_0 > 0$) in the initial cushion $W_0 - F^0$, the slope is nontrivial.

When the risky asset evolves according to (2.4.1) with lognormal jumps (Equation (2.4.2)), there is an analytical solution for a vanilla European call with spot price S, strike X, maturity T, and the market parameters defined in Section 2.4.1:

$$\mathcal{C}(S; X, T) = \sum_{\ell=0}^{\infty} \left[S e^{-\lambda(\kappa+1)T} \frac{\left(\lambda(\kappa+1)T\right)^\ell}{\ell!} \Phi(d_{1,\ell}) - e^{-(r+\lambda)T} X \frac{\left(\lambda T\right)^\ell}{\ell!} \Phi(d_{2,\ell}) \right], \quad (4.1.1)$$

$$\text{where} \quad d_{1,\ell} \equiv \frac{\ln\left(\frac{S}{X}\right) + \left[r + \frac{\sigma^2}{2} - \lambda\kappa\right] T + \ell(\mu + \gamma^2)}{\sqrt{\sigma^2\delta + \ell\gamma^2}},$$

$$\text{and} \quad d_{2,\ell} \equiv d_{1,\ell} - \sqrt{\sigma^2\delta + \ell\gamma^2}.$$

Here Φ is the standardised normal cumulative distribution function. The analytical solution for vanilla European options with lognormal jumps is a Poisson-weighted sum of the Black-Scholes prices given that ℓ jumps have occurred. This result was first presented by Merton in [35]. Although this expression is not closed-form, it is well-approximated by a suitably high partial sum [25].

For the purposes of validating our numerical results we are interested in one final simplification:

Proposition 4.1.1 (Analytical special case valuation of a discrete classical CPPI claim)**.** *If*

- *the risky asset follows a Merton jump diffusion with constant parameters over the entire investment horizon,*

- *the risk-free asset and the guaranteed CPPI floor both evolve at the same rate, and*
- *reallocations are uniformly spaced,*

then the time-zero risk-neutral value of a classical CPPI claim with initial wealth W_0 *is*

$$v_J(W_0,0) = \max\left\{W_0 - F^0, 0\right\}\left[\mathcal{C}\left(m; e^{r\delta}(m-1), \delta\right)\right]^{K+1},$$

where

$$\begin{aligned}
\mathcal{C}\left(m; e^{r\delta}(m-1), \delta\right) &= \sum_{\ell=0}^{\infty} E_\ell, \\
E_\ell &\equiv m e^{-\lambda(\kappa+1)\delta}\frac{(\lambda(\kappa+1)\delta)^\ell}{\ell!}\Phi(d_{1,\ell}) - (m-1)e^{-\lambda\delta}\frac{(\lambda\delta)^\ell}{\ell!}\Phi(d_{2,\ell}), \\
\delta &\equiv t^{k+1} - t^k \equiv \tfrac{T}{K+1}, \\
d_{1,\ell} &\equiv \frac{\ln\left(\frac{m}{m-1}\right) + \left[\frac{\sigma^2}{2} - \lambda\kappa\right]\delta + \ell(\mu+\gamma^2)}{\sqrt{\sigma^2\delta + \ell\gamma^2}}, \\
\text{and} \quad d_{2,\ell} &\equiv d_{1,\ell} - \sqrt{\sigma^2\delta + \ell\gamma^2}.
\end{aligned}$$

By Equation (2.6.8) *the corresponding liability is*

$$v_L(W_0,0) = W_0 - \rho^0_{K+1}F^T - \max\left\{W_0 - F^0, 0\right\}\left[\mathcal{C}\left(m; e^{r\delta}(m-1), \delta\right)\right]^{K+1}.$$

4.1.2 Limiting behaviour

Next we use Lemma 3.6.5 to determine the limiting behaviour for Proposition 4.1.1 as $K \to \infty$.

Preliminaries. The function $\Phi(x)$ is bounded and approaches 1 as $x \to \infty$.

By direct evaluation, we see that $\lim_{K\to\infty} d_{1,\ell}$ is finite for $\ell > 0$. The same can be said for:

$$\begin{aligned}
\lim_{K\to\infty} d_{2,\ell} &= \lim_{K\to\infty} d_{1,\ell} - \sqrt{\ell}\gamma, \\
\lim_{K\to\infty} -(K+1)^2 \frac{\partial d_{1,\ell}}{\partial K} &= \frac{(\frac{\sigma^2}{2} - \lambda\kappa)T}{\sqrt{\ell}\gamma} - \frac{\sigma^2 T \lim_{K\to\infty} d_{1,\ell}}{2\ell\gamma^2}, \\
\text{and } \lim_{K\to\infty} -(K+1)^2 \frac{\partial d_{2,\ell}}{\partial K} &= \lim_{K\to\infty} -(K+1)^2 \frac{\partial d_{1,\ell}}{\partial K} - \frac{\sigma^2 T}{2\sqrt{\ell}\gamma}.
\end{aligned}$$

On the other hand, when $\ell = 0$ we have

$$\lim_{K\to\infty} d_{1,0} = \infty = \lim_{K\to\infty} d_{2,0}.$$

Let $\mathbf{1}_A(x)$ denote an indicator function that is 1 when x is in set A, and 0 otherwise. Applying the above results yields

$$\lim_{K\to\infty} E_\ell = m\mathbf{1}_{\{0\}}(\ell) - (m-1)\mathbf{1}_{\{0\}}(\ell) = \mathbf{1}_{\{0\}}(\ell),$$

since all but the 0^{th} case of E_ℓ are nonzero degree polynomials in $\frac{1}{N}$ that vanish in the limit. Summing over ℓ confirms that $\lim_{K\to\infty} \mathcal{C}\left(m; e^{r\delta}(m-1), \delta\right) = 1$.

Applying Lemma 3.6.5. For convenience define

$$G \equiv \frac{\ln \frac{m-1}{m} - \mu}{\gamma}. \tag{4.1.2}$$

Then for nonzero ℓ,

$$\begin{aligned}
-(K+1)^2\frac{\partial E_\ell}{\partial K} =& -\lambda T(\kappa+1)me^{-\lambda(\kappa+1)\delta}\frac{(\lambda(\kappa+1)\delta)^\ell}{\ell!}\Phi(d_{1,\ell}) \\
&+\lambda T(m-1)e^{-\lambda\delta}\frac{(\lambda\delta)^\ell}{\ell!}\Phi(d_{2,\ell}) \\
&+\lambda T(\kappa+1)me^{-\lambda(\kappa+1)\delta}\frac{(\lambda(\kappa+1)\delta)^{\ell-1}}{(\ell-1)!}\Phi(d_{1,\ell}) \\
&-\lambda T(m-1)e^{-\lambda\delta}\frac{(\lambda\delta)^{\ell-1}}{(\ell-1)!}\Phi(d_{2,\ell}) \\
&+me^{-\lambda(\kappa+1)\delta}\frac{(\lambda(\kappa+1)\delta)^\ell}{\ell!}\Phi'(d_{1,\ell})\left(-(K+1)^2\frac{\partial d_{1,\ell}}{\partial K}\right) \\
&-(m-1)e^{-\lambda\delta}\frac{(\lambda\delta)^\ell}{\ell!}\Phi'(d_{2,\ell})\left(-(K+1)^2\frac{\partial d_{2,\ell}}{\partial K}\right).
\end{aligned}$$

The common factor of $\left(\frac{1}{K+1}\right)^{(\ell-1)}$ arising from the appearance of $\delta^{(\ell-1)}$ causes most terms to vanish:

$$\lim_{K\to\infty} -(K+1)^2\frac{\partial E_\ell}{\partial K} = \begin{cases}\lambda T\left[m(\kappa+1)\Phi(\gamma-G)-(m-1)\Phi(-G)\right], & \ell=1,\\ 0, & \ell>1.\end{cases}$$

On the other hand,

$$\begin{aligned}
-(K+1)^2\frac{\partial E_0}{\partial K} =& -\lambda T(\kappa+1)me^{-\lambda(\kappa+1)\delta}\Phi(d_{1,0}) \\
&+\lambda T(m-1)e^{-\lambda\delta}\Phi(d_{2,0}) \\
&+me^{-\lambda(\kappa+1)\delta}\Phi'(d_{1,0})\left(-(K+1)^2\frac{\partial d_{1,0}}{\partial K}\right) \\
&-(m-1)e^{-\lambda\delta}\Phi'(d_{2,0})\left(-(K+1)^2\frac{\partial d_{2,0}}{\partial K}\right).
\end{aligned}$$

Adding the last two terms together produces an expression that vanishes in the limit because the Gaussian decay dominates. Hence

$$\begin{aligned}
&\lim_{K\to\infty} -(K+1)^2\frac{\partial \mathcal{C}\left(m;e^{r\delta}(m-1),\delta\right)}{\partial K} \\
=& -\lambda T(\kappa+1)m+\lambda T(m-1)+m\lambda T(\kappa+1)\Phi(\gamma-G)-(m-1)\lambda T\Phi(-G) \\
=& \;(m-1)\lambda T\Phi(G)-m\lambda T(\kappa+1)\Phi(G-\gamma)
\end{aligned}$$

and we conclude that under the assumptions of Proposition 4.1.1 (constant financial parameters, Merton jumps, nonautonomous CPPI floors and uniform reallocations)

$$\lim_{K\to\infty} v_J(W_0, 0) = e^{\lambda T\left((m-1)\Phi(G)-m(\kappa+1)\Phi(G-\gamma)\right)} \max\{W_0 - F^0, 0\}. \tag{4.1.3}$$

In the no-jumps case, the exponential factor is unity. This is consistent with the result in [4] for risk-neutral drift.

4.2 Continuous case

Next we present an alternative derivation of the above result. Our work in this section closely follows the proof of Proposition 3.2 in [15] which addresses expected CPPI shortfalls for general Lévy processes. The difference is that here we present a more explicit set of calculations for the specific case where the stock dynamics are described by a diffusion process with lognormally distributed jumps.

In the following we use the notation $\cdot_t$ to denote a continuous-time process.

State variable

Previously, we used the values of the risky and risk-free assets as our state variables. This permitted us to impose constraints on the CPPI portfolio's composition. However, for the unconstrained, continuous case it is preferable to describe the CPPI portfolio using the *discounted cushion process*:

$$\bar{C}_t \equiv \exp\left(\int_{\min\{t,t^\star\}}^{0} r(u)\,\mathrm{d}u\right)\left(S_{\min\{t,t^\star\}} + B_{\min\{t,t^\star\}} - F_{\min\{t,t^\star\}}\right), \quad 0 < t \leq T, \tag{4.2.1}$$

with $\bar{C}_0 = W_0 - F_0 \geq 0$.

The random variable $t^\star$ is a *stopping time* representing the first instant where the CPPI strategy fails (i.e. the CPPI portfolio is worth less than the prevailing CPPI floor F_t). More formally,

$$t^\star \equiv \inf\{\, t \mid S_t + B_t - F_t < 0 \,\} = \inf\{\, t \mid \bar{C}_t < 0 \,\}. \tag{4.2.2}$$

If $t^\star$ occurs within the investment horizon then all remaining wealth is subsequently invested in the risk-free asset. Consequently, $\bar{C}_t$ is constant and negative on the interval $[t^\star, T]$.

Continuous-time CPPI dynamics

For the continuous-time processes S_t, B_t and F_t we use the models presented in Section 2.4. Once again we model the risk-free rate as a deterministic function of time. Additionally, we assume that the CPPI floor appreciates at the risk-free rate. This leads to the following characterisation of the continuous-time CPPI strategy.

Proposition 4.2.1. *The pre-shortfall CPPI strategy's discounted cushion process satisfies the stochastic differential equation*

$$\frac{\mathrm{d}\bar{C}_t}{m\bar{C}_{t^-}} = (-\lambda\kappa)\,\mathrm{d}t + \sigma_t\,\mathrm{d}Z_t + (J_t - 1)\mathrm{d}q_t, \qquad 0 \le t \le t^{\star^-}. \tag{4.2.3}$$

Proof. As an intermediate step we will formulate the undiscounted cushion dynamics.

Recall that the CPPI strategy is wealth-preserving: $S_{t^-} + B_{t^-} = S_t + B_t$. As in Section 2.4, the subscript t^- represents the instant preceding time t. Since the process F_t is continuous, $S_{t^-} + B_{t^-} - F_{t^-} = S_t + B_t - F_t + \epsilon$.

The continuous-time analogue to Equation 2.2.3 requires that—at each instant t—the risky holding be worth $m(S_{t^-} + B_{t^-} - F_{t^-})$. Since the CPPI strategy is self-financing, the risk-free holding is worth $(1-m)(S_{t^-} + B_{t^-}) + mF_{t^-}$. It then follows that the difference between the risk-free asset and the CPPI floor is $(1-m)(S_{t^-} + B_{t^-} - F_{t^-})$.

Consider the undiscounted cushion process $S_t + B_t - F_t$. This can be treated as a two-asset *wealth process* [16] involving (i) the risky asset, and (ii) the difference between the risk-free asset and the floor. For the risky asset, the change in value from t^- to t is the product of the risky position (at t^-) and the unit change in S. By the above findings, this product can be expressed as $m(S_{t^-} + B_{t^-} - F_{t^-})\frac{dS_t}{S_{t^-}}$. The other asset class can be handled with similar reasoning, recalling that both the risk-free asset and the CPPI floor value are assumed to appreciate at the risk-free rate. It follows that the undiscounted CPPI cushion dynamics are

$$\frac{\mathrm{d}\left(S_t + B_t - F_t\right)}{S_{t^-} + B_{t^-} - F_{t^-}} = m\frac{\mathrm{d}S_t}{S_{t^-}} + (1-m)\frac{\mathrm{d}B_t}{B_{t^-}}$$

The final result is attained by substituting Equations (2.4.1) and (2.4.3), and then applying Itō's lemma. ∎

Remark 4.2.2 (Relation to a single power option)**.** For completeness, we note that when $\varrho = r$ and $\lambda = 0$, the continuous-reallocation dynamics (Equation (4.2.3)) have a tractable solution that involves $(S_t/S_0)^m$ [10, 36]. This observation allows this special case of CPPI-backed guarantee to be treated as a power option written on the risky asset [36]. However, in a risk-neutral context, this observation offers us little additional insight because the m^{th}-order terms all cancel out; after simplification the risk-neutral valuation has no dependence on the underlying assets, apart from linear dependence on the initial cushion. This is consistent with our previous findings. ∎

An expression for gap risk

The justification for using $\bar{C}_t$ rather than the undiscounted cushion is as follows. We seek the time-0 fair-value liability on a continuously-reallocated CPPI instrument, for an initial endowment of W_0. This quantity was previously denoted as $\lim_{K\to\infty} v_L(W_0, 0)$. As before, we need to determine the risk-neutral time-0 expectation of the discounted payoff:

$$\mathrm{E}^{\mathbb{Q}}\left\{ \exp\left(\int_T^0 r(u)\,\mathrm{d}u\right) \max\left\{F_T - S_T - B_T, 0\right\} \,\middle|\, S_0 + B_0 = W_0 \right\},$$

noting that the reallocation behaviour will change if a shortfall is experienced in the lifetime of the instrument. By Equation 4.2.1, this is equivalent (in the context of continuous-time reallocation) to determining

$$\mathrm{E}^{\mathbb{Q}}\left\{ -\max\left\{-\bar{C}_T, 0\right\} \;\middle|\; \bar{C}_0 = W_0 - F_0 \right\} = \mathrm{E}^{\mathbb{Q}}\left\{ \min\left\{\bar{C}_T, 0\right\} \;\middle|\; \bar{C}_0 = W_0 - F_0 \right\}.$$

This expression would be more complicated had we instead used the undiscounted cushion. Here $\bar{C}_t$ obeys Equation (4.2.3) for t in the interval $[0, t^\star]$.

Applying the law of total expectation yields

$$\begin{aligned}\lim_{K\to\infty} v_L(W_0, 0) = \quad & \int_0^T \mathrm{E}^{\mathbb{Q}}\left\{ \min\left\{\bar{C}_T, 0\right\} \mid t^\star = u,\ \bar{C}_0 = W_0 - F_0 \right\} \mathrm{P}^{\mathbb{Q}}\left\{t^\star \in \mathrm{d}u\right\}\ \mathrm{d}u \\ + \quad & \mathrm{E}^{\mathbb{Q}}\left\{ \min\left\{\bar{C}_T, 0\right\} \mid t^\star > T,\, \bar{C}_0 = W_0 - F_0 \right\} \mathrm{P}^{\mathbb{Q}}\left\{t^\star > T\ \right\},\end{aligned}$$

and this simplifies to

$$\lim_{K\to\infty} v_L(W_0, 0) = \int_0^T \mathrm{E}^{\mathbb{Q}}\left\{\bar{C}_T \mid t^\star = u,\, \bar{C}_0 = W_0 - F_0\right\} \mathrm{P}^{\mathbb{Q}}\left\{t^\star \in \mathrm{d}u\right\}\ \mathrm{d}u \qquad (4.2.4)$$

because the expectation conditional upon no shortfall taking place vanishes. We can therefore solve the problem at hand by determining the expected shortfall under the risk-neutral measure.

Characterising the first shortfall

Before continuing it is necessary to introduce some notation and concepts from the realm of stochastic calculus.

Recall that the ordinary differential equation $\mathrm{d}y = y(x)\ \mathrm{d}x$ with initial condition $y(0) = y_0$ has the solution $y(x) = y_0 e^x$. The stochastic abstraction of the exponential function is called the *Doléans-Dade exponential*.

Definition 4.2.3 ([14, 15]). The Doléans-Dade exponential $\mathcal{E}(\cdot)_t$ is the solution to the stochastic differential equation $\mathrm{d}Y_t = Y_t\ \mathrm{d}X_t$ with the initial condition $Y_0 = 1$. ■

The Doléans-Dade exponential has two pertinent properties [14, 15]:

1. If X_t is a Lévy Process with jump component $(\Delta X)_t$ then $\mathcal{E}(X)_t = \mathcal{E}(X)_{t^-}\left[1+(\Delta X)_t\right]$. The rightmost factor is a random variable and is in general not strictly positive. So, unlike the standard exponential function, the Doléans-Dade exponential has a nonzero probability of attaining nonpositive values.
2. If X_t is a Lévy Process then $\ln \mathcal{E}(X)_t$ is also a Lévy Process.

We can characterise the right-hand side of Equation (4.2.3) with the Lévy triplet $\left(-\lambda\kappa,\ \sigma^2,\ \nu\left(\mathrm{d}\zeta\right)\right)$, where $\nu(\mathrm{d}\zeta)$ is the Lévy measure representing the probability of a jump in $\frac{\mathrm{d}\bar{C}_t}{m\bar{C}_{t^-}}$ of magnitude $\zeta \equiv J - 1$ happening in a given instant. Since the jump magnitude and jump intensity are assumed independent, λ is finite, and J has the density $p(J)$, we have

$$\nu(\mathrm{d}\zeta) = \lambda p(J)\,\mathrm{d}J.$$

To proceed, we decompose the right-hand side of Equation (4.2.3) into the subprocesses L_t^{A} and L_t^{B}, where

1. $L_t^{\mathrm{A}} \sim \Big(-\lambda\kappa,\ \sigma^2,\ \nu\left(d\zeta\right)\mathbf{1}_{\left\{J_t > \frac{m-1}{m}\right\}}(J_t)\Big)$ is a jump-diffusion process that will almost surely not cause a shortfall, and
2. $L_t^{\mathrm{B}} \sim \Big(0,\ 0,\ \nu\left(d\zeta\right)\mathbf{1}_{\left\{J_t \le \frac{m-1}{m}\right\}}(J_t)\Big)$ is a pure-jump process of stock price drops significant enough to cause a shortfall.

Since the Merton model has finite activity jumps, so does L_t^{A}. This observation will simplify later calculations.

The following confirms that only L_t^{B} induces shortfalls. Equation (4.2.3) can now be written as

$$\frac{\mathrm{d}\bar{C}_t}{\mathrm{d}(L_t^{\mathrm{A}} + L_t^{\mathrm{B}})} = m\bar{C}_{t^-},$$

which has the solution

$$\begin{aligned}\bar{C}_t &= \bar{C}_0 \mathcal{E}\left(mL^{\mathrm{A}} + mL^{\mathrm{B}}\right)_t \\ &= \bar{C}_0 \mathcal{E}\left(mL^{\mathrm{A}} + mL^{\mathrm{B}}\right)_{t^-} \left[1 + m(J_t - 1)\mathrm{d}q_t\right] \\ &= \bar{C}_0 \mathcal{E}\left(mL^{\mathrm{A}}\right)_{t^-} \left[1 + m(J_t - 1)\mathrm{d}q_t\right]\end{aligned}$$

for t in the interval $[0, t^\star]$. The second equality follows from the first property of the Doléans-Dade exponential; the third equality holds because if $t \leq t^\star$ then the realised value of $L_{t^-}^{\mathrm{B}}$ is zero.

In the event of a jump at time $t^\star$, $\mathrm{d}q_{t^\star} = 1$ and the discounted cushion scales by a factor of $\big[1 + m(J_{t^\star} - 1)\big]$. It then follows that $\bar{C}_t$ ceases to be positive at

$$t^\star = \inf\left\{t \mid J_t \leq \tfrac{m-1}{m},\, \mathrm{d}q_t = 1\right\}.$$

We can now state the CPPI discounted dynamics (for $0 \leq t \leq T$) as

$$\bar{C}_t = \bar{C}_0 \mathcal{E}\left(mL^{\mathrm{A}}\right)_t \mathbf{1}_{\{t^\star > t\}}(t^\star) + \bar{C}_0 \mathcal{E}\left(mL^{\mathrm{A}}\right)_{(t^\star -)} \Big[1 + m(J_{t^\star} - 1)\Big] \mathbf{1}_{\{t^\star \leq t\}}(t^\star)$$

and hence write Equation (4.2.4) as

$$\begin{aligned}&\lim_{K\to\infty} v_L(W_0, 0) \\ &= \int_0^T \mathrm{E}^{\mathbb{Q}}\left\{(W_0 - F_0)\mathcal{E}\left(mL^{\mathrm{A}}\right)_{(t^\star -)}\Big[1 + m(J_{t^\star} - 1)\Big] \;\Big|\; t^\star = u\right\} \mathrm{P}^{\mathbb{Q}}\left\{t^\star \in \mathrm{d}u\right\}\, \mathrm{d}u. \\ &= (W_0 - F_0)\, \mathrm{E}^{\mathbb{Q}}\Big\{1 + m(J_{t^\star} - 1)\Big\} \int_0^T \mathrm{E}^{\mathbb{Q}}\left\{\mathcal{E}\left(mL^{\mathrm{A}}\right)_{(t^\star -)} \;\Big|\; t^\star = u\right\} \mathrm{P}^{\mathbb{Q}}\left\{t^\star \in \mathrm{d}u\right\}\, \mathrm{d}u.\end{aligned}$$

The last equality is a consequence of J being independent of $t^\star$.

At this stage the result still does not look very tractable. The key observation [15] is that $\ln \mathcal{E}(mL^A)_t$ is also a Lévy Process, and if its characteristic function —which we can calculate using the Lévy-Khinchin representation [14]—is of the form $\mathrm{E}^{\mathbb{Q}}\left\{e^{\mathrm{i}t\varphi(z)}\right\}$, then

$$\mathrm{E}^{\mathbb{Q}}\left\{\mathcal{E}(mL^A)_{t^\star-} \mid t^\star = u\right\} = e^{\varphi(-\mathrm{i})u}.$$

The occurrence of jumps is governed by a Poisson process with rate λ, so the occurrence of shortfall-inducing jumps in $(L^B)_t$ is governed by a Poisson process with rate

$$\lambda^\star \equiv \lambda\,\mathrm{P}^{\mathbb{Q}}\left\{J_t \leq \frac{m-1}{m}\right\} = \lambda\Phi(G),$$

where $\Phi(\cdot)$ is the standardised normal cumulative distribution function and G is as defined in Equation (4.1.2). Therefore $t^\star$ is exponentially distributed with density $\lambda^\star e^{-\lambda^\star u}$.

Incorporating these developments yields

$$\begin{aligned}\lim_{K\to\infty} v_L(W_0, 0) &= (W_0 - F_0)\lambda^\star\,\mathrm{E}^{\mathbb{Q}}\left\{1 + m(J_{t^\star} - 1)\right\}\int_0^T e^{[\varphi(-\mathrm{i})-\lambda^\star]u}\,\mathrm{d}u \\ &= (W_0 - F_0)\lambda^\star\,\mathrm{E}^{\mathbb{Q}}\left\{1 + m(J_{t^\star} - 1)\right\}\frac{e^{\left(\varphi(-i)-\lambda^\star\right)T} - 1}{\varphi(-i) - \lambda^*}.\end{aligned}$$

after directly integrating. This is valid because $\varphi(-i)$ is independent of t. The following calculation will confirm this.

Final steps

The challenge here is to find an appropriate Lévy-Khinchin representation for the process $\ln \mathcal{E}(mL^A)_t$. Since L_t^A is a finite-activity process we can use a simpler version of the Lévy-Khinchin representation [15, Remark 3.1] :

$$\begin{aligned}\varphi(-i) &= -m\lambda\kappa + m\int_{\zeta>-\frac{1}{m}} \zeta\,\nu(\mathrm{d}\zeta) \\ &= -m\lambda\,\mathrm{E}^{\mathbb{Q}}\{J-1\} + m\lambda\,\mathrm{E}^{\mathbb{Q}}\left\{J-1 \,\middle|\, J > \frac{m-1}{m}\right\}\mathrm{P}^{\mathbb{Q}}\left\{J > \frac{m-1}{m}\right\} \\ &= -m\lambda^\star\,\mathrm{E}^{\mathbb{Q}}\left\{J-1 \,\middle|\, J \leq \frac{m-1}{m}\right\} \qquad (4.2.5) \\ &= -m\lambda^\star\,\mathrm{E}^{\mathbb{Q}}\left\{J \,\middle|\, J \leq \frac{m-1}{m}\right\} + m\lambda^\star \\ &= m\lambda^\star - m\lambda(\kappa+1)\Phi(G-\gamma)\end{aligned}$$

The last equality follows from the partial expectation of a lognormal random variable [2, Equation 9.3] and the property $\Phi(-x) = 1 - \Phi(x)$.

From Equation (4.2.5) we see—perhaps surprisingly—that

$$\varphi(-i) - \lambda^\star = -\lambda^\star \, \mathrm{E}^{\mathbb{Q}} \Big\{ 1 + m(J_{t^\star} - 1) \Big\},$$

so the desired limit simplifies to

$$\lim_{K \to \infty} v_L(W_0, 0) = -(W_0 - F_0) \Big[e^{\big(\varphi(-i) - \lambda^\star\big)T} - 1 \Big]$$

or more revealingly,

$$\lim_{K \to \infty} v_L(W_0, 0) = -(W_0 - F_0) \left[e^{-\lambda^\star T \, \mathrm{E}^{\mathbb{Q}} \Big\{ 1 + m(J_{t^\star} - 1) \Big\}} - 1 \right].$$

After the appropriate substitutions we get

$$\lim_{K \to \infty} v_L(W_0, 0) = -(W_0 - F_0) \left[e^{\lambda T \big((m-1)\Phi(G) - m(\kappa+1)\Phi(G-\gamma) \big)} - 1 \right].$$

Moreover, by Equation (2.6.8) and the fact that the initial cushion was assumed to be nonnegative,

$$\lim_{K \to \infty} v_J(W_0, 0) = e^{\lambda T \big((m-1)\Phi(G) - m(\kappa+1)\Phi(G-\gamma) \big)} \max\{W_0 - F_0, 0\}$$

which agrees with the previous result from Equation (4.1.3).

5 Numerical results and validation

5.1 Overview

Here we present numerical experiments that demonstrate how this framework agrees with —and extends—existing CPPI models. Our valuations are functions of the initial wealth W_0. To facilitate comparisons across various CPPI floor trajectories we will also state the initial cushion, $C_0 = W_0 - F^0$. Unless noted otherwise, our computational tests' financial parameters take the values listed in Table 5.1.

Table 5.1: Financial parameters

Symbol	Value	Description
		Contractually specified
m	5	Leverage factor
T	1 year	Contract term
F_T	150	CPPI floor at maturity
ϱ	0.05	Constant CPPI floor rate
K	250	CPPI portfolio reallocations
		Market-calibrated
r	0.05	Constant risk-free rate
σ	0.2	Constant volatility
λ	0.61	Jump frequency
μ	-0.7	Mean log jump size
γ	0.85	Standard deviation of log jump size

These financial parameters were introduced in Chapter 2. The default value of K roughly corresponds to one reallocation per business day. By *market-calibrated* we refer to financial parameters which in practice should be estimated from market data. The values in Table 5.1 are *not* calibrated to current market conditions; rather, we chose artificial values that would challenge the numerical framework.

The first two experiments (Sections 5.2 and 5.3) validate our framework against the analytical results derived in Chapter 4. More precisely, we verify that (i) increasing the resolution of the computational grid lowers the error between the numerical results and the analytical solutions, and (ii) that the convergence behaviour of the results is consistent with theory. This is done by comparing the results of trials run on successively finer grids. We start with the timestep $\Delta\tau$ and a coarse initial (S, B) grid. This corresponds to *refinement level* (RL) 0. From $\text{RL} = N$ to $\text{RL} = N + 1$ (i) the timestep is halved, and (ii) for the two prototypical one-dimensional grids, new gridpoints are added equidistantly between each of the old ones. So an $n \times m$ grid refines to a $(2n - 1) \times (2m - 1)$ grid. Grids were scaled about the prevailing allocation locus, following the design described in Appendix B. For the sake of simplicity, each trial uses constant timesteps, although the framework does permit adaptive timestepping.

For the other experiments our trials are arranged similarly, except that there are no analytical results against which we can compare directly. In the penultimate experiment, we begin with a high-resolution grid and observe the sensitivity to artificially imposed borrowing limits.

We use two metrics for assessing our results. Let $V(\text{RL})$ represent the computational approximation of $v^0(W_0, 0)$ (for some fixed W_0) at refinement level RL. The convergence ratio , CR, is defined at $\text{RL} = N$ by

$$\text{CR} \equiv \frac{V(\text{RL} = N - 1) - V(\text{RL} = N - 2)}{V(\text{RL} = N) - V(\text{RL} = N - 1)}, \tag{5.1.1}$$

with all other parameters remaining unchanged (unless noted otherwise). It is customary to assume that in the error between theoretical and computational results, the higher-order timestep and grid spacing terms are negligible. So as RL approaches infinity, a convergence ratio of 2 corresponds to linear convergence, and similarly a ratio of 4 is theoretically consistent with quadratic convergence.

Convergence ratios are useful for quantifying the uniformity of convergence and estimating the incremental tradeoff between computational cost and approximation error. However, this metric says nothing about the accuracy on the initial grid. So, whenever possible we also compute the percentage error (%RE) for a computed value $V(\text{RL} = N)$ relative to the theoretical value THEO:

$$\%\text{RE} \equiv \frac{V(\text{RL} = N) - \text{THEO}}{\text{THEO}}. \tag{5.1.2}$$

In Section 3.6.2 it was shown that the numerical scheme is monotone when using fully-implicit timestepping. Our framework also accommodates Crank-Nicolson timestepping. Despite the Crank-Nicolson scheme being only conditionally monotone for the chosen discretisation [18], it was found that—in terms of convergence ratio consistency—using Crank-Nicolson timestepping with Rannacher smoothing (two initial fully-implicit timesteps for each stage of the PIDE solve) was usually preferable to using the fully-implicit scheme at all timesteps. The datasets from each of the two schemes were consistent, but as expected, the results with Crank-Nicolson timestepping converged more quickly since this scheme is theoretically $O(\Delta\tau^2)$.

5.2 Daily reallocation and unlimited borrowing

We begin by applying this framework towards solving the problem treated in Section 4.1: Merton jump diffusion in the underlying, discrete reallocation, unlimited borrowing and a CPPI floor value appreciating at the risk-free rate. This is an appropriate starting point because an analytical solution exists and is piecewise linear in the cushion, as given by Proposition 4.1.1. Moreover, the homogeneity property (Proposition 3.3.3) holds, and the similarity extrapolant is—neglecting truncation errors—exact. The numerical results, with comparisons to the analytical results, are presented in Tables 5.2 and 5.3.

This experiment—and the next—should be viewed as validation exercises; for speed and accuracy one would in practice favour using the analytical solution to a model whenever possible. It should be recalled that this computational framework is intended to be used with (arguably more realistic) models where an analytical solution to the CPPI gap risk problem is not tractable. Such cases will be explored in Section 5.4 onward, but it is prudent to first test the framework on easier problems.

The simplicity of this problem permits adequate results to be achieved with relatively coarse initial grid dimensions, Crank-Nicolson timestepping and the wealth-indexed linear interpolation described in Section 3.4. The percentage relative error decreases with each refinement. Moreover, the reported convergence ratios are consistent with quadratic convergence. This is in agreement with [19], where Crank-Nicolson timestepping achieved quadratic convergence for a vanilla option, even when linear interpolation was used (to transfer information, at each timestep, between a non-uniform S grid and a uniform FFT grid).

The values in Table 5.4 are obtained by adding the corresponding computational results

Table 5.2: Values for v_J^0 with jumps, unlimited borrowing and discrete, daily ($K = 250$) reallocation. These results were computed using Crank-Nicolson timestepping, linear interpolation and the far-field similarity extrapolant, for initial cushions C_0 in the interval $[0, 250000]$. A representative subset of the data is presented. Refinement level (RL) 0 corresponds to a 52×52 initial grid and a timestep $\Delta\tau = \frac{T}{K+1}$. The percentage error (%RE) relative to the analytical value (THEO) is defined in Equation (5.1.2) and the convergence ratio (CR) is defined in Equation (5.1.1).

	$W_0 = 143.684414$ $C_0 = 1.000000$			$W_0 = 160.184414$ $C_0 = 17.500000$			$W_0 = 267.684414$ $C_0 = 125.000000$		
RL	Value	%RE	CR	Value	%RE	CR	Value	%RE	CR
0	2.477334	1.073		43.525177	1.474		312.338895	1.945	
1	2.458994	0.325		43.073772	0.421		308.002875	0.530	
2	2.453107	0.085	3.115	42.936092	0.100	3.279	306.718445	0.111	3.376
3	2.451568	0.022	3.826	42.903454	0.024	4.218	306.463650	0.028	5.041
4	2.451171	0.006	3.884	42.895566	0.006	4.138	306.397907	0.006	3.876
5	2.451068	0.001	3.821	42.893655	0.001	4.128	306.382660	0.001	4.312
THEO	2.451031			42.893043			306.378878		

Table 5.3: Values for v_L^0 with jumps, unlimited borrowing and discrete, daily ($K = 250$) reallocation, computed under the same conditions as Table 5.2

	$W_0 = 143.684414$ $C_0 = 1.000000$			$W_0 = 160.184414$ $C_0 = 17.500000$			$W_0 = 267.684414$ $C_0 = 125.000000$		
RL	Value	%RE	CR	Value	%RE	CR	Value	%RE	CR
0	-1.462018	0.757		-25.654894	1.031		-183.884516	1.381	
1	-1.453396	0.163		-25.456334	0.249		-181.966206	0.324	
2	-1.451626	0.041	4.870	-25.406363	0.052	3.973	-181.467020	0.049	3.843
3	-1.451178	0.010	3.955	-25.396126	0.012	4.882	-181.406408	0.015	8.236
4	-1.451069	0.003	4.092	-25.393757	0.003	4.322	-181.385198	0.003	2.858
5	-1.451041	0.001	3.915	-25.393223	0.001	4.432	-181.380348	0.001	4.373
THEO	-1.451031			-25.393043			-181.378878		

Table 5.4: Confirming the parity relationship (Equation (2.6.8)) for the unlimited borrowing, daily reallocation case. The Value columns arise from element-wise addition of the Value columns in Tables 5.2 and 5.3. The percentage error (%RE) relative to the analytical value (THEO) is defined in Equation (5.1.2) and the convergence ratio (CR) is defined in Equation (5.1.1).

	$W_0 = 143.684414$ $C_0 = 1.000000$			$W_0 = 160.184414$ $C_0 = 17.500000$			$W_0 = 267.684414$ $C_0 = 125.000000$		
RL	Value	%RE	CR	Value	%RE	CR	Value	%RE	CR
0	1.015316	1.532		17.870284	2.116		128.45438	2.764	
1	1.005598	0.560		17.617438	0.671		126.036669	0.829	
2	1.001481	0.148	2.361	17.529729	0.170	2.883	125.251424	0.201	3.079
3	1.000389	0.039	3.772	17.507328	0.042	3.915	125.057242	0.046	4.044
4	1.000103	0.010	3.805	17.501809	0.010	4.059	125.012709	0.010	4.360
5	1.000027	0.003	3.786	17.500432	0.002	4.011	125.002312	0.002	4.283
THEO	1.000000			17.500000			125.000000		

for v_J^0 and v_L^0 from Tables 5.2 and 5.3. This data confirms that the parity result (2.6.8) is obeyed.

5.3 Continuous reallocation and unlimited borrowing

In the previous section we saw that for a fixed reallocation frequency, our computational results converge to the exact discrete solution. Additionally, in the previous chapter we showed that the exact discrete solution approaches the exact continuous solution. Now we confirm that our computational results do the same, by successively halving the interval between reallocations. We again use Crank-Nicolson timestepping and the wealth-indexed linear interpolation described in Section 3.4.

Our implementation is parameterised by the number of reallocations, K. So in this experiment we let K tend to infinity, with one timestep between reallocations (in addition to the standard grid refinements). In particular, we start with a 64-stage PIDE solve and double this number at each refinement. This corresponds to K taking values in the sequence $\{2^6 - 1, 2^7 - 1, 2^8 - 1, \ldots\}$. The starting value of this sequence was chosen with computational time in mind; with one timestep per stage of the PIDE solve, starting instead with twice as many reallocations would double the computational time for each refinement level.

Results are presented in Tables 5.5 and 5.6. Again, the practical value of this test is limited to validating our implementation and showing that it is stable for large values of K.

Some difficulty was encountered in finding grid dimensions that were suitable for achieving well-behaved convergence ratios for both v_J^0 and v_L^0. The initial grid dimensions used to produce Tables 5.5 and 5.6 were well-suited for v_L^0; smaller dimensions were found to produce more favourable results (not reported) for v_J^0.

The computational results were found to converge to the sequence of theoretical, discrete reallocation results (THEO), which in turn appear to converge (albeit slowly) to the theoretical result for continuous reallocation (INF). The theoretical data shows that even as $K = 2047$, the differences between daily sub-daily reallocation and continuous reallocation is not negligible for the set of financial parameters listed in Table 5.1. The computational convergence ratios (CR) are eventually consistent with linear convergence. This agrees with the theoretical findings for Asian options, where the discrete-reallocation model converges to the continuous-reallocation result with a first-order discrete-observation error [48].

In a separate trial, stable results were achieved with $K = 500000$ and $\text{RL} = 1$. This is consistent with the results of Section 3.6.1.

Table 5.7 confirms that the parity relation (2.3.5) is satisfied. Quadratic convergence is achieved, despite the results of Tables 5.5 and 5.6 only achieving linear convergence. This is explained by noting that the process $v_J^0 + v_L^0$ is constant when the CPPI floor moves at the risk-free rate. More precisely, it is worth C_0 for all t. This is readily verified using the parity result (2.6.8), and the definitions of the cushion and the CPPI floor value. Moreover, the value of $v_J^0 + v_L^0$ does not depend on the interval between allocations. Consequently, there are no $\mathrm{O}(\Delta\tau) = \mathrm{O}(t_{\mathrm{o}}^{k+1} - t_{\mathrm{o}}^{k})$ terms in the error; instead, the second-order grid discretisation and interpolation errors dominate.

Table 5.5: Values for v_J^0 with jumps, unlimited borrowing and reallocation approaching the continuous case. These results were computed using fully-implicit timestepping, linear interpolation and the large-cushion similarity extrapolant, for initial cushions C_0 in the interval $[0, 250000]$. A representative subset of the data is presented. Refinement level (RL) 0 corresponds to a 52×52 initial grid, $2^6 - 1$ reallocations and a timestep $\Delta\tau = \frac{T}{K+1}$. Percentage errors (see Equation (5.1.2)) relative to the discrete analytical value (THEO, calculated from Proposition 4.1.1) and the continuous analytical value (INF, calculated from Equation (4.1.3)) are respectively represented by $\%\mathrm{RE_d}$ and $\%\mathrm{RE_c}$. The convergence ratio (CR) is defined in Equation (5.1.1).

	$W_0 = 143.684414$, $C_0 = 1.000000$					$W_0 = 267.684414$, $C_0 = 125.000000$				
RL	Value	THEO	$\%\mathrm{RE_d}$	$\%\mathrm{RE_c}$	CR	Value	THEO	$\%\mathrm{RE_d}$	$\%\mathrm{RE_c}$	CR
0	2.448644	2.433147	0.637	-0.356		308.407008	304.143426	1.402	0.401	
1	2.451243	2.445070	0.252	-0.250		306.997008	305.633702	0.446	-0.058	
2	2.452833	2.451179	0.067	-0.185	1.634	306.684136	306.397353	0.094	-0.159	4.507
3	2.454706	2.454272	0.018	-0.109	0.849	306.859065	306.783942	0.024	-0.102	-1.789
4	2.455943	2.455828	0.005	-0.059	1.515	306.996630	306.978445	0.006	-0.058	1.272
5	2.456639	2.456608	0.001	-0.031	1.777	307.080377	307.076001	0.001	-0.030	1.643
INF		2.457390					307.173760			

Table 5.6: Values for v_L^0 with jumps, unlimited borrowing and reallocation approaching the continuous case, computed under the same conditions as Table 5.5.

	$W_0 = 143.684414$, $C_0 = 1.000000$					$W_0 = 267.684414$, $C_0 = 125.000000$				
RL	Value	THEO	$\%\mathrm{RE_d}$	$\%\mathrm{RE_c}$	CR	Value	THEO	$\%\mathrm{RE_d}$	$\%\mathrm{RE_c}$	CR
0	-1.434114	-1.433147	0.067	-1.597		-180.364687	-179.143426	0.6817	-0.993	
1	-1.445774	-1.445070	0.049	-0.797		-180.998229	-180.633702	0.2018	-0.645	
2	-1.451358	-1.451179	0.012	-0.414	2.088	-181.433632	-181.397353	0.0200	-0.406	1.455
3	-1.454315	-1.454272	0.003	-0.211	1.888	-181.798457	-181.783942	0.0080	-0.206	1.193
4	-1.455839	-1.455828	0.001	-0.106	1.941	-181.981674	-181.978445	0.0018	-0.105	1.991
5	-1.456612	-1.456608	0.0002	-0.053	1.974	-182.076689	-182.076001	0.0004	-0.053	1.928
INF		-1.457390					-182.173760			

Table 5.7: Confirming the parity relationship (Equation (2.6.8)) for the unlimited borrowing, continuous reallocation case. The Value columns arise from element-wise addition of the Value columns in Tables 5.5 and 5.6. The percentage error (%RE) relative to the analytical value (THEO) is defined in Equation (5.1.2) and the convergence ratio (CR) is defined in Equation (5.1.1).

	$W_0 = 143.684414$ $C_0 = 1.000000$				$W_0 = 267.684414$ $C_0 = 125.000000$			
RL	Value	THEO	%RE	CR	Value	THEO	%RE	CR
0	1.014530	1.000000	1.453		128.042321	125.000000	2.434	
1	1.005469	1.000000	0.547		125.998779	125.000000	0.799	
2	1.001475	1.000000	0.148	2.269	125.250504	125.000000	0.200	2.731
3	1.000391	1.000000	0.039	3.684	125.060608	125.000000	0.048	3.940
4	1.000103	1.000000	0.010	3.770	125.014957	125.000000	0.012	4.160
5	1.000027	1.000000	0.003	3.777	125.003687	125.000000	0.003	4.051
INF		1.000000				125.000000		

5.4 Daily reallocation with limited borrowing

We now apply our framework to scenarios with limited borrowing, where we do not have a tractable analytical solution. These problems are more complicated than the previous ones, and require a few computational adjustments in order to obtain satisfactory convergence ratios.

In the previous experiments linear interpolation and Crank-Nicolson timestepping were used, and this combination was (somewhat serendipitously) found to be sufficient for obtaining quadratic convergence. The same was not observed in the limited-borrowing case, probably because the similarity extrapolant (which is no longer exact) is not used, and the result is no longer linear in the cushion.

For the limited-borrowing case, the combination of fully-implicit timestepping and quadratic interpolation was found to be more appropriate for achieving quadratic convergence. Standard quadratic Lagrange interpolation was found to be inadequate, so two variants (introduced in Section 3.4) were used instead: (i) an adaptation of the limited quadratic interpolation used in [48], and (ii) a piecewise modification of the standard scheme, with wealth-indexed quadratic Lagrange interpolation on each of the three intervals (corresponding to the three segments of Figure 2.2). The latter scheme prevents interpolation across these segments' intersections, where v is generally nonsmooth. Between these two methods, the results were marginally different, with neither alternative performing dominantly over the other. However, both methods were an improvement over the standard quadratic scheme.

Secondly, the imposition of a borrowing limit raises the issue of how to distribute each k^{th} grid's B ordinates. We settled on uniform distribution over the interval $[B^k_{\min}, F^k]$; Chebyshev spacing [44] was also implemented but was found to produce more erratic convergence ratios.

The computational results for limited borrowing are presented in Tables 5.8 and 5.9. Like previous experiments, quadratic convergence was only achieved when the grids were sufficiently dense and the timestep sufficiently small. In the absence of an analytical solution, the best validation tool is the parity result (applied in Table 5.10).

5.5 Continuous reallocation with limited borrowing

In order to further verify the stability of the limited-borrowing case, we repeat the previous experiment with the interval between reallocations tending towards zero. Consequently, K follows the same sequence as in Section 5.3. The results are presented in Tables 5.11 and 5.12. Despite quadratic convergence being obtained for the finite reallocation case, here only linear convergence is observed. This is again consistent with the theoretical first-order behaviour predicted for the convergence of a discretely-observed Asian model to a continuously-observed Asian model[48].

The parity relation was obeyed (not shown), with quadratic convergence for the same reasons as in Section 5.3. Another parallel with Section 5.3 is that the chosen numerical parameters were found to be better suited for computing v^0_L. Nevertheless, the convergence ratios from Table 5.12 can also be indirectly achieved for v^0_J, by calculating v^0_L and then applying the parity result. While this will improve the convergence behaviour for the calculation of v^0_J, it cannot be concluded that this will also result in smaller errors relative to the actual value.

Table 5.8: Values for v_J^0 with jumps, limited borrowing and daily reallocation ($K = 250$, $\varrho = r$). These results were computed using Crank-Nicolson timestepping and limited quadratic interpolation. A representative subset of the data is presented. The grids are designed to circumvent extrapolation for $W \to \infty$, using a fixed borrowing limit of $\hat{B} = 0$. Refinement level (RL) 0 corresponds to a 52×52 initial grid and a timestep $\Delta\tau = \frac{T}{K+1}$. The convergence ratio (CR) is defined in Equation (5.1.1).

	$W_0 = 146.881014$, $C_0 = 4.196600$		$W_0 = 160.170249$, $C_0 = 17.485835$		$W_0 = 176.956650$, $C_0 = 34.272237$	
RL	Value	CR	Value	CR	Value	CR
0	9.207987		32.632119		54.803378	
1	9.210330		32.629499		54.789261	
2	9.213594	0.718	32.633930	-0.591	54.787978	10.997
3	9.214412	3.992	32.635070	3.887	54.787474	2.547
4	9.214611	4.108	32.635360	3.936	54.787358	4.337
5	9.214660	4.060	32.635432	4.014	54.787328	3.890

Table 5.9: Values for v_L^0 with jumps, limited borrowing and daily reallocation ($K = 250, \varrho = r$). The conditions of Table 5.8 apply here, too.

	$W_0 = 146.881014$, $C_0 = 4.196600$		$W_0 = 160.170249$, $C_0 = 17.485835$		$W_0 = 176.956650$, $C_0 = 34.272237$	
RL	Value	CR	Value	CR	Value	CR
0	-4.978182		-15.121826		-20.495311	
1	-5.006248		-15.137278		-20.508177	
2	-5.015230	3.125	-15.146491	1.677	-20.513535	2.401
3	-5.017375	4.187	-15.148829	3.942	-20.514676	4.697
4	-5.017901	4.084	-15.149421	3.942	-20.514977	3.786
5	-5.018032	4.013	-15.149570	3.978	-20.515054	3.946

Table 5.10: Confirming the parity relationship (Equation (2.6.8)) for the limited borrowing, daily reallocation case. The Value columns arise from element-wise addition of the Value columns in Tables 5.8 and 5.9, and the THEO values match the cushions, C_0. The percentage error (%RE) relative to the analytical value (THEO) is defined in Equation (5.1.2) and the convergence ratio (CR) is defined in Equation (5.1.1).

	$W_0 = 146.881014$ $C_0 = 4.196600$			$W_0 = 160.170249$ $C_0 = 17.485835$			$W_0 = 176.956650$ $C_0 = 34.272237$		
RL	$V_J + V_L$	%RE	CR	$V_J + V_L$	%RE	CR	$V_J + V_L$	%RE	CR
0	4.229805	0.7912		17.510293	0.1399		34.308066	0.1045	
1	4.204082	0.1783		17.492220	0.0365		34.281085	0.0258	
2	4.198364	0.0420	4.498	17.487439	0.0092	3.780	34.274442	0.0064	4.062
3	4.197036	0.0104	4.307	17.486242	0.0023	3.995	34.272798	0.0016	4.038
4	4.196710	0.0026	4.070	17.485938	0.0006	3.947	34.272380	0.0004	3.939
5	4.196628	0.0007	3.985	17.485862	0.0002	3.945	34.272274	0.0001	3.930
THEO	4.196600			17.485835			34.272237		

Table 5.11: Values for v_J^0 with jumps, limited borrowing and reallocation approaching the continuous case ($\varrho = r$). These results were computed using fully-implicit timestepping and limited quadratic interpolation. A representative subset of the data is presented. The grids are designed to circumvent extrapolation for $W \to \infty$, using a fixed borrowing limit of $\hat{B} = 0$. Refinement level (RL) 0 corresponds to a 52×52 initial grid, $2^6 - 1$ reallocations and a timestep $\Delta\tau = \frac{T}{K+1}$. The convergence ratio (CR) is defined in Equation (5.1.1).

	$W_0 = 146.881014$ $C_0 = 4.196600$		$W_0 = 160.170249$ $C_0 = 17.485835$		$W_0 = 176.956650$ $C_0 = 34.272237$	
RL	Value	CR	Value	CR	Value	CR
0	9.193331		32.647635		54.851529	
1	9.207486		32.639050		54.808178	
2	9.215270	1.819	32.637032	4.254	54.789493	2.320
3	9.219532	1.826	32.637202	-11.919	54.781606	2.369
4	9.221737	1.932	32.637566	0.464	54.778124	2.265

Table 5.12: Values for v_L^0 with jumps, limited borrowing and reallocation approaching the continuous case ($\varrho = r$). The conditions of Table 5.11 apply here, too.

	$W_0 = 146.881014$ $C_0 = 4.196600$		$W_0 = 160.170249$ $C_0 = 17.485835$		$W_0 = 176.956650$ $C_0 = 34.272237$	
RL	Value	CR	Value	CR	Value	CR
0	-4.966138		-15.138107		-20.545773	
1	-5.003415		-15.146535		-20.526581	
2	-5.016880	2.768	-15.149526	2.818	-20.514941	1.649
3	-5.022488	2.401	-15.150945	2.107	-20.508790	1.892
4	-5.025025	2.210	-15.151626	2.087	-20.505742	2.018

5.6 Convergence to the unlimited borrowing case

Next we examine the sensitivity of v_L^0 with respect to the borrowing limit $\hat{B}$. For simplicity we impose the same borrowing limit at each reallocation stage k, and assume that the CPPI floor moves at the risk-free rate.

It is natural to suppose that the limited-borrowing results will approach the classical (i.e. unlimited borrowing) case as $\hat{B} \to -\infty$. This hypothesis is supported by the data presented in Figure 5.1. Moreover, we observe a similarity between the results for all five borrowing limits. Outside of this figure's range, the computed values for the three most negative borrowing limits diverge further from the analytical values. Thus, this experiment suggests that an artificial borrowing limit $\hat{B}$ can always be chosen sufficiently large to ensure that the distance between the limited- and unlimited-borrowing cases—over an interval (of initial cushion or initial wealth values)—is within a specified tolerance.

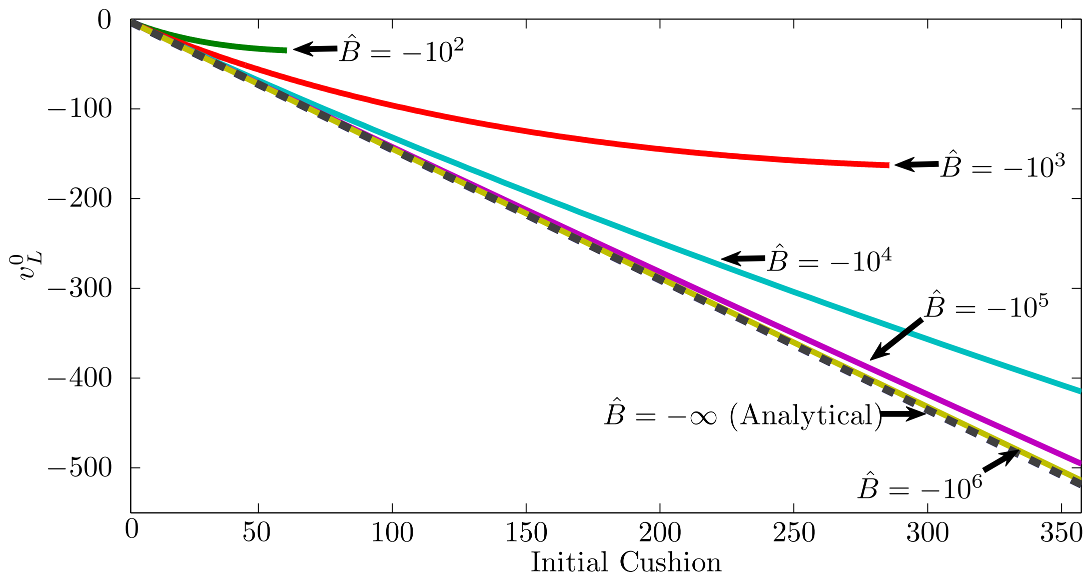

Figure 5.1: For varying $\hat{B}$, v_L^0 was computed for initial cushions ($C_0 = W_0 - F^0$) corresponding to B^0 in the range $[\hat{B}, F^0]$.

Sharpening the preceding statement requires methodological adjustments; the data presented in Figure 5.1 is suitable for qualitative comparisons, but even with interpolation the difference in scale between datasets' domains hinders quantitative comparisons. To compensate, we perform a new experiment, where each sequence $\mathbf{B}^k$ (the B ordinates for the k^{th} grid) is held identical across trials—except for $B^k_{\min}$ which is set to the prevailing borrowing limit. So, unlike the B ordinate distribution described in Section 5.4, this construction results in grids where all but the nodes corresponding to $B_{\min}$ are independent of the borrowing limit.

The data presented in Table 5.13 demonstrates that (for a fixed refinement level), doubling the artificial borrowing limit results in linear convergence to the unlimited borrowing case's theoretical result. This finding allows for the approximation of a pointwise upper bound on $\hat{B}$. Details are presented in Appendix C. As $B_{\min} \to -\infty$ the truncation error remains. This residual error varies between nodes (and grid spacings), but is observed to decrease as the grid is refined.

Table 5.13: Artificial borrowing limit sensitivity for v_J^0 with jumps, limited borrowing and daily reallocation ($K = 250$, $\varrho = r$). These results were computed using Crank-Nicolson timestepping and limited quadratic interpolation. A representative subset of the data is presented. A refinement level of 4 was used throughout. The convergence ratio (CR) is defined in Equation (5.1.1), the theoretical value for unlimited borrowing (THEO) is calculated using Equation (4.1.3) and the error (%RE) relative to this value is defined in Equation (5.1.2). The computed values presented here do not converge exactly to the THEO values as $\hat{B}$ decreases; a discretisation error persists because of the refinement level being held fixed throughout this trial.

	$W_0 = 142.871914$ $C_0 = 0.187500$			$W_0 = 156.043789$ $C_0 = 13.359375$			$W_0 = 258.309414$ $C_0 = 115.625000$		
$\hat{B}$	Value	%RE	CR	Value	%RE	CR	Value	%RE	CR
-2^{12}	-0.271534	0.196		-18.552353	4.295		-138.735085	17.309	
-2^{13}	-0.271714	0.130		-18.909642	2.452		-150.035858	10.573	
-2^{14}	-0.271817	0.092	1.7425	-19.132228	1.303	1.6052	-157.950327	5.856	1.4279
-2^{15}	-0.271871	0.072	1.9181	-19.255337	0.668	1.8081	-162.651847	3.054	1.6834
-2^{16}	-0.271898	0.062	1.9811	-19.319285	0.338	1.9251	-165.168946	1.554	1.8678
-2^{17}	-0.271912	0.057	1.9901	-19.351767	0.171	1.9688	-166.460890	0.784	1.9483
-2^{18}	-0.271919	0.055	1.9936	-19.368132	0.086	1.9849	-167.114468	0.394	1.9767
-2^{19}	-0.271922	0.054	1.9966	-19.376345	0.044	1.9924	-167.443138	0.198	1.9886
-2^{20}	-0.271924	0.053	1.9983	-19.380460	0.023	1.9963	-167.607938	0.100	1.9943
-2^{21}	-0.271925	0.053	1.9990	-19.382519	0.012	1.9980	-167.690461	0.051	1.9970
-2^{22}	-0.271925	0.053	1.9996	-19.383549	0.007	1.9992	-167.731750	0.026	1.9987
-2^{23}	-0.271925	0.053	1.9998	-19.384064	0.004	1.9996	-167.752402	0.014	1.9993
THEO	-0.272068			-19.384868			-167.775462		

5.7 Limited borrowing with an independent CPPI floor

Finally, we demonstrate that our framework can handle cases where borrowing is limited and the CPPI floor moves independently of the risk-free rate. Such a scenario arises if the CPPI floor rate is contractually fixed, or if it is set to float at a nonzero distance relative to the risk-free rate. To our knowledge, this class of problems has not been examined in the CPPI literature. For simplicity we consider the scenarios where (i) $\varrho = 0$ and (ii) $\varrho = 2r$. Our findings are tabulated respectively in Tables 5.14 and 5.15, and plotted in Figure 5.2.

Table 5.14: Values for v_L^0 with jumps, limited borrowing and daily reallocation ($K = 250, \varrho = 0$). These results were computed using Crank-Nicolson timestepping and piecewise quadratic interpolation. A representative subset of the data is presented. The grids are designed to circumvent extrapolation for $W \to \infty$, using a fixed borrowing limit of $\hat{B} = 0$. Refinement level (RL) 0 corresponds to a 52×52 initial grid and a timestep $\Delta\tau = \frac{T}{K+1}$. The convergence ratio (CR) is defined in Equation (5.1.1).

	$W_0 = 154.411765$, $C_0 = 4.411765$		$W_0 = 168.382353$, $C_0 = 18.382353$		$W_0 = 186.029412$, $C_0 = 36.029412$	
RL	Value	CR	Value	CR	Value	CR
0	-6.890316		-15.788886		-20.234672	
1	-6.892573		-15.796509		-20.238710	
2	-6.897004	0.509	-15.802839	1.204	-20.240589	2.148
3	-6.899759	1.608	-15.804904	3.066	-20.241449	2.186
4	-6.900416	4.196	-15.805417	4.022	-20.241665	3.991
5	-6.900564	4.434	-15.805542	4.121	-20.241716	4.153

Table 5.15: Values for v_L^0 with jumps, limited borrowing and daily reallocation ($K = 250, \varrho = 2r$). These results were computed using Crank-Nicolson timestepping and piecewise quadratic interpolation. A representative subset of the data is presented. The grids are designed to circumvent extrapolation for $W \to \infty$, using a fixed borrowing limit of $\hat{B} = 0$. Refinement level (RL) 0 corresponds to a 52×52 initial grid and a timestep $\Delta\tau = \frac{T}{K+1}$. The convergence ratio (CR) is defined in Equation (5.1.1).

	$W_0 = 139.717542$, $C_0 = 3.991930$		$W_0 = 152.358653$, $C_0 = 16.633041$		$W_0 = 168.326373$, $C_0 = 32.600760$	
RL	Value	CR	Value	CR	Value	CR
0	-5.080131		-14.229497		-20.569731	
1	-5.047407		-14.233321		-20.574730	
2	-5.045118	14.295	-14.240384	0.541	-20.579155	1.130
3	-5.045562	-5.148	-14.242394	3.515	-20.580449	3.417
4	-5.045742	2.474	-14.242935	3.715	-20.580771	4.027
5	-5.045787	3.968	-14.243076	3.821	-20.580853	3.919

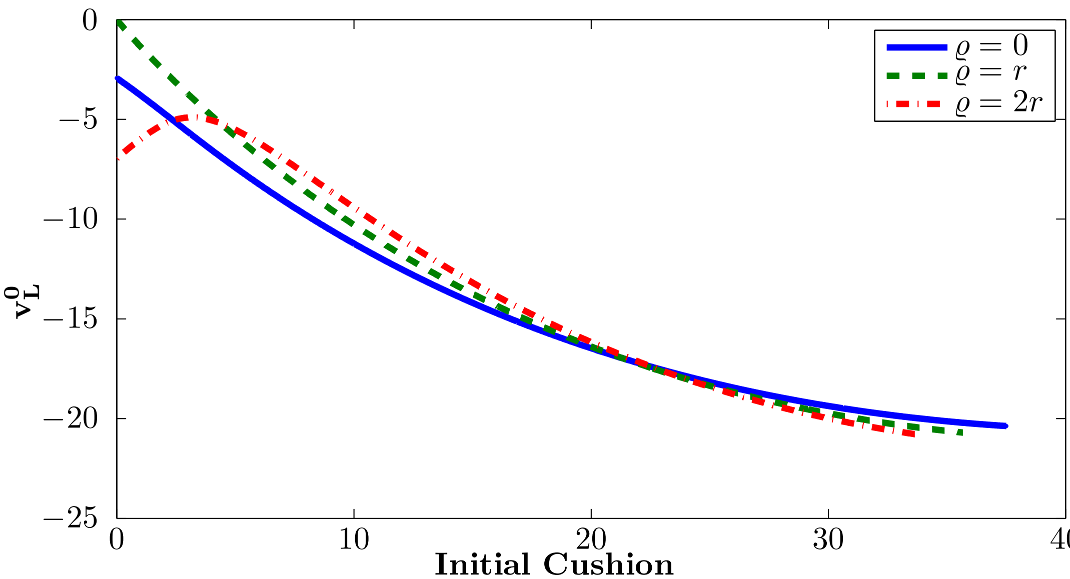

Figure 5.2: The effect of ϱ on v_L^0. These results correspond to Tables 5.9, 5.14 and 5.15.

Interestingly, both the $\varrho = 0$ and the $\varrho = 2r$ cases are riskier than the $\varrho = r$ case, because both variants dictate larger allocations in the risky asset. Recall from Remark 2.4.1 that our formulation of the CPPI jump conditions permits a negative-cushion state to eventually regain positive-cushion status when $\varrho < r$.

For brevity, analogous results for v_J^0 are not presented, but both scenarios did obey the parity relationship of Equation (2.6.8).

6 Conclusion

6.1 Summary of contributions

The CPPI portfolio allocation strategy has existed for about twenty-five years and has an established role in the multibillion-dollar capital guarantee niche of finance. However, the vulnerabilities of CPPI-backed guarantees to portfolio shortfalls have only recently received attention in the literature. Motivated by this, we have developed a robust computational framework for valuing discretely-reallocated CPPI-backed contingent claims in the presence of risky-asset jumps.

Our framework models CPPI portfolios with a two-asset state space, in order to accommodate composition-dependent variants of the classical strategy. From this, a two-dimensional partial integro-differential equation (PIDE) was derived to represent the pricing dynamics of the contingent claim in between reallocations. Discrete reallocations are imposed as instantaneous, global shocks. More precisely, at each discrete reallocation instant the domain is repopulated using information from a subset of the domain just solved in the previous PIDE stage. Therefore, the pricing problem is equivalent to solving a cascading sequence of 2D PIDEs.

Two types of CPPI reallocation strategy were considered: the classical scheme and a limited-borrowing variant. The images of these reallocation operations were examined so that the grid design and interpolation scheme could be tailored accordingly. This led to a sequence of computational grids that updates with each stage of the PIDE solve. From a dynamic programming perspective (solving backwards in time), both reallocation mappings were found to have expansive regions. In the classical case this was handled by using a similarity extrapolant that is exact in special cases. We showed that in the fixed-borrowing-limit case the grid can be constructed so that the computational domain of dependence is bounded.

In order to facilitate computation, the problem was reformulated as a system of 1D PIDEs, using a Lagrangian transformation. Financially, this is equivalent to deferring the interest paid on the risk-free asset until the instant before reallocation. Information is only exchanged between 1D PIDE domains at the reallocation instants, permitting the inter-reallocation calculations to be performed with parallel instances of a general 1D PIDE solver.

For our implementation of the fixed-borrowing-limit case we proved robust stability and monotonicity. For our implementation of the classical CPPI case we have proven monotonicity; to date we can only conjecture numerical stability, guided by our numerical results and by our proof of stability for a special analytical case. For this reason we advocate the use of limited borrowing computational models over their unlimited borrowing counterparts. The former approach is also more appealing from financial and regulatory perspectives.

A central theme of this work was the development of analytical results to complement the computational framework. Each approach helps to advance the other: the analytical results help validate the computational framework, which in turn (in addition to its general applicability) provides insight that may inspire further analytical findings. In this work we developed analytical results for a special case of the classical CPPI strategy, for both continuous and discrete reallocation.

Our implementation used the PIDE discretisation of [18]. We confirmed our framework's ability to price CPPI products with absolute borrowing limits. Convergence to the continuous-reallocation case was demonstrated. A guideline was established for approximating the unlimited borrowing case using an artificially imposed borrowing limit. A result akin to put-call parity was introduced, enabling the risk-neutral expected values of the claim and the guarantor's liability to be determined from the same computation. Finally, we examined situations where the floor's movement was independent of the risk-free rate.

6.2 Future work

A desirable feature of this framework would be the ability to handle proportional borrowing limits (i.e. restricting borrowing to a percentage of the portfolio value, rather than imposing an absolute borrowing limit). This can be viewed as a compromise between the two CPPI allocation strategies considered herein. Accordingly, we propose a CPPI variant where a proportional borrowing limit yields to an absolute borrowing limit when the portfolio wealth is above a suitably high artificial threshold. Graphically, this modification corresponds to a 'chamfered' transition between the oblique and horizontal components of Figure 2.2. This can be implemented with minimal change to the existing grid design (Appendix B). We suspect that conditions analogous to those in Section B.3 can be devised so that the need for a similarity extrapolant can be avoided.

CPPI strategies with a ratcheting feature switch to a more ambitious CPPI floor trajectory if the risky component of the portfolio has performed well. Our implementation can be extended—at the expense of increased computational load—to permit contractually predetermined, discrete-time ratcheting events with a finite number of CPPI floor trajectories. This is achieved by parallelly solving (S, B) planes for each CPPI floor function. Information is exchanged between planes at each discrete ratcheting event. Such an extension would not have been possible had our modelling assumed that the CPPI floor value always appreciates at the risk-free rate.

Transaction costs are another practical consideration that may deserve attention. At a given discretely-observed reallocation instant, transaction costs can avoided if the current CPPI portfolio state is suitably close to the prescribed reallocated state. Referring to Figure 2.1 (resp. Figure 2.2), consider a region on the (S, B) plane that contains the relevant allocation locus. States outside of this region follow the classical (resp. limited-borrowing) reallocation strategy developed herein and will incur transaction costs. In contrast, states within this region will at reallocation jump in the B direction (as a consequence of the Lagrangian transformation) but will not incur transaction costs. It follows that for this modification, the domain of dependence between reallocations is no longer just the prevailing reallocation locus. This has interpolation and grid design implications.

It should be possible to derive a semi-analytical solution for the limited-borrowing case when the CPPI floor moves at the risk-free rate. The key insight is that at each reallocation instant, the difference between values for the limited- and unlimited-borrowing strategies is only nonzero for wealth above a threshold (corresponding to $\hat{B}$). Therefore this difference can be viewed as a (typically nonlinear) call payoff. Moreover, the payoff can be approximated as the payoff of a polynomial option, which can in turn be decomposed into a linear combination of power options [33]. Even if this approach turns out to be computationally intractable it may help sharpen the result presented in Appendix C. This decomposition of a limited-borrowing CPPI-backed guarantee into simpler financial instruments could also provide insight into how to hedge this guarantee in incomplete markets.

Lastly, the issue of calibration must be addressed; our ultimate goal is to assess the suitability of CPPI-backed guarantees and this can only go so far without empirically-grounded financial parameters.

Appendix A Positive coefficient discretisation

For convenience we state the positive coefficient discretisation for a 1D PIDE. This was developed in [18]. Define the *centred difference coefficients* as

$$
\begin{aligned}
\bar{\alpha}_{i,j} &\equiv \frac{\sigma_i^2 S_{i,j}^2}{(S_{i,j} - S_{i-1,j})(S_{i+1,j} - S_{i-1,j})} - \frac{(r - \lambda\kappa) S_{i,j}}{S_{i+1,j} - S_{i-1,j}} \\
\bar{\beta}_{i,j} &\equiv \frac{\sigma_i^2 S_{i,j}^2}{(S_{i+1,j} - S_{i,j})(S_{i+1,j} - S_{i-1,j})} + \frac{(r - \lambda\kappa) S_{i,j}}{S_{i+1,j} - S_{i-1,j}} ,
\end{aligned}
$$

forward difference coefficients as

$$
\begin{aligned}
\acute{\alpha}_{i,j} &\equiv \frac{\sigma_i^2 S_{i,j}^2}{(S_{i,j} - S_{i-1,j})(S_{i+1,j} - S_{i-1,j})} \\
\acute{\beta}_{i,j} &\equiv \frac{\sigma_i^2 S_{i,j}^2}{(S_{i+1,j} - S_{i,j})(S_{i+1,j} - S_{i-1,j})} + \frac{(r - \lambda\kappa) S_{i,j}}{S_{i+1,j} - S_{i,j}} ,
\end{aligned}
$$

and *backward difference coefficients* as

$$
\begin{aligned}
\grave{\alpha}_{i,j} &\equiv \frac{\sigma_i^2 S_{i,j}^2}{(S_{i,j} - S_{i-1,j})(S_{i+1,j} - S_{i-1,j})} - \frac{(r - \lambda\kappa) S_{i,j}}{S_{i+1,j} - S_{i,j}} \\
\grave{\beta}_{i,j} &\equiv \frac{\sigma_i^2 S_{i,j}^2}{(S_{i+1,j} - S_{i,j})(S_{i+1,j} - S_{i-1,j})} .
\end{aligned}
$$

Then, applying the following algorithm ensures both $\alpha_{i,j}$ and $\beta_{i,j}$ are non-negative, while maximising the use of centred finite differences:

- If $\bar{\alpha}_{i,j} \geq 0$ and $\bar{\beta}_{i,j} \geq 0$ then $\alpha_{i,j} \equiv \bar{\alpha}_{i,j}$ and $\beta_{i,j} \equiv \bar{\beta}_{i,j}$;
- otherwise, if $\acute{\beta}_{i,j} \geq 0$ then $\alpha_{i,j} \equiv \acute{\alpha}_{i,j}$ and $\beta_{i,j} \equiv \acute{\beta}_{i,j}$;
- otherwise, $\alpha_{i,j} \equiv \grave{\alpha}_{i,j}$ and $\beta_{i,j} \equiv \grave{\beta}_{i,j}$.

This discretisation accommodates local volatilities, represented as $\sigma_i \equiv \sigma(S_{i,j}^k, t)$. In this case $\alpha_{i,j}$ and $\beta_{i,j}$ will vary over the PIDE solve but will still retain the desired properties.

Appendix B Grid design

B.1 Objectives and design constraints

Here we present the details of our computational grids. We proceed with the jump conditions (2.6.4) and (2.6.5) in mind, and end up with distinct grid designs for each. Each design is a sequence of bounded grids indexed by k.

We require that our grid designs satisfy the following objectives, in descending order of importance:

(**O1**) grids must be consistent with the reallocation scheme specified in the CPPI contract;

(**O2**) grids must exploit the Lagrangian formulation of Section 2.6;

(**O3**) grid nodes should be distributed in a fashion that hastens convergence and simplifies interpolation;

(**O4**) in instances where the similarity extrapolant applied in [47] is not appropriate, the jump conditions should not require off-grid data.

The first objective is easily addressed. If there is no borrowing limit then the domain must be artificially truncated in the B direction. In light of the large shortfall boundary condition (Section 3.3.1) we require that this artificial borrowing limit be negative; in practice its magnitude should be suitably large to restrict its influence on the initial wealth range for which we wish to solve. Numerical tests in Section 5.6 show the effect of this artificial borrowing limit. Conversely, if the contract specifies a borrowing limit $\hat{B}^k$ then the k^{th} grid must have adequate coverage of the $B = \hat{B}^k$ row, and no nodes below this row.

Objective (B.1.O2) suggests that all grids should be organized in rows, with each gridpoint in a given row having the same B ordinate. This in turn allows us to model the inter-observation dynamics as a system of PIDEs in one spatial dimension. Moreover, since no information need be exchanged between rebalancing instants, the problem is *embarrassingly parallel* and lends itself very well to parallel processing [46].

In light of (B.1.O2) alone, a *regular grid* would suffice. However, to meet (B.1.O3) we instead use a sequence of *scaled* two-dimensional scaled grids. This is motivated by similar studies for other instruments (such as [48, 17, 47, 5]) and their use of grids that are tailored to the appropriate jump conditions. The difference here is that *our* jump conditions change at each reallocation, so our grids must as well.

Additionally, we take the kink in each PIDE stage's initial conditions into account. There is a payoff kink in the K^{th} stage, where one choice in the payoff function overtakes the other. Likewise, there is also a *reallocation kink* in the other stages, at the interface between information propagated from the vertical and oblique segments of the k^{th} allocation locus.

So, to improve the quality of the numerical solution we impose the additional requirement that each row should have nodes situated where the row intersects (i) the payoff kink, and (ii) the oblique segment of the appropriate allocation locus. The second constraint allows for diagonal interpolation [47, 5] instead of the more-general, less-accurate method of two-dimensional interpolation.

Each resultant grid is *structured* and can be indexed by the subscript pair (i, j). For design flexibility we will allow our grid sequences to vary with k: the $(i, j)^{\text{th}}$ node of grid k need not have the same coordinates as the $(i, j)^{\text{th}}$ node of grid $k+1$. Nor do we require that each row have the same number of nodes.

Objective (B.1.O4) is the most demanding of all, requiring that we find a sequence of computational grids where the range of wealth required to populate the k^{th} grid falls within the range of wealth supplied by the $(k+1)^{\text{th}}$ grid's allocation locus. In Section B.3 we determine conditions under which the fixed-borrowing-limit variant satisfies (B.1.O4).

B.2 Grid construction

Our construction begins with a two-dimensional sequence $\left\{\mathbf{B}^k\right\}_{k=0}^{K} \equiv \left\{\left\{B_j^k\right\}_{j=0}^{j_{\max}}\right\}_{k=0}^{K}$, with B_J^k representing the j^{th} *ordinate* of grid k. We constrain the endpoints and require that for each k, the sequence $\mathbf{B}^k$ be monotonically increasing in j, from $B_0^k = B_{\min}^k$ to $B_{j_{\max}}^k = F^k$. In the limited-borrowing case, $B_{\min}^k$ is $\hat{B}^k$ and in the classical case we set $B_{\min}^k$ to be suitably low. The interior points of each $\mathbf{B}^k$ should be concentrated at the ordinates of the kinks in the k^{th} CPPI allocation locus, since this is where one would expect the greatest nonlinearity to arise.

Next we construct our grid's S coordinates (*abscissæ*). Each B_j^k has the corresponding sequence $\{S_{i,j}^k\}_{i=0}^{i_{\max}}$. Consider the prototypical grid sequence $\mathbf{s}$ with which we will construct each row's abscissæ $\{S_{i,j}^k\}_{i=0}^{i_{\max}-1}$. Let $\mathbf{s} \equiv \{s_i\}_{i=0}^{i_{\max}-1}$, constrained such that

1. the gridpoints of $\mathbf{s}$ are concentrated about a gridpoint $s^\dagger$ contained within $\mathbf{s}$,
2. $\mathbf{s}$ is strictly increasing in i, and
3. $0 \equiv s_0 < s^\dagger \ll s_{i_{\max}-1}$.

Having introduced our notation, we can now describe our grid construction procedure. The limited-borrowing case requires a few grid parameter restrictions (see Section B.3) in order to avoid needing a large-cushion boundary condition; the grid construction process itself is identical for the classical and limited-borrowing cases. The result is a sequence of grids, with each grid scaled about the prevailing reallocation locus. Additionally, each grid has nodes coincident with the relevant reallocation locus and reallocation kink.

Step I. Grid scaling

Concentrating row j of grid k about $S = x_j^k$ is a simple matter of scaling each element of $\mathbf{s}$ by $\frac{x_j^k}{s^\dagger}$. In practice, numerical complications arise when the grid spacing falls within the machine epsilon range, so we will ensure that the scale factor exceed a threshold of $\epsilon_1 > 0$.

Despite the Lagrangian state space transformation of Section 2.5, $\mathcal{A}^k$ and $\hat{\mathcal{A}}^k$ (as defined in Equations (2.2.4) and (2.2.6)) are still a valid representations of the allocation locus in effect at time $t_{\mathrm{o}}^{k^+}$, since at this instant no interest on the risk-free asset has accrued since the last update at $t_{\mathrm{o}}^{k^-}$. Rearranging the oblique segment of either previously mentioned equation yields $x_j^k = \left(F^k - B_j^k\right)\frac{m}{m-1}$ and hence the scaled grid abscissæ are defined by

$$S_{i,j}^k = \max\left\{\left(F^k - B_j^k\right)\frac{m}{m-1}, \epsilon_1\right\}\frac{s_i}{s^\dagger} \tag{B.2.1}$$

for $0 \le i < i_{\max}$.

The alternative approach of scaling our grids about the payoff kinks is more complicated: the payoff kink does not always span the computational domain's full range of B ordinates. Such a situation arises under reasonable financial circumstances when the function F grows slower than the prevailing risk-free rate.

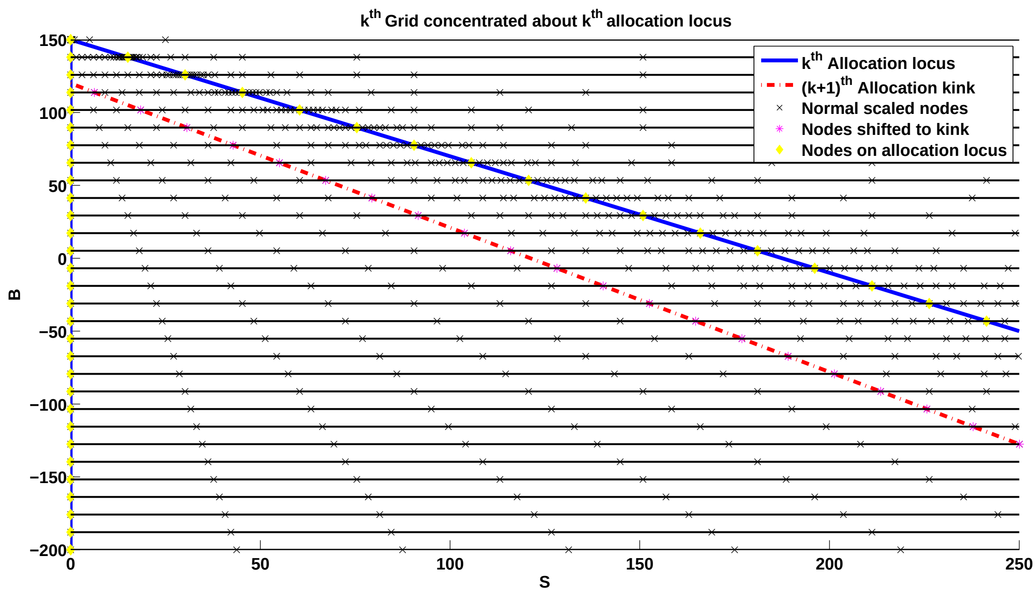

Figure B.1: This is a typical grid centred about the allocation locus, with $F^k = 150$ and $m = 5$.

Step II. Adding nodes of interest

The measures taken in the previous step have already guaranteed coincidence with the appropriate allocation locus. Next, we adjust our scaled grids so that they are coincident the relevant allocation kink. For each grid and row, the abscissa $\tilde{S}_j^k$ is calculated, representing the reallocation kink's intersection with row j of grid k. These abscissæ are then inserted into the grids, preserving row-wise abscissa monotonicity. No adjustments are made to rows that do not intersect the allocation kink.

Suppose (i) that we find $\tilde{S}_j^k$ lies between the pre-existing abscissæ $S_{\tilde{i},j}^k$ and $S_{\tilde{i}+1,j}^k$, and furthermore (ii) that $\tilde{S}_j^k$ is within a threshold $\epsilon_2 > 0$ of one or both of these nodes. Then it might be prudent to reposition the closer of $S_{\tilde{i},j}^k$ and $S_{\tilde{i}+1,j}^k$ to overlie $\tilde{S}_j^k$, instead of inserting a new node.

A sample grid is illustrated in Figure B.1.

Step III. Grid extension

Finally, it is necessary to extend each grid row in order to counteract our numerical scheme's susceptibility to FFT pollution (see [18], particularly Appendix B). This modification is consequential to our grid design because it influences the maximum wealth represented on each grid. In the same reference the task of determining an appropriate extension factor is posed as finding Δy^+ such that $p(\ln \Delta y^+) < -2\Delta y^+ \epsilon_3$. For general density functions it is not possible to precisely solve this without a root-finding algorithm; any answer larger than the minimum will suffice.

In the special case where the jump probability density is lognormal (see Equation (2.4.2)) then we can explicitly solve for Δy^+:

$$\Delta y^+ > \gamma^2 + \gamma\sqrt{\gamma^2 + 2\mu - \ln\left(2\pi\gamma^2\epsilon_3^2\right)} + \mu.$$

In practice we will err on the side of caution and scale this result by a safety factor, C_2. What is important here is that we calculate a grid extension factor that is independent of the row, j, and the grid number, k. Hence we need only calculate Δy^+ once. This property will be used to simplify our calculations in the next section.

For notational convenience we represent the extension factor as

$$\Upsilon \equiv e^{\Delta y^+ + C_2}$$

and the abscissa arising from this extension as

$$S^k_{i_{\max},j} \equiv \Upsilon S^k_{i_{\max}-1,j}.$$

B.3 Boundedness of the limited-borrowing grid sequence

We end this appendix by showing that the fixed-borrowing-limit CPPI discretisation does not require a far-field boundary condition at reallocations, under reasonable financial assumptions and mild conditions on the grid bounds. This section proves the result alluded to in Section 3.3.

Proposition B.1. *Consider the sequence of computational* (S,B) *grids proposed in Section B.2 and characterised by the abscissæ*

$$S_{i,j}^k = \begin{cases} \max\left\{\left(F^k - B_j^k\right)\frac{m}{m-1}, \epsilon_1\right\}\frac{s_i}{s^\dagger}, & 0 \le i < i_{\max} \\ \Upsilon S_{i_{\max}-1,j}^k, & i = i_{\max} \end{cases} \tag{B.3.1}$$

with $\Upsilon \gg 1$. *If*

- ***(i)*** $B_0^k = \hat{B} \le 0$ *for all* k,
- ***(ii)*** *the largest prototypical grid value* $s_{i_{\max}-1}$ *satisfies*

$$\frac{s_{i_{\max}-1}}{s^\dagger} > \frac{1}{\Upsilon}\cdot\frac{\rho_0^{K+1}(F_T - \hat{B})}{(F_T - \hat{B})\frac{m}{m-1} - \epsilon_1} > \frac{\rho_0^{K+1}}{\Upsilon}\cdot\frac{m-1}{m},$$

- ***(iii)*** $(F^0 - \hat{B})\frac{m}{m-1} > \epsilon_1$, *and*
- ***(iv)*** *the CPPI floor sequence* $\{F^k\}$ *samples a nondecreasing function*

then the S *coordinate resulting from the composition* $\hat{f}^K \circ \hat{f}^{K-1} \circ \cdots \circ \hat{f}^{k+1} \circ \hat{f}^k\left(S_{i,j}^k, B_j^k\right)$ *is bounded above by* $\Upsilon\frac{s_{i_{\max}-1}}{s^\dagger}\left(F_T - \hat{B}\right)\frac{m}{m-1}$, *for all* $i_{\max}$, $j_{\max}$ *and* K. *In words, conditions (i) through (iv) are sufficient for the limited-borrowing CPPI case not needing a large cushion boundary condition.*

Proof. The fixed-borrowing-limit CPPI discretisation does not require a large-cushion boundary condition at each t_{o}^{k+1} if, for any positive-cushion node (S,B) on grid k, $\hat{f}^{k+1}(S,B)$ lies within the wealth range of $\hat{\mathcal{A}}^{k+1}$ on the $(k+1)^{\text{th}}$ grid (thus permitting the interpolation described in Section 3.4). Since $\hat{f}^{k+1}$ depends solely on the time $t_{\mathrm{o}}^{(k+1)^-}$ wealth, an equivalent condition (for the fixed-borrowing-limit case) is that

$$W_{\max}^{(k+1)^-} \equiv \max_{i,j}\left\{S_{i,j}^k + \rho_k^{k+1}B_j^k\right\} < W_{\max}^{(k+1)^+} \equiv S_{i_{\max},0}^{k+1} + \hat{B} \quad \text{for all } k. \tag{B.3.2}$$

First we calculate $W_{\max}^{(k+1)^-}$. Since $S_{i,j}^k$ is increasing in i, the maximum occurs when $i = i_{\max}$. So, by Equation (B.3.1), we seek to maximise $\Upsilon\max\left\{\left(F^k - B_j^k\right)\frac{m}{m-1}, \epsilon_1\right\}\frac{s_{i_{\max}-1}}{s^\dagger} + \rho_k^{k+1}B_j^k$ over j. The quantity $\left(F^k - B_j^k\right)\frac{m}{m-1}$ is decreasing in j, so if $\left(F^k - B_{j^\star}^k\right)\frac{m}{m-1} > \epsilon_1$

then the same can be said for $0 \leq j \leq j^{\star}$. Conditions (iii) and (iv) guarantee that such a $j^{\star}$ exists.

For $0 \leq j \leq j^{\star}$ we have

$$\begin{aligned} & \Upsilon\left(F^k - B_j^k\right) \frac{m}{m-1} \frac{s_{i_{\max}-1}}{s^{\dagger}} + \rho_k^{k+1} B_j^k \\ = \quad & B_j^k \left(\rho_k^{k+1} - \Upsilon \frac{s_{i_{\max}-1}}{s^{\dagger}} \frac{m}{m-1}\right) + \Upsilon \frac{s_{i_{\max}-1}}{s^{\dagger}} F^k \frac{m}{m-1}. \end{aligned} \tag{B.3.3}$$

The second inequality of condition (ii) guarantees that the above quantity in the parentheses is negative for all k. So, since B_j^k is increasing in j, (B.3.3) is decreasing in j and is optimised at $j = 0$.

For $j > j^{\star}$ the optimal index is $j = j_{\max}$ because B_j^k is increasing in j.

Combining these two cases, we have

$$\begin{aligned} & \max_{i,j} \left\{S_{i,j}^k + \rho_k^{k+1} B_j^k\right\} \\ = \quad & \max\left\{\Upsilon\left(F^k - \hat{B}\right) \frac{m}{m-1} \frac{s_{i_{\max}-1}}{s^{\dagger}} + \rho_k^{k+1} \hat{B},\ \Upsilon \epsilon_1 \frac{s_{i_{\max}-1}}{s^{\dagger}} + \rho_k^{k+1} F^k\right\}. \end{aligned}$$

The first inequality of condition (ii) guarantees that—for all k—the above maximum is achieved at $j = 0$, so that

$$W_{\max}^{(k+1)^-} = S_{i_{\max},0}^k + \rho_k^{k+1} \hat{B} = \Upsilon\left(F^k - \hat{B}\right) \frac{m}{m-1} \frac{s_{i_{\max}-1}}{s^{\dagger}} + \rho_k^{k+1} \hat{B}.$$

Next we verify (B.3.2). By Equation (B.3.1) we have

$$W_{\max}^{(k+1)^+} - W_{\max}^{(k+1)^-} = \Upsilon\left(F^{k+1} - F^k\right) \frac{m}{m-1} \frac{s_{i_{\max}-1}}{s^{\dagger}} - \hat{B}\left(\rho_k^{k+1} - 1\right).$$

Conditions (i) and (iv) guarantee that this quantity is positive for all k, as desired.

The upper bound on $S_{i,j}^k$ is the risky position of the portfolio with wealth $W_{\max}^{K+1}$. ∎

Appendix C Approximate bound for artificial $\hat{B}$

Consider the scenario where the unlimited-borrowing (classical) case is to be approximated by the limited-borrowing case (with an artificial borrowing limit $\hat{B}$). This raises the issue of how to choose a value for $\hat{B}$ so that the classical case is approximated within a desired tolerance.

Let V_h represent the computed limited-borrowing value $v^0(W_0, t = 0; \hat{B} = -2^h)$ at a fixed refinement level, and let e_d represent the discretisation error between $V_\infty \equiv \lim_{h\to\infty} V_h$ and the theoretical classical value $\bar{V} \equiv v^0(W_0, t = 0)$. For simplicity we restrict h to integer values.

An examination of the data gathered in Section 5.6—of which Table 5.13 is a subset—shows that the convergence ratios are (in the interior of the grid) all very close to 2 when $\hat{B}$ is sufficiently small (i.e. h is sufficiently large). The value 2, corresponding to ideal linear convergence, was only ever exceeded by less than 1% in this experiment. It is therefore reasonable to state that

$$V_h - V_{h+1} \lesssim 2(V_{h+1} - V_{h+2}).$$

If equality is achieved for all h then $(V_h - V_{h+1})$ follows a geometric progression. So

$$V_h - V_\infty \gtrsim 2(V_h - V_{h+1}).$$

With equality, it is also true that for any fixed value of h, if $|V_{h+1} - V_h|$ is less than a tolerance δ_h, then

1. $|V_{h+1+\ell} - V_{h+\ell}| < 2^{-\ell}\delta_h$, and
2. $|V_\infty - V_h| < 2\delta_h$.

Let $\epsilon > |e_d|$. It then follows that for $h^\star \equiv h + \left\lceil \log_2\left(\frac{2\delta_h}{\epsilon - |e_d|}\right)\right\rceil$,

$$|V_{h^\star+1} - V_{h^\star}| < \frac{\epsilon - |e_d|}{2}$$

and

$$\left|V_\infty - V_{h^\star}\right| < \epsilon - \left|e_d\right|,$$

so that

$$\begin{aligned}\left|\bar{V} - V_{h^\star}\right| &= \left|V_\infty - e_d - V_{h^\star}\right| \\ &< \left|V_\infty - V_{h^\star}\right| + \left|e_d\right| \\ &< \epsilon.\end{aligned}$$

This analysis shows that given a target tolerance ϵ, and knowing from prior computations that $|V_{h+1} - V_h| < \delta_h$, then $\hat{B} = -2^{h+\left\lceil \log_2\left(\frac{2\delta_h}{\epsilon - |e_d|}\right)\right\rceil}$ is an approximate upper bound on the artificial borrowing limits that will ensure the computed value differs from the theoretical value by no more than ϵ. As should be expected, a bound does not exist if the discretisation error is greater than ϵ.

This is a pointwise result; the values δ_h and e_d will naturally vary with W_0 (and with the grid spacing).

Finally, it is worth repeating that this is only an approximate bound because there is no theoretical reason that the convergence ratios for varying values of h should be bounded above by 2. Indeed, the computed convergence ratios did occasionally slightly exceed this value. For this same reason—if the convergence ratios obtained with the Chapter 4 analytical results (varying K) are any indication—the bound derived here is also approximate for the exact values of $\{V_h\}$ (i.e. when e_d is zero at all gridpoints, for all h).

References

[1] The Bank of Nova Scotia Deposit Notes – Linked to the Scotia Canadian Dividend Fund. Information statement, Scotiabank, June 2006. 4

[2] J. Aitchison and J.A.C. Brown. *The Lognormal Distribution.* Cambridge University Press, 1957. 59

[3] Leif B. Andersen and Jesper Andreasen. Jump-Diffusion Processes: Volatility Smile Fitting and Numerical Methods for Option Pricing. *Rev. Derivatives Res.*, 4(3):231–262, 2000. 16

[4] Sven Balder, Michael Brandl, and Antje Mahayni. Effectiveness of CPPI strategies under discrete-time trading. *J. Econom. Dynam. Control*, 33(1):204–220, 2009. 2, 3, 6, 45, 48, 53

[5] A.C. Belanger and P.A. Forsyth. Infinite reload options: Pricing and analysis. *J. Comput. Appl. Math.*, 222:54–81, 2008. 25, 37, 38, 81

[6] Fischer Black and Andre F. Perold. Theory of constant proportion portfolio insurance. *J. Econom. Dynam. Control*, 16(3-4):403–426, 1992. 1, 2

[7] Fisher Black and Robert Jones. Simplifying portfolio insurance. *J. Portfol. Manage.*, 14(1):48 – 51, 1987. 2

[8] Adrian Blundell-Wignall. An Overview of Hedge Funds and Structured Products: Issues in Leverage and Risk. Technical report, Organization for Economic Co-operation and Development, May 2007. 5

[9] Scott Blyth. Principal considerations. *Advisor's Edge Report*, page 6, November 2006. 5

[10] Jean-François Boulier and Anu Kanniganti. Expected performance and risks of various portfolio insurance strategies. In *AFIR Colloquium, Brussels, Belgium.* International Actuarial Association, September 1995. 1, 55

[11] John Philip Boyd. *Chebyshev and Fourier Spectral Methods*. Courier Dover Publications, 2001. 19

[12] Michael Brandl. *CPPI Strategies in Discrete Time*. PhD thesis, Rheinischen Friedrich-Wilhelms-Universität Bonn (University of Bonn), 2009. 3

[13] Alessandro P. Cipollini. Capital Protection: Modeling the CPPI Portfolio. *SSRN eLibrary*, 2008. 2, 3, 14

[14] Rama Cont and Peter Tankov. *Financial Modelling with Jump Processes*. CRC Press, 2004. 18, 56, 58

[15] Rama Cont and Peter Tankov. Constant proportion portfolio insurance in presence of jumps in asset prices. *Math. Finance*, 18(3):379–401, 2009. 2, 3, 8, 14, 16, 53, 56, 58

[16] Jakša Cvitanić and Fernando Zapatero. *Introduction to the Economics and Mathematics of Financial Markets*. The MIT press, 2004. 54

[17] Y. d'Halluin, P. A. Forsyth, and G. Labahn. A semi-lagrangian approach for American Asian options under jump diffusion. *SIAM J. Sci. Comput.*, 27:315–345, 2005. 19, 25, 81

[18] Y. d'Halluin, P. A. Forsyth, and K. R. Vetzal. Robust numerical methods for contingent claims under jump diffusion processes. *IMA J. Num. Anal.*, 25:87–112, 2003. 37, 38, 39, 40, 62, 77, 79, 84

[19] Yann d'Halluin. *Numerical Methods for Real Options in Telecommunications*. PhD thesis, University of Waterloo, 2004. 27, 46, 62

[20] P.A. Forsyth and G. Labahn. Numerical methods for controlled Hamilton–Jacobi–Bellman PDEs in finance. *J. Comput. Finance*, 11:1–44, 2007/2008. 38

[21] P.A. Forsyth and K.R. Vetzal. *Numeric Computation for Financial Modelling: CS 476/676 Course Notes*. University of Waterloo, 2009. 18, 40

[22] P.A. Forsyth, H.A. Windcliff, and K.R. Vetzal. *PathDepPricer: a user's overview*. David R. Cheriton School of Computer Science, University of Waterloo, 2005. 22, 38

[23] Sanford J. Grossman and Jean-Luc Vila. Optimal dynamic trading with leverage constraints. *J. Finan. Quant. Anal.*, 27(2):151–168, 1992. 1

[24] Paul Halpern and Poonam Puri. 'Canada Steps Up' - Task Force to Modernize Securities Legislation in Canada: Recommendations and Discussions. *Capital Markets Law J.*, 2(2):191–221, 2007. 4

[25] John Hull. *Options, Futures and other Derivative Securities.* Prentice–Hall, 1993. Second Edition. 49

[26] Cathrine Jessen. Constant proportion portfolio insurance: Discrete-time trading and gap risk coverage. Working paper on SSRN; `http://ssrn.com/abstract=1513914`, November 2009. 3

[27] Mark Suresh Joshi. *The Concepts and practice of mathematical finance.* Cambridge University Press, 2003. 31, 35

[28] Raul Kangro and Roy Nicolaides. Far field boundary conditions for black-scholes equations. *SIAM J. Numer. Anal.*, 38(4):1357–1368, 2000. 27

[29] Geoffrey Kingston. Theoretical foundations of constant-proportion portfolio insurance. *Econ. Letters*, 29(4):345 – 347, 1989. 1

[30] S. G. Kou. A Jump-Diffusion Model for Option Pricing. *Manage. Sci.*, 48(8):1086–1101, 2002. 16

[31] Vincent-Antonin Lépinay. Decoding finance: Articulation and liquidity around a trading room. In Donald MacKenzie, Fabian Muniesa, and Lucia Siu, editors, *Do Economists Make Markets? On the Performativity of Economics.* Princeton University Press, 2007. 1

[32] Donald MacKenzie. The big, bad wolf and the rational market: portfolio insurance, the 1987 crash and the performativity of economics. *Economy Society*, 33(3):303–334, 2004. 5

[33] Stefan Macovschi and François Quittard-Pinon. On the pricing of power and other polynomial options. *J. Derivatives*, 13(4):61–71, 2006. 78

[34] Donna Mann-Campbell. Session ind-6: Segregated funds update. *Proceedings of the Canadian Institute of Actuaries*, XXXVII(2), 2006. 4, 5

[35] Robert C. Merton. Option pricing when underlying stock returns are discontinuous. Working papers 787-75., Massachusetts Institute of Technology (MIT), Sloan School of Management, 1975. 15, 16, 36, 49

[36] Marcus Overhaus, Ana Bermúdez, Hans Buehler, Andrew Ferraris, Christopher Jordinson, and Aziz Lamnouar. *Equity Hybrid Derivatives.* Wiley, 2007. 2, 3, 12, 55

[37] Darren Pain and Jonathan Rand. Recent Developments in Portfolio Insurance. *Bank of England Quarterly Bulletin, 2008 Q1*, 2008. 2, 3, 5

[38] K. Parrott and N. Clarke. A parallel solution of early exercise asian options with stochastic volatility. *Proceedings of the 11th Domain Decomposition Conference, Greenwich*, 1998. 19

[39] Louis Paulot and Xavier Lacroze. Efficient pricing of CPPI using markov operators. Working paper on SSRN; `http://ssrn.com/abstract=1326297`, January 2009. 3

[40] Louis Paulot and Xavier Lacroze. One-dimensional pricing of CPPI. Working paper on SSRN; `http://ssrn.com/abstract=1406600`, February 2010. 3

[41] André F. Perold. Constant proportion portfolio insurance. Unpublished Manuscript, Harvard School of Business, 1986. 2

[42] André F. Perold and William F. Sharpe. Dynamic strategies for asset allocation. *Financ. Anal. J.*, 44(1):16–27, 1988. 1, 2

[43] D.M. Pooley, P.A. Forsyth, and K.R. Vetzal. Numerical convergence properties of option pricing PDEs with uncertain volatility. *IMA J. Num. Anal.*, 23:241–267, 2003. 37

[44] Lloyd N. Trefethen. *Spectal methods in MATLAB.* SIAM, 2000. 68

[45] H. Windcliff, P. A. Forsyth, and K. R. Vetzal. Analysis of the stability of the linear boundary condition for the Black–Scholes equation. *J. Comput. Finance*, 8:65–92, 2004. 27

[46] H. Windcliff, K. R. Vetzal, P. A. Forsyth, A. Verma, and T. F. Coleman. An object-oriented framework for valuing shout options on high-performance computer architectures. *J. Econ. Dyn. Control*, 27:1133–1161, 2003. 80

[47] H.A. Windcliff and P.A. Forsyth. Numerical methods and volatility models for valuing cliquet options. *Appl. Math. Finance*, 13:353–386, 2006. 4, 16, 25, 29, 37, 80, 81

[48] R. Zvan, P.A. Forsyth, and K.R. Vetzal. Discrete Asian barrier options. *J. Comput. Finance*, 3(Fall):41–68, 1999. 25, 37, 42, 65, 67, 68, 81